

1-1-1988

# Vibrational spectroscopic studies of restructuring of chain conformations [sic]/

Laurence D. Coyne

*University of Massachusetts Amherst*

Follow this and additional works at: [https://scholarworks.umass.edu/dissertations\\_1](https://scholarworks.umass.edu/dissertations_1)

---

## Recommended Citation

Coyne, Laurence D., "Vibrational spectroscopic studies of restructuring of chain conformations [sic]/" (1988). *Doctoral Dissertations 1896 - February 2014*. 738.

[https://scholarworks.umass.edu/dissertations\\_1/738](https://scholarworks.umass.edu/dissertations_1/738)

This Open Access Dissertation is brought to you for free and open access by ScholarWorks@UMass Amherst. It has been accepted for inclusion in Doctoral Dissertations 1896 - February 2014 by an authorized administrator of ScholarWorks@UMass Amherst. For more information, please contact [scholarworks@library.umass.edu](mailto:scholarworks@library.umass.edu).

UMASS/AMHERST



312066007651579

C

VIBRATIONAL SPECTROSCOPIC STUDIES  
OF RESTRUCTURING OF CHAIN CONFORMATIONS

A Dissertation Presented

by

LAURENCE D. COYNE

Submitted to the Graduate School of the  
University of Massachusetts in partial fulfillment  
of the requirements for the degree of

DOCTOR OF PHILOSOPHY

February 1988

Polymer Science and Engineering

Laurence D. Coyne 1988

© All Rights Reserved

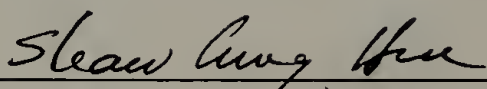
VIBRATIONAL SPECTROSCOPIC STUDIES  
OF RESTRUCTURING OF CHAIN CONFORMATIONS

A Dissertation Presented

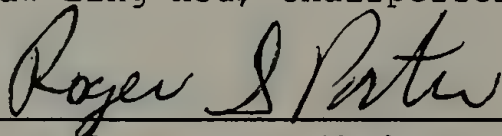
by

LAURENCE D. COYNE

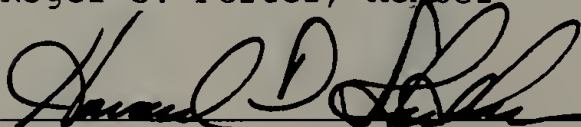
Approved as to style and content by:



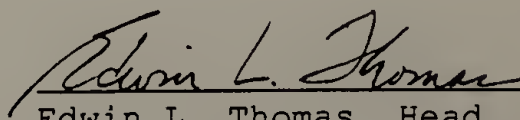
Shaw Ling Hsu, Chairperson of Committee



Roger S. Porter, Member



Howard D. Stidham, Member



Edwin L. Thomas, Head  
Polymer Science and Engineering

## ACKNOWLEDGEMENTS

I would like to acknowledge the support, guidance, and encouragement of my thesis advisor, Professor Shaw Ling Hsu. I would also like to thank Professors Roger S. Porter and Howard D. Stidham for their helpful comments and assistance.

I am grateful for the friendship and help extended to me by my co-workers including Dr. Peter Kim, David Waldman, Bruce Reinhold, and especially Dr. Chih Chang.

I would like to thank as a whole the faculty, students, and post-doctoral fellows of the Polymer Science and Engineering Department for providing a stimulating and richly rewarding environment for academia and research.

I also thank Sue Rusiecki and Wendy Lajoie for typing and compiling this thesis.

Finally, I thank my mother, father, sister, and brothers for their love and encouragement during my education.

## ABSTRACT

### VIBRATIONAL SPECTROSCOPIC STUDIES OF RESTRUCTURING OF CHAIN CONFORMATIONS

(February, 1988)

Laurence D. Coyne, B.S. Tufts University  
Ph.D. University of Massachusetts

Directed by: Professor Shaw Ling Hsu

Vibrational spectroscopy was used to investigate conformational restructuring of polymer chains in two systems. In the first system of study, miscible blends of polystyrene (PS) and poly(vinyl methyl ether) (PVME), the interactions responsible for miscibility have been observed to enhance ordering of the polymer chains during deformation of the blends. As an attempt to understand this phenomenon, a vibrational spectroscopic study was performed on a miscible blend undergoing stress relaxation. Measurements of relaxation in chain orientation from this study demonstrated that long term relaxations in these blends arise solely from the PS component. Indications were also found that the short term relaxations of the PS component arise from the destruction of chain entanglements between the two components.

In the second system of study, solutions of polydiacetylenes, various aspects of the chromic and conformational transition of this system were investigated using spectroscopic techniques. It was shown that a unimolecular

chain mechanism cannot describe in a generic fashion the chromic transition of polydiacetylenes in all solvent systems and that any observed properties of these solutions are highly solvent dependent. An unambiguous correlation was demonstrated for changes in intramolecular hydrogen bonding and changes in extent of backbone conjugation for solvated polydiacetylenes. Related experiments showed that the absence or presence of gelation does not affect the chromic transition, that the transition can be generated below room temperature despite the presence of moderately strong hydrogen-bonding solvents, and that substantial ordering can occur in polydiacetylene gels under certain circumstances.



## TABLE OF CONTENTS

ACKNOWLEDGEMENTS . . . . .	iv
ABSTRACT . . . . .	v
LIST OF TABLES . . . . .	ix
LIST OF FIGURES . . . . .	x
Chapter	
1 INTRODUCTION . . . . .	1
1.1 Vibrational Spectroscopy in Studies of Chain Structure and Conformation . . . . .	1
1.2 Chain Structure Dynamics in Miscible Blends. .	4
1.3 Chain Structure Transitions in Polydiacetylenes . . . . .	6
2 SPECTROSCOPIC STUDIES OF CHAIN RELAXATION MECHANISMS IN MISCIBLE BLENDS . . . . .	9
2.1 Introduction . . . . .	9
2.2 Experimental . . . . .	24
2.3 Results and Discussion . . . . .	33
2.3.1 Molecular Model . . . . .	36
2.3.2 Orientation Function. . . . .	42
2.3.3 Data Analysis . . . . .	46
2.4 Conclusions . . . . .	60
3 SPECTROSCOPIC STUDIES OF THE CHROMIC TRANSITION IN POLYDIACETYLENE SOLUTIONS . . . . .	62
3.1 Introduction . . . . .	62
3.1.1 Initial Observations of Solution Behavior . . . . .	62
3.1.2 Models for Chain Structure in Yellow Solutions . . . . .	68
3.1.3 Models for Mechanism of Transition. . .	73
3.2 Experimental . . . . .	89
3.3 Results and Discussion . . . . .	92
3.3.1 Solvatochromic Transition . . . . .	92

3.3.2	Thermochromic Transition . . . . .	.100
3.4	Conclusions. . . . .	.103
4	SPECTROSCOPIC STUDIES OF HYDROGEN BONDING IN SOLUTIONS, GELS, AND FILMS OF POLYDIACETYLENES. .107	
4.1	Introduction . . . . .	.107
4.2	Experimental . . . . .	.120
4.3	Results and Discussion . . . . .	.132
4.3.1	Correlation Between Backbone Structure and Hydrogen Bonding in Sidegroups. .132	
4.3.2	Hydrogen Bonding and Order in Gels. . .150	
4.3.3	Hydrogen Bonding in Quenched Solutions .156	
4.4	Conclusions. . . . .	.162
5	GENERAL RESULTS AND FUTURE WORK . . . . .	.164
	REFERENCES. . . . .	.169

## LIST OF TABLES

1. . Calculated relaxation times for second moment orientation function of PS during stress relaxation experiments. . . . . 54
2. Listing of structures, abbreviations, and solvent types for some soluble polydiacetylenes. . . . . 66

## LIST OF FIGURES

1.	Orientation function measured for PS in 50% PS/ 50% PVME blends as a function of strain rate. . .	13
2.	Stress-strain behavior for 50% PS/50% PVME blends at different strain rates. . . . .	15
3.	PS orientation in PS-PVME blends at different compositions . . . . .	18
4.	Average orientation function of plasticized PS versus draw ratio. . . . .	20
5.	Schematic of typical stress relaxation behavior of a noncross-linked, amorphous polymer . . . .	23
6.	Schematic of the hydraulic stretcher. . . . .	27
7.	Schematic diagram of the method by which mechanical data is relayed to the FTIR spectrometer. . . . .	29
8.	Infrared spectrum obtained for a 50% PS/50% PVME miscible blend . . . . .	32
9.	Relaxation of orientation function of PS component in 40% PS/60% PVME blend. . . . .	35
10.	Different relaxation stages for a primitive chain after a step uniaxial stretch . . . . .	38
11.	Modification of path of primitive chain due to retraction of constraining chains . . . . .	41
12.	Definitions of dichroic ratio and second moment orientation function . . . . .	44
13.	Relaxation of orientation function of PS components of varying molecular weight in 40% PS/60% PVME blends. . . . .	50
14.	Relaxation of orientation function of PS components in PS/PVME blends of varying composition . . . . .	52
15.	Relaxation of stress in 40% PS/60% PVME blends with varying molecular weight of PS component .	57

16.	Relaxation of stress in PS/PVME blends with varying composition . . . . .	59
17.	Planar hydrogen-bonded conformations of poly(3BCMU) and poly(4BCMU) . . . . .	64
18.	Patel, Heeger, and Wegner models for chromic transition. . . . .	71
19.	Application of visible spectroscopic data on chromic transition to Zimm-Bragg model for helix-coil transition . . . . .	76
20.	Hydrodynamic diameter of poly(4BCMU) in toluene as a function of polymer concentration. . . . .	82
21.	Hydrodynamic diameter of poly(4BCMU) in toluene as a function of temperature. . . . .	84
22.	Partial phase diagram for poly(3BCMU) in mixed solvents of CHCl <sub>3</sub> and n-hexane. . . . .	87
23.	Fraction of total intensity of visible absorption spectra associated with the red phase of poly(4BCMU) in mixed solvents of CHCl <sub>3</sub> and n-hexane as a function of temperature . . . . .	91
24.	Visible absorption spectra obtained for solutions of poly(3BCMU) in 43% CHCl <sub>3</sub> /57% CCl <sub>4</sub> and poly(3BCMU) in 60% CHCl <sub>3</sub> /40% CCl <sub>4</sub> . . . . .	94
25.	Partial phase diagram for poly(3BCMU) in mixed solvents of CHCl <sub>3</sub> and CCl <sub>4</sub> . . . . .	97
26.	Visible absorption spectra of poly(3BCMU)/15% CHCl <sub>3</sub> /85% CCl <sub>4</sub> obtained as a function of temperature . . . . .	102
27.	The absorbance of the 540 nm (red phase) peak observed for poly(4BCMU)/15% CHCl <sub>3</sub> /85% CCl <sub>4</sub> solution as a function of temperature . . . . .	105
28.	Visible absorption and Fourier transform infrared spectra of poly(3BCMU) in various mixtures of CHCl <sub>3</sub> and n-hexane. . . . .	111

29.	Infrared spectrum of a poly(4BCMU)/toluene gel.	123
30.	Comparison of infrared spectra in the NH stretching region for film, toluene gel, and o-DCB solution in the red phase . . . . .	125
31.	Comparison of infrared spectra in the NH stretching region for yellow film, yellow toluene solution, and yellow o-DCB solution . .	127
32.	Block diagram of polarization modulation experiment. . . . .	130
33.	Temperature dependence of integrated intensity of NH stretching vibrations and absorbance of the 540 nm peak for a poly(4BCMU)/toluene system. . . . .	134
34.	FTIR spectra (NH stretching region) of poly(4BCMU) in toluene. . . . .	136
35.	Temperature dependence of integrated intensity of NH stretching vibrations and absorbance of the 540 nm peak for a poly(4BCMU)/o-DCB solution. . . . .	141
36.	FTIR spectra (Amide I region) of poly(4BCMU) in toluene . . . . .	144
37.	Integrated intensity of the 1691 $\text{cm}^{-1}$ band as a function of temperature for a toluene system. .	146
38.	Temperature dependence of integrated intensity of NH stretching vibrations and absorbance of the 540 nm peak for a film. . . . .	148
39.	A typical distribution of Fourier frequencies in a detection signal of a polarization modulation experiment . . . . .	153
40.	Single beam spectrum and modulation spectrum for a 0.2% (w/v) gel of poly(4BCMU) in toluene at 4 $\text{cm}^{-1}$ resolution. . . . .	155
41.	FTIR spectra (carbonyl stretching region) for a 2% (w/v) solution of poly(4BCMU) in $\text{CHCl}_3$ during a cooling experiment . . . . .	159

42. FTIR spectra (carbonyl stretching region) for a 4% (w/v) solution of poly(4BCMU) in a mixed solvent of 65% CCl<sub>4</sub>/35% CHCl<sub>3</sub> during a cooling experiment. . . . . 161

## CHAPTER 1

### INTRODUCTION

#### 1.1 Vibrational Spectroscopy in Studies of Chain Structure and Conformation

There are a number of inherent advantages in using vibrational spectroscopy as a tool for studying conformational or structural changes in systems of polymer chains. Firstly, the technique is selective in that many of the absorption bands in infrared spectra are reflective of localized conformations or environments. For the same reason, vibrational spectroscopy can be used to simultaneously obtain information about all components in a polymer system. The differing components may exist within single chains as in the chemically differing hard and soft segmental units of polyurethanes, as morphologically differing regions in semicrystalline polyethylene, or as species composed of two or more components as in the case of the polystyrene/poly(vinyl methyl ether) blends studied in this work.

A second advantage of the vibrational spectroscopic technique is its capacity for orientation measurements. If polarized infrared radiation is sent to a molecular species, then that radiation is absorbed at those frequencies at which its electric field component is parallel to the normal vibrational modes of molecular species vibrating at the same fre-



quencies. In particular, if the molecular species is aligned, then differing degrees of absorption will occur depending upon the relative average orientations of the normal modes with respect to the direction of the incident polarized radiation. As outlined in Chapter 2, infrared dichroic measurements, in which absorption is measured both parallel and perpendicular to the direction of orientation in a sample, can be used to calculate second moment orientation functions. This method was used in this work to obtain orientation measurements in deformed miscible polymeric blends.

A third useful aspect of vibrational spectroscopy is its sensitivity to certain molecular interactions not involving covalently bonded species. Hydrogen bonding is one prime example; many vibrational spectroscopic studies of hydrogen bonding in polymers can be found in the literature (see, for example, references 1-3). In certain conformational studies of polymers the strengths of these interactions directly reflect large scale changes in polymer conformation as is true for polypeptides. Formation of helices from coils in polypeptides is induced by formation of hydrogen bonding within the chain backbones, and this can be easily observed with vibrational spectroscopic techniques. As will be seen in Chapter 4, polydiacetylenes containing hydrogen bonding substituents undergo similar dramatic conformational changes with accompanying formations or dissociations of intramolecu-

lar hydrogen bonding in solution. This system, along with miscible blends of polystyrene and poly(vinyl methyl ether), was chosen for this study to demonstrate the overall scope and utility of vibrational spectroscopy in conformational studies of polymers.

Miscible polymeric blends and polydiacetylenes are two very different systems which upon closer inspection share some common features. In both systems it has been found that dramatic changes in conformations of the polymeric chains can occur due to a subtle coupling with a particular type of molecular interaction. In blends, interactions responsible for miscibility between components have been shown to induce additional ordering during deformation of these materials (4). In polydiacetylenes, changes in the degree of  $\pi$ -electron delocalization of the conjugated molecular backbones result in dramatic conformational transitions of the molecules. These transitions, as will be shown, can be altered by changes in polymer-solvent interactions. Determining the particular mechanisms by which these molecular interactions induce conformational changes and the magnitudes of these changes are problems that can be investigated by the technique of vibrational spectroscopy. In the studies presented in this thesis vibrational spectroscopy is applied to the investigation of conformational changes in polydiacetylenes and a miscible polymeric blend.

## 1.2 Chain Structure Dynamics in Miscible Blends

In miscible blends of polystyrene (PS) and poly(vinyl methyl ether) (PVME) the intermolecular attractive forces necessary for miscibility induce by an unknown mechanism enhanced orientation of the polystyrene component during deformation (4). As well as quantifying the effects of these interactions upon chain conformations during deformation, vibrational spectroscopy has also been used to probe the source of the interactions themselves in PS/PVME blends (5). Miscibility induced perturbations of absorption bands associated with the ether group in PVME and the phenyl group in PS suggest interactions between these substituents to be the source of this compatibility.

The precise manner in which these interactions induce additional ordering of the PS component during blend deformation is still unknown. It is known, however, that the macromolecular nature of the PVME component is important to the induced ordering effect in PS since no such effect is observed for deformed blends of PS and low molecular weight ethers (6). The possibility then arises that the physical processes necessary for molecular chain entanglements, which greatly restrict the motions and numbers of possible conformations of polymeric chain segments, are coupled to some de-

gree with the attractive interactions between components of the miscible blend.

In order to investigate this hypothesis more thoroughly it is necessary to have a better understanding of the molecular mechanisms responsible for the creation and destruction of chain entanglement points and the effects on orientation and motions of chain segments in the blend. The first study presented in this thesis will show a possible approach of using vibrational spectroscopy to characterize segmental motion and orientation in PS/PVME blends.

Uniaxial step strains were applied to miscible blends of PS and PMVE and held. Subsequent decays in chain orientation of the two components were measured in the form of second moment orientation functions. Decays in stress were measured simultaneously with the optical measurements. Stress relaxation experiments of this type are known to separate modes of molecular response according to their respective time scales (7). It will be demonstrated how analysis of the experimental data obtained by this approach can be used to formulate a picture at the molecular level of the chain mechanisms responsible for the deformation behavior of the blends. These molecular descriptions will aid in understanding the effects of miscibility-favoring interactions upon this deformation behavior.

### 1.3 Chain Structure Transitions in Polydiacetylenes

Several polydiacetylenes display conformational changes that may be induced by changes in temperature or solvent composition (8-10). These conformational changes are believed to alter the extent of electronic delocalization within the conjugated backbones of these materials. Changes in the degree of conjugation give rise to visual color changes (chromic transitions) in polydiacetylenes (10,11).

The molecular interactions or mechanisms responsible for the conformational and chromic transitions are a subject of controversy. Proposed sources or driving forces for these transitions have included formation and dissociation of intramolecular hydrogen bonding in side groups of these molecules (10-14), entropic disordering of the side groups (15), and alterations in the strength of interactions of delocalized electrons in the conjugated backbone with polarizable solvent molecules or polarizable substituents on other polymer molecules (16,17).

Vibrational spectroscopy can be used to study the role of intramolecular hydrogen bonding between urethane side group substituents in the conformational and chromic transitions. As will be shown by one study presented in this thesis, large scale changes in intramolecular hydrogen bonding, as measured by vibrational spectroscopy, were seen to corre-

late very closely with large scale changes in conjugation for polydiacetylenes in solution. The changes in conjugation arise from an order-disorder transition in the chain backbones of these molecules with disordering occurring at high temperatures or within good quality solvents. In films of polydiacetylene it was observed in this study that the correlation between hydrogen bonding in sidegroups and changes in backbone structure does not occur. Thus, in films at least, the formation and dissociation of hydrogen bonding is ruled out as a potential driving force for the transition, whereas the possibility still remains for transitions in solution.

The observed correlation between hydrogen bonding and changes in backbone structure for polydiacetylenes in solution can be used to extend the applicability of vibrational spectroscopic techniques in studies of polydiacetylenes in solution. Experiments outlined in Chapter 4 of this thesis will demonstrate how vibrational spectroscopy can be used to characterize structure of polydiacetylenes in gels, possible effects of gelation on the chromic transition, and structures of polydiacetylenes in solutions at low temperatures in which it is found that the rod-like conformations of polydiacetylenes can still exist even in the presence of strongly hydrogen bonding, conformationally disrupting solvents.

The experiments delineated in Chapter 3 of this thesis serve as an introduction to the vibrational spectroscopic

studies of hydrogen bonding and conformational structure of polydiacetylenes related in Chapter 4. The former experiments concern intricate studies of the chromic transition in solvent systems differing from those commonly used in such studies. It was found that many of the conclusions derived from these experiments concerning the mechanism and kinetics of the chromic transition do not represent intrinsic properties of polydiacetylenes in solution but rather are highly dependent upon the particular solvent system used for the experiments.

## CHAPTER 2

### SPECTROSCOPIC STUDIES OF CHAIN RELAXATION MECHANISMS IN MISCIBLE BLENDS

#### 2.1 Introduction

Mechanical properties of miscible blends are generally more difficult to analyze than those of homopolymers. The mechanical response arises from various mechanisms of orientation and relaxation occurring at the molecular level. The understanding of these molecular processes can be further complicated by the presence of the strong interactions between components responsible for the compatibility of the blend. The relative rates of the orientation and relaxation mechanisms, as well as the relative degree to which these mechanisms are perturbed by attractive interactions, will in the general case depend upon the physical nature of the blend and the conditions under which it is deformed.

For blends of polystyrene (PS) and poly(vinyl methyl ether) (PVME), the system under consideration here, it has previously been shown that the response to deformation is strongly dependent upon blend composition, miscibility, strain rate, and temperature, particularly with respect to the glass transition (4,18). It has also been shown that for miscible blends containing polystyrene, the presence of the second interacting component induces greater orientation of



the polystyrene component than is found for homopolymeric polystyrene subjected to drawing at similar ranges of temperature above its respective glass transition temperature (4,19). This study then had the purposes of further quantifying the former results and providing a means for explaining the latter results in terms of the molecular mechanisms responsible for the enhanced orientation of polystyrene in these miscible blends.

In the earlier experiments of Lu et al. (18) the method of vibrational-mechanical spectroscopy was used to characterize the response of PS/PVME blends subjected to constant strain rates. Orientation measurements were obtained using polarized infrared spectroscopy, and measurements of stress and strain were recorded simultaneously. These results were evaluated in terms of a rubber network model.

For rubber networks the true stress (ratio of load to deformed cross-sectional area),  $\sigma_T$ , on the draw ratio of the sample as follows (20):

$$\sigma_T = C(\lambda^2 - 1/\lambda) \quad (1)$$

$C$  = modulus; a constant related to temperature, sample volume, and crosslink density of the material

$\lambda$  = draw ratio (ratio of deformed length to undeformed length)

Optical properties of a deformed rubber network have been derived as well by Stein (21), and Roe and Krigbaum (22). The second moment orientation function (discussed in detail in section II.3.2),  $F$ , for a uniaxially deformed sample is dependent upon the draw ratio as follows:

$$F \cong \frac{1}{5N} \left( \lambda^2 - \frac{1}{\lambda} \right) + \text{higher order terms} \quad (2)$$

where  $N$  is the number of Kuhn equivalent segments between crosslinks. (A Kuhn equivalent segment is comprised of that number of real chain segments, per monomeric unit, statistically equivalent to a segment of a freely jointed chain.)

For molecularly entangled amorphous polymers above their glass transition temperatures the chain entanglement points can be considered as transient crosslinks. Thus, unlike true rubbers, the modulus and number of Kuhn equivalent segments between junction points are time dependent parameters, i.e. dependent upon the deformation rate.

Lu et al. (18) used the rubber network approach to determine for miscible PS/PVME blends the stress moduli and numbers of Kuhn equivalent segments between entanglement points as functions of strain rate, blend composition, temperature, and molecular weights of components. Representative mechanical and optical data is shown in Figures 1 and 2. From the data in Figure 1 it was determined that the number of Kuhn equivalent segments between entanglements increases

Figure 1. Orientation function measured for PS in 50% PS/  
50% PVME blends as a function of strain rate;  
(  $\square$  ) strain rate: 6%/min; (  $\circ$  ) strain rate:  
2%/min.  
(from Lu et al., ref. 18).

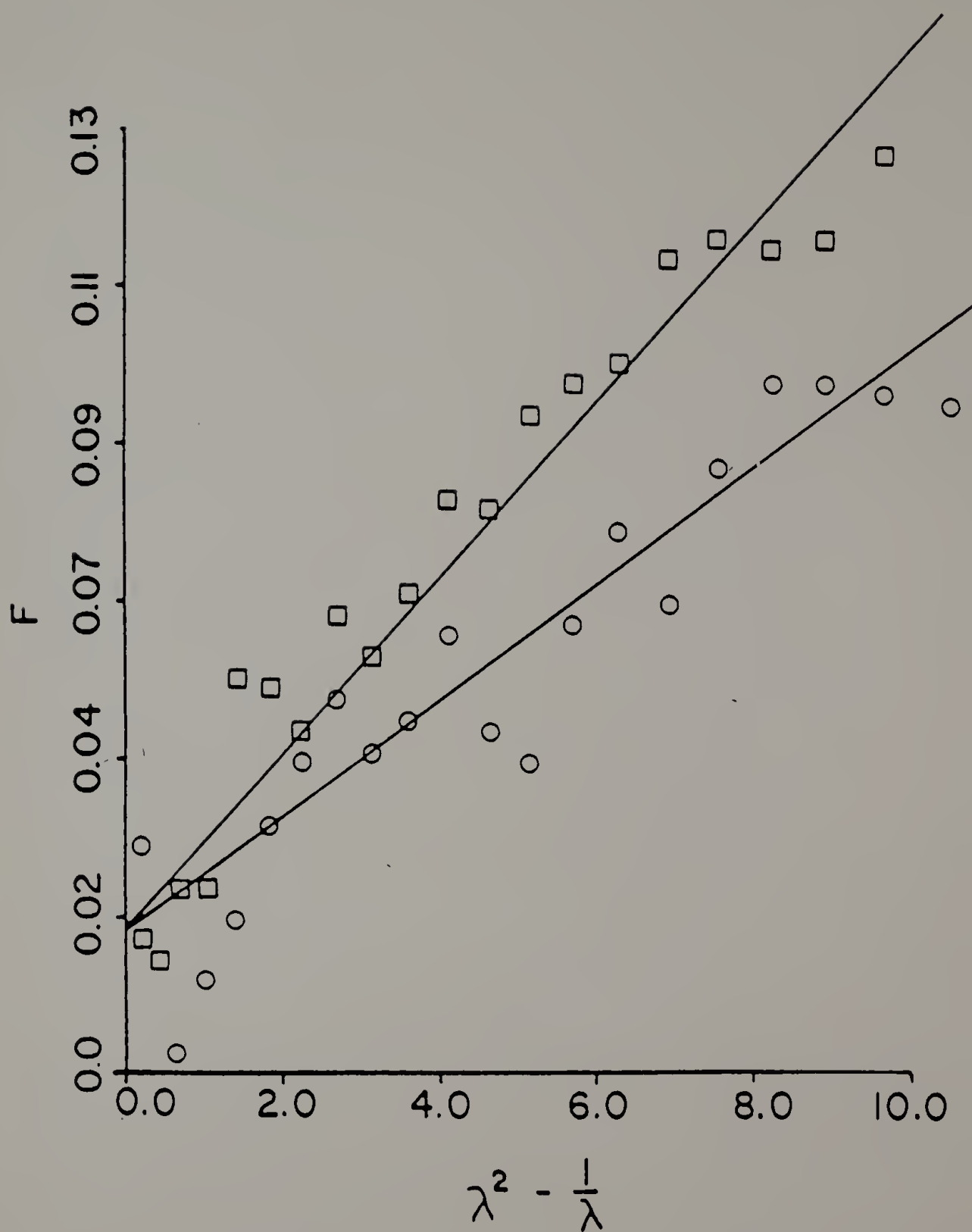


Figure 1.

Figure 2. Stress-strain behavior for 50% PS/50% PVME blends at different strain rates.  
(from Lu et al., ref. 18).

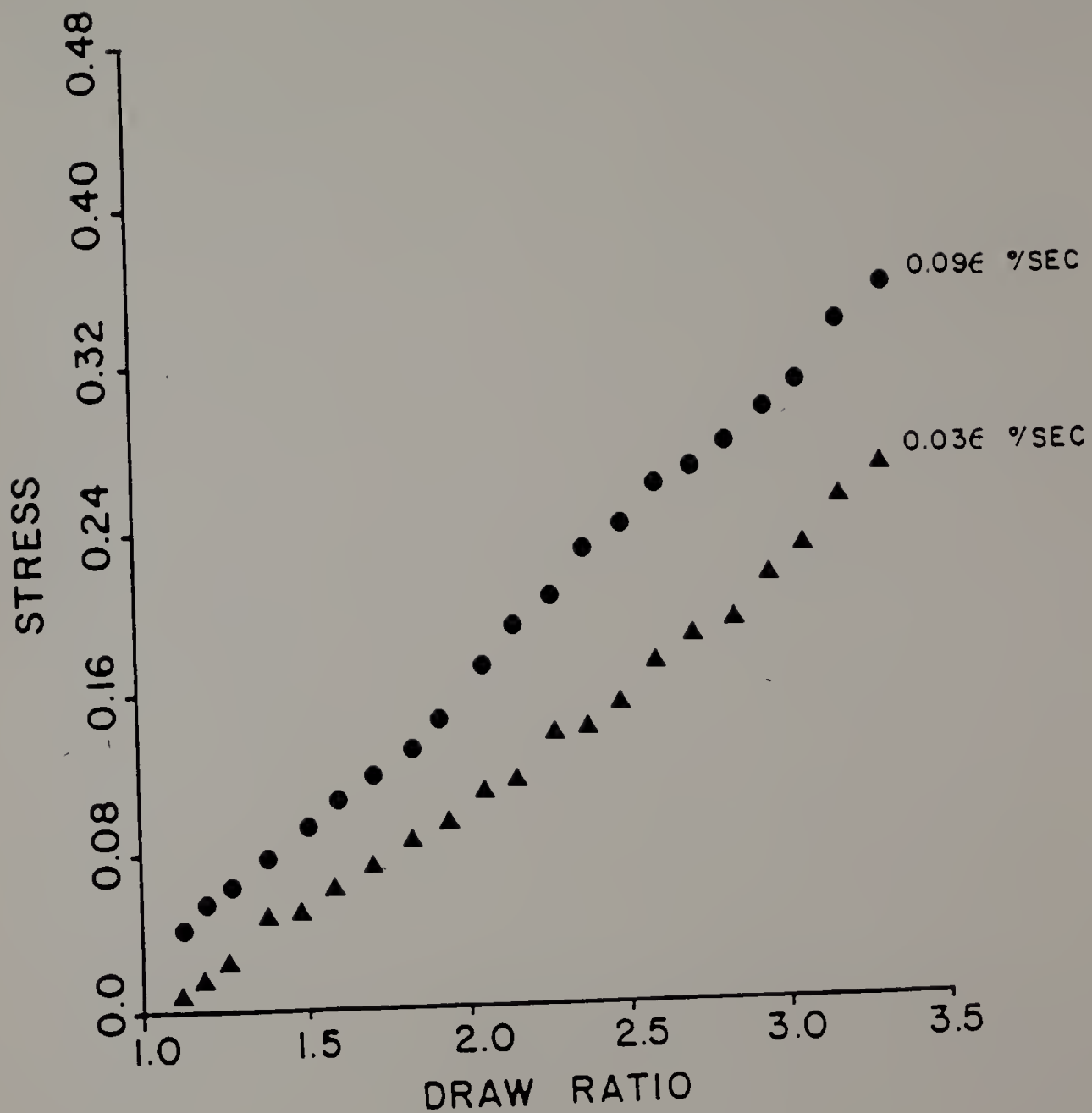


Figure 2.

from 23 to 35 when the strain rate is decreased by 67%. Their most important observation, however, was that the orientation function determined for a set draw ratio decreases linearly with temperature relative to the glass transition temperature.

In the experiments of Faivre et al. (4) miscible blends of PS and PVME were deformed under constant strain rates and under constant shear. As was found by Lu et al. (18), polarized infrared spectroscopy detected little or no orientation for the PVME component. However, it was determined that the presence of the PVME component enhanced orientation of the PS component when comparisons were made with studies of homopolymeric PS deformed at the same rate at similar temperatures with respect to the glass transition temperature (Figure 3). Interestingly, similar orientation enhancement of the PS component was also found in miscible blends of PS and poly(2,6-dimethyl 1,4-phenylene oxide) (19) but not in PS films plasticized with small molecules (tetraethylene glycol dimethyl ether, etc.) with chemical substituents similar to the ether side group in PVME (6) (Figure 4). Although, in the latter study, the interactions between PS and small molecular weight ethers would be similar to those found in miscible PS and PVME blends, the second interacting component must be macromolecular in nature to enhance orientation of the PS component under deformation. These results reinforce

Figure 3. PS orientation in PS-PVME blends at different compositions; PVME content: (1) ▲ , 0 %; (2) ● , 5%; (3) \* , 10 %; (4) ■ , 15%; (5) ○ , 20%; (6) ● , 25%; strain rate: 0.115 s<sup>-1</sup>; stretching temperatures:  $T = T_g + 11.5^\circ\text{C}$ . (from Faivre et al., ref. 4).



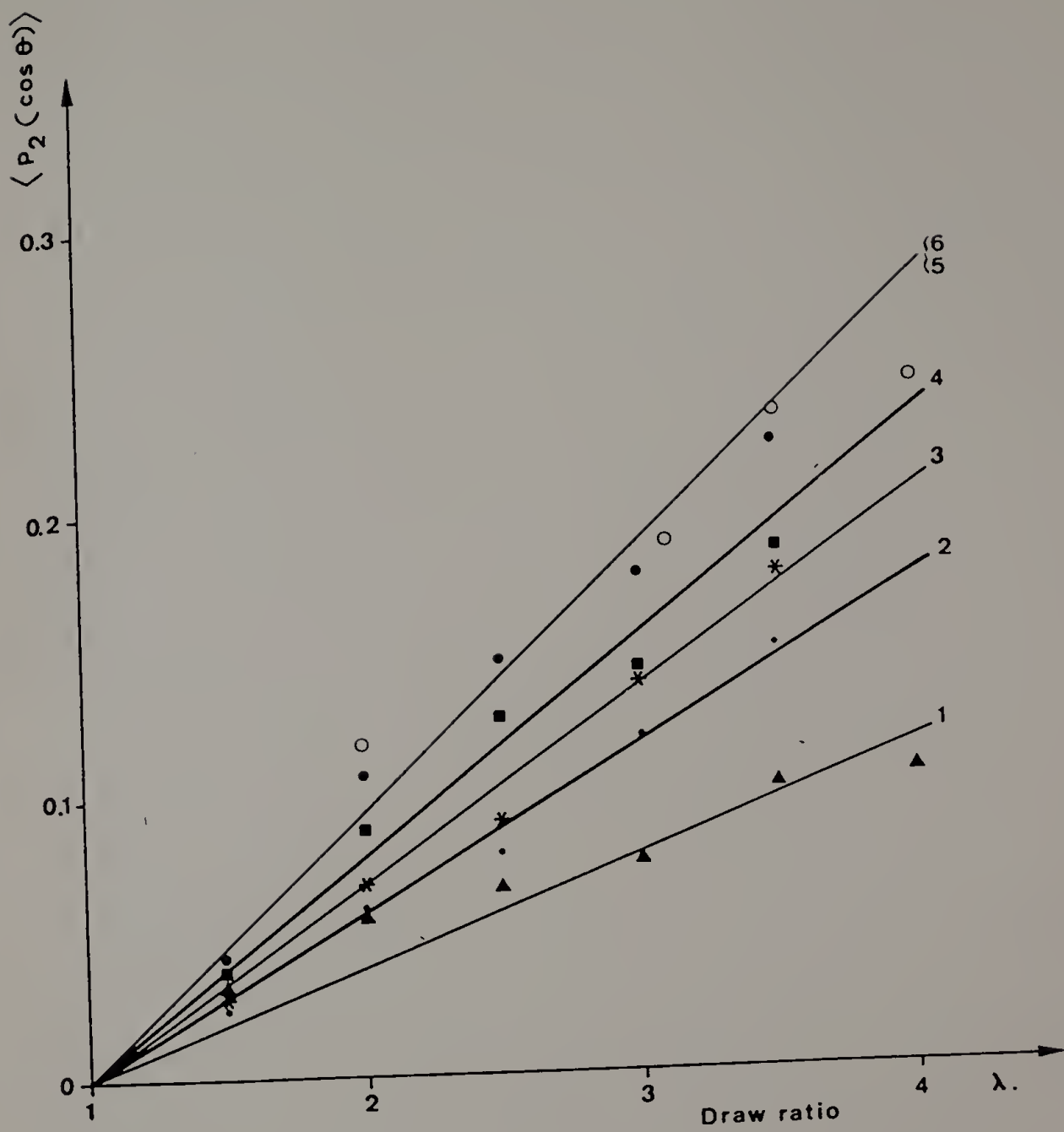


Figure 3.

Figure 4. Average orientation function  $\langle P_2(\cos\theta) \rangle$  of plasticized PS versus draw ratio  $\lambda$ ; strain rate:  $0.115 \text{ s}^{-1}$ ;  $T = T_g + 11.5^\circ\text{C}$ ; (1) unplasticized PS; (2) 95% PS/5% PVME blend; (3) 90% PS/10% PVME blend; plasticized PS; (  $\circ$  ) decaline; (  $\bullet$  ) triethylene glycol dimethyl ether; (  $\blacktriangle$  ) tetraethylene glycol dimethyl ether; (  $\square$  ) stearate of butyl 6%.  
(from Zhao et al., ref. 6).

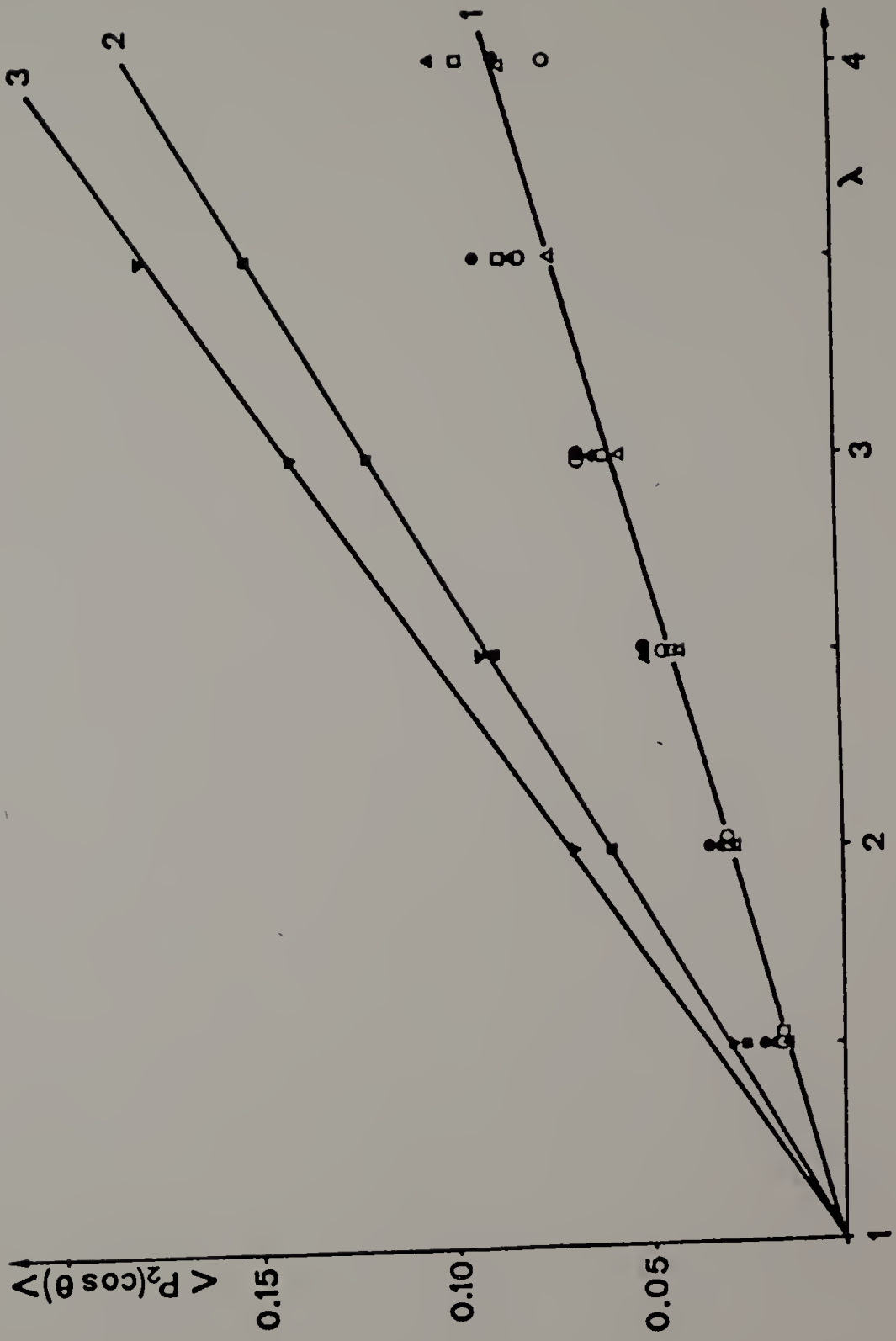


Figure 4.

the importance of molecular chain entanglements in the mechanical properties of these blends.

In both of the studies of Lu et al. and Faivre et al. it was not possible to quantitatively predict the effects of varying a molecular parameter (e.g. molecular weight) or varying an experimental parameter (e.g. temperature). Nor was it possible to formulate a picture at the molecular level concerning mechanisms for chain relaxation and how these mechanisms could conceivably be affected by molecular interactions between components. Amendments of these deficiencies served as the motivation for the study presented here.

The particular approach presented here consisted of application of uniaxial step strains to compatible blends of PS and PVME and measuring subsequent decays in chain orientation of components and stress. The same vibrational-mechanical spectroscopic method, mentioned previously, was employed. The inherent advantage of using stress and orientation relaxation experiments of this type is that modes of mechanical response are separated according to their respective time scales (Figure 5) (7).

These various chain relaxation mechanisms are best delineated by analyzing experimental results according to a molecular model describing segmental motions at the microstructural level. The Doi and Edwards (DE) model (23,24), in particular, predicts discrete mechanisms of relaxation for

Figure 5. Schematic of typical stress relaxation behavior of a noncross-linked, amorphous polymer.

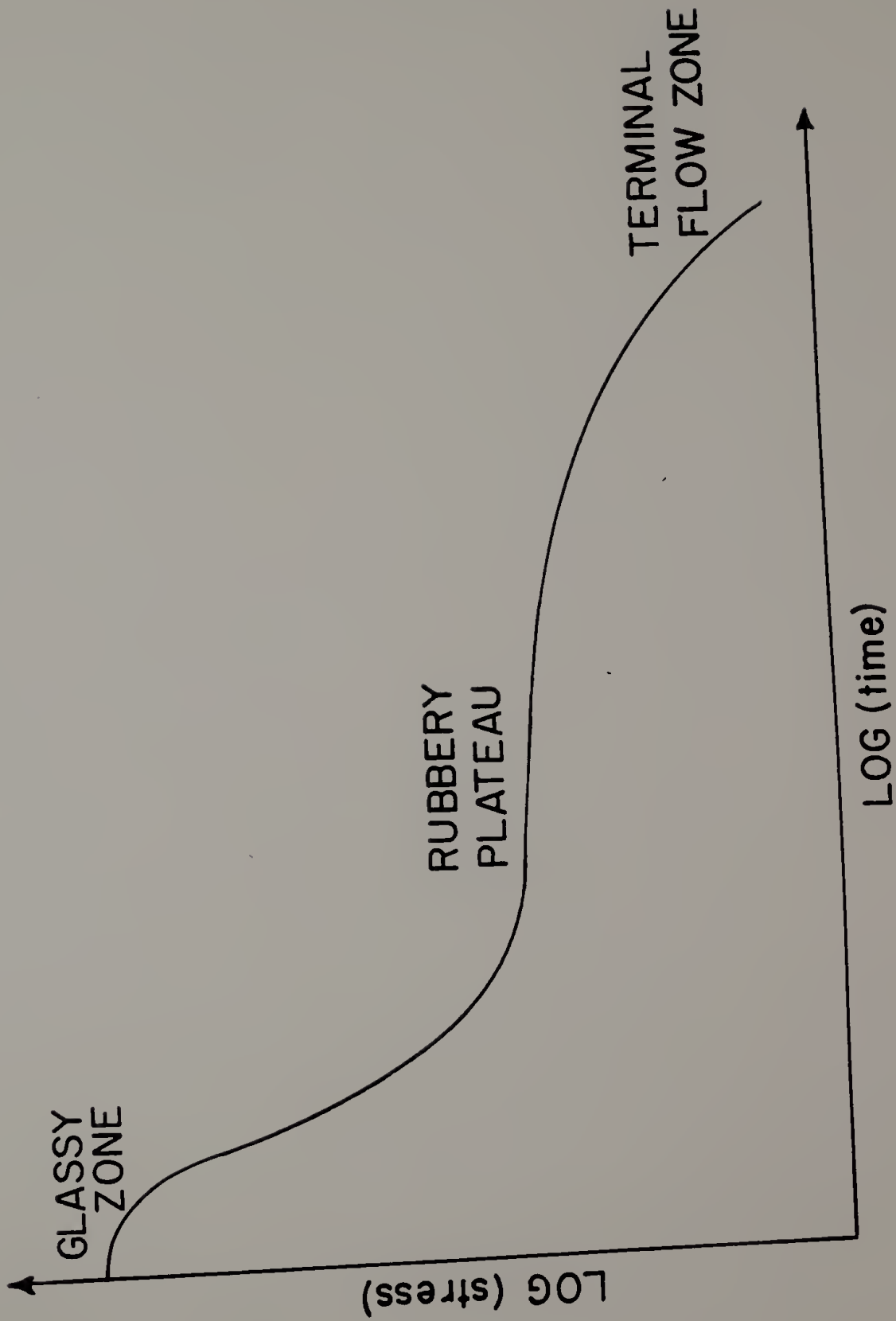


Figure 5.

strained polymer chains and incorporates the effects of molecular parameters such as friction coefficients or chain molecular weights. Incorporation of additional mechanisms for chain relaxation, as proposed by Viovy, Monnerie, and Tassin (VMT) (25), are also necessary due to the multicomponent nature of the system.

In the study presented here the experimental results proved to be inconclusive in answering many of the questions posed above. However, the particular experimental approach and means of analysis should prove with proper refinement to be of great value in future investigations of molecular mechanisms responsible for the deformation behavior of compatible polymeric blends. (26)

## 2.2 Experimental

Thin films of miscible blends of atactic polystyrene (PS) and poly(vinyl methyl ether) (PVME) were prepared. Monodisperse PS samples used in this experiment with molecular weight 233,000 ( $M_w/M_n=1.06$ ), 410,000 ( $M_w/M_n=1.06$ ) and 600,000 ( $M_w/M_n=1.10$ ) were obtained from Polysciences. PVME ( $M_w=98,000$  and  $M_n=46,500$ ) was obtained from Scientific Polymer Products, Inc. Mixtures of PS and PVME were prepared with PS content ranging from 30% to 40%. The solutions were dissolved in 5% (by weight) toluene solutions for 48 hours. The solutions were then cast onto clean glass plates, and

solvent was allowed to evaporate under ambient conditions for three hours. The films were subsequently vacuum dried at 70°C for 72 hours to remove all traces of toluene. Samples were then cut, carefully removed from the glass plates and then mounted on a special hydraulic stretcher (27) (Figure 6).

The stretcher, which was adapted to the optical bench of a Nicolet 7199 Fourier transform spectrometer, was interfaced to the Nicolet computer (27,28) (Figure 7). In this apparatus the polymer films were stretched between a pair of sample mounts directly coupled to a hydraulic piston. In these experiments the servocontroller was programmed so as to deliver a single stroke of the piston and hold so that the conditions of a stress relaxation experiment could be met. Load values were measured by a Data Instruments JP10 load cell attached directly to a fixed sample mount. The strain was measured by a Trans-Tek 243-000 linear DC to DC position gauge (LVDT). The analog outputs from the load cell and LVDT were digitized, sent to the Nicolet computer, and stored with their respective infrared data files. Thus, this apparatus allowed the simultaneous collection of both optical measurements in the form of infrared spectra and mechanical measurements of stress and strain.

The films of PS/PVME blends were subjected to step strains of 200% at room temperature and allowed to relax for



Figure 6. Schematic of the hydraulic stretcher.

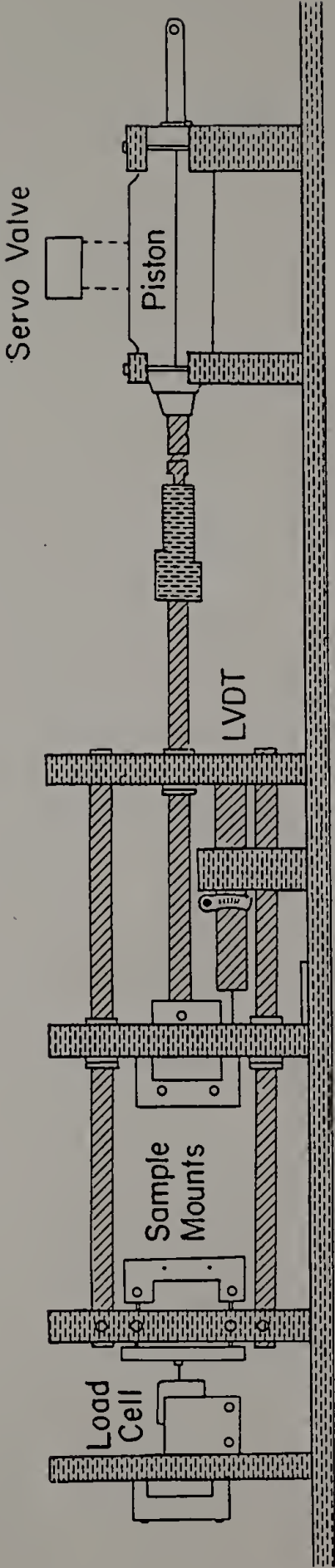


Figure 6.

Figure 7. Schematic diagram of the method by which mechanical data is relayed to the FTIR spectrometer.

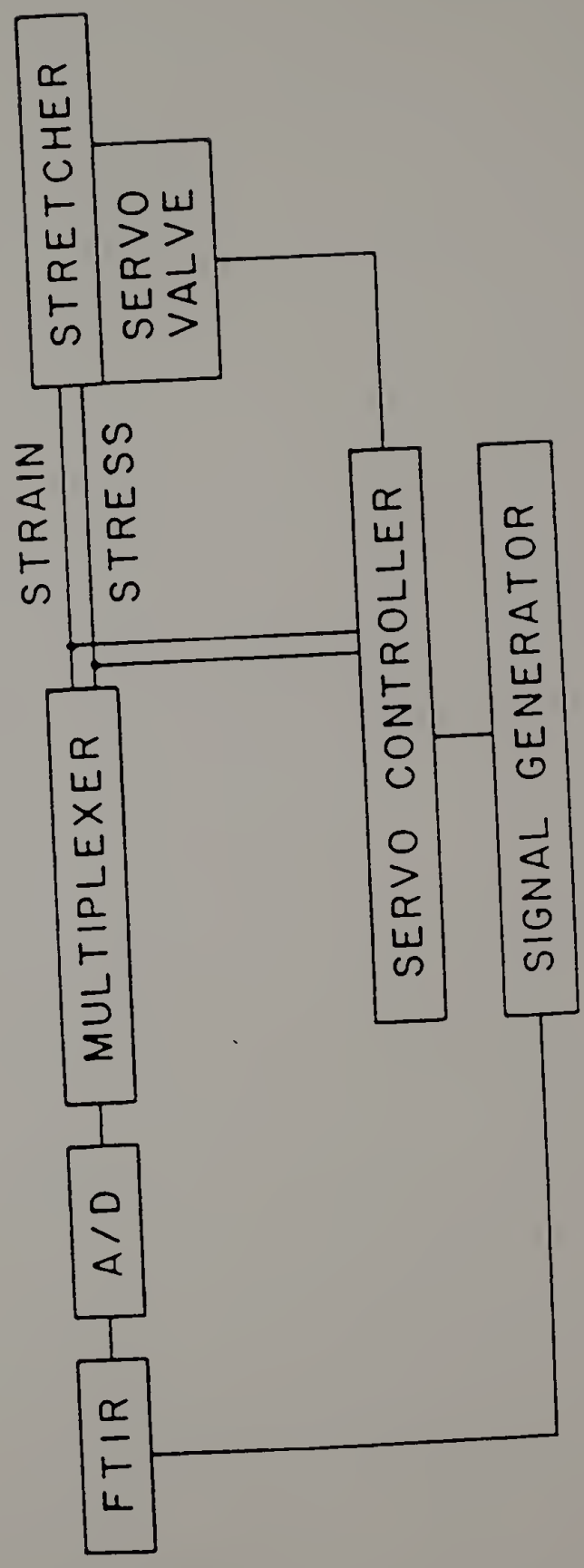


Figure 7.

times greater than  $2 \times 10^4$  seconds. Stress measurements were taken simultaneously with polarized infrared spectra collected at  $4 \text{ cm}^{-1}$  resolution. Shown in Figure 8 is a typical infrared spectrum for a compatible blend of 40% PS/60% PVME. The band at  $3026 \text{ cm}^{-1}$  (C-H stretch in the ring) was used to determine polystyrene segmental orientation. The C-H stretching vibration at  $2819 \text{ cm}^{-1}$  was used to calculate orientation of the PVME component. In all cases, absorptions did not exceed the limit denoted by Beer's law.

The spectra were collected in three stages. For the first three minutes following deformation, files of 15 coadded scans were taken sequentially for both parallel and perpendicular polarizations. The number of coadded scans was then increased to 50 for the next 25 minutes. Absorbances from sequential files for parallel polarization were averaged so that they would correspond to the same times at which perpendicular polarized spectra were collected. Files of 100 coadded scans were collected every 5 minutes for 5.5 hours thereafter.

The above scheme for collection was used to optimize the required time resolution with respect to signal resolution. As will be seen, the first relaxation for PS/PVME blends in our experiments occurs over a period of approximately 200 seconds. This necessitates collection of a large number of files at relatively short times to quantitatively character

Figure 8. Infrared spectrum obtained for a 50% PS/50% PVME miscible blend; 2  $\text{cm}^{-1}$  resolution.

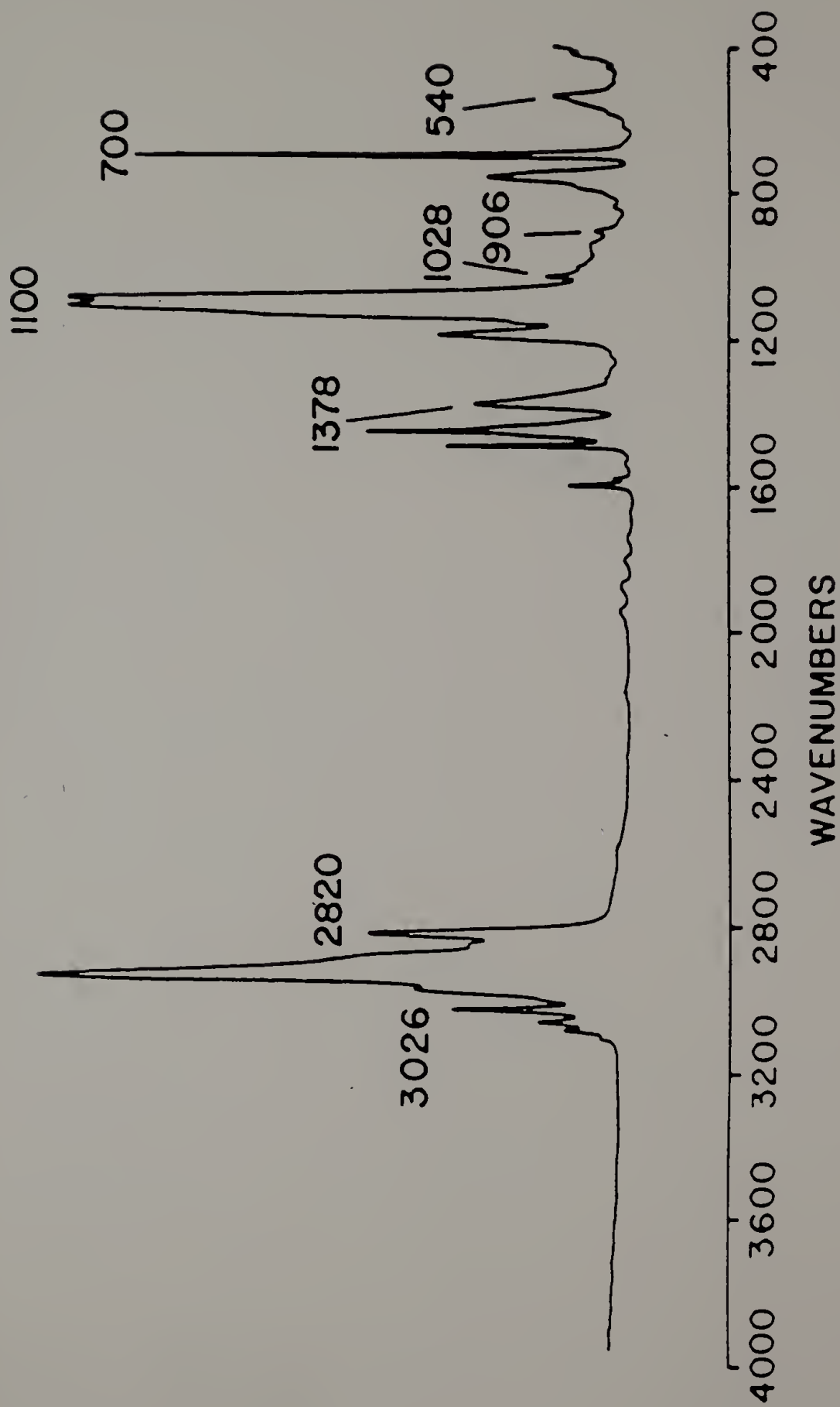


Figure 8.

ize this relaxation period. However, the signal-to-noise ratio of the obtained spectra increases as the square of the number of coadded scans. Therefore, the number of scans at short times represents a compromise between the required time and signal resolutions. This accounts for the appreciably greater scatter of data points at short times as seen in Figure 9. For the longer term relaxations, changes in the measured orientation function proceed more slowly. Thus, the number of scans per file can be increased so as to achieve a greater signal-to-noise ratio. However, there is somewhat greater uncertainty in the measured dichroic ratio as the strained sample disorients. This is due to the fact that the integrated intensities for parallel and perpendicular absorbances approach one another and their ratio is prone to greater fluctuations.

### 2.3 Results and Discussion

As was stated previously, the molecular chain motions responsible for the macroscopic deformation behavior of compatible blends can become very complicated, much more so than would be the case for homopolymers. Understanding of these complex motions and speculation on the effects of attractive interactions between blend components requires application of a molecular model. While scatter in the experimental results makes the conclusions drawn by application of this model un



Figure 9. Relaxation of orientation function of PS component ( $M_n = 410,000$ ) in 40% PS/60% PVME blend.

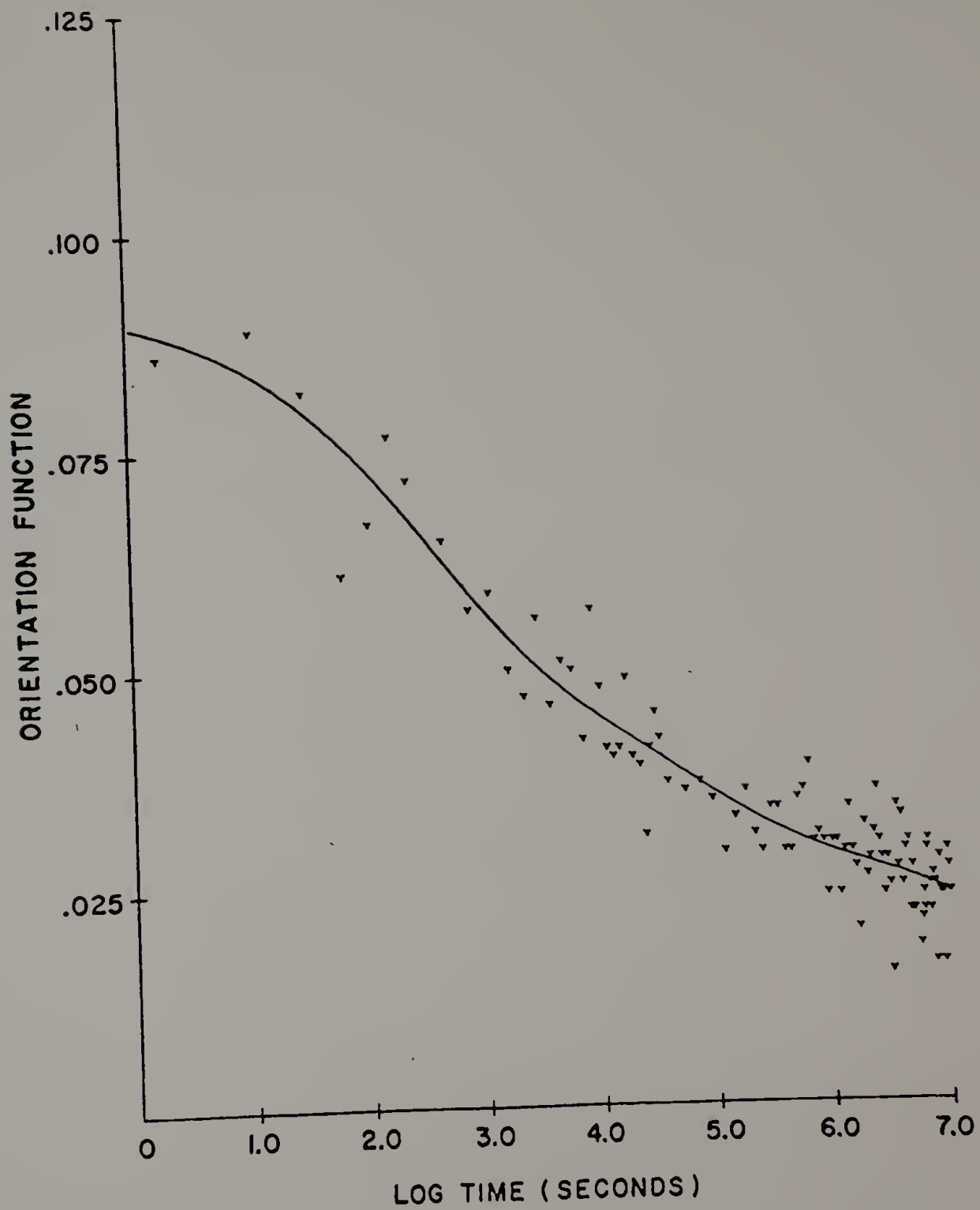


Figure 9.

certain, the particular approach taken to understand molecular motions in deformed blends will nonetheless be seen as both valid and important.

### 2.3.1 Molecular Model

The Doi-Edwards (DE) theory (23,24) of deformation proposes three distinct relaxation mechanisms for a strained polymer chain (Figure 10). The first mechanism consists of a rapid re-equilibration of chain segments between entanglement points. The second is retraction of the chain within the tube defined by chain entanglements points. The third mechanism has the longest time constant, consisting of tube renewal arising from reptative motions of the chain.

The three relaxations have respective characteristic times of (23)

$$T_A = \frac{\zeta b^2 N_e^2}{6\pi^2 kT} \quad (\text{local re-equilibration}) \quad (3)$$

$$T_B = \frac{\zeta b^2 N_0^2}{3\pi^2 kT} \quad (\text{retraction}) \quad (4)$$

$$T_C = \frac{\zeta b^2 N_0^3}{\pi^2 kT N_e} \quad (\text{reptation}) \quad (5)$$

where  $\zeta$  = monomeric friction coefficient

Figure 10. Different relaxation stages for a primitive chain after a step uniaxial stretch; chain entanglement points are represented by small circles; (a) initial isotropic state; (b) step-strained primitive chain at time  $0+$ ; (c) primitive chain at end of self-retraction; (d) primitive chain during reptation; (e) primitive chain after complete disengagement (isotropic state). (Primitive chain defined as a hypothetical chain of straight segments between chain entanglement points). (from Viovy et al., ref. 25).

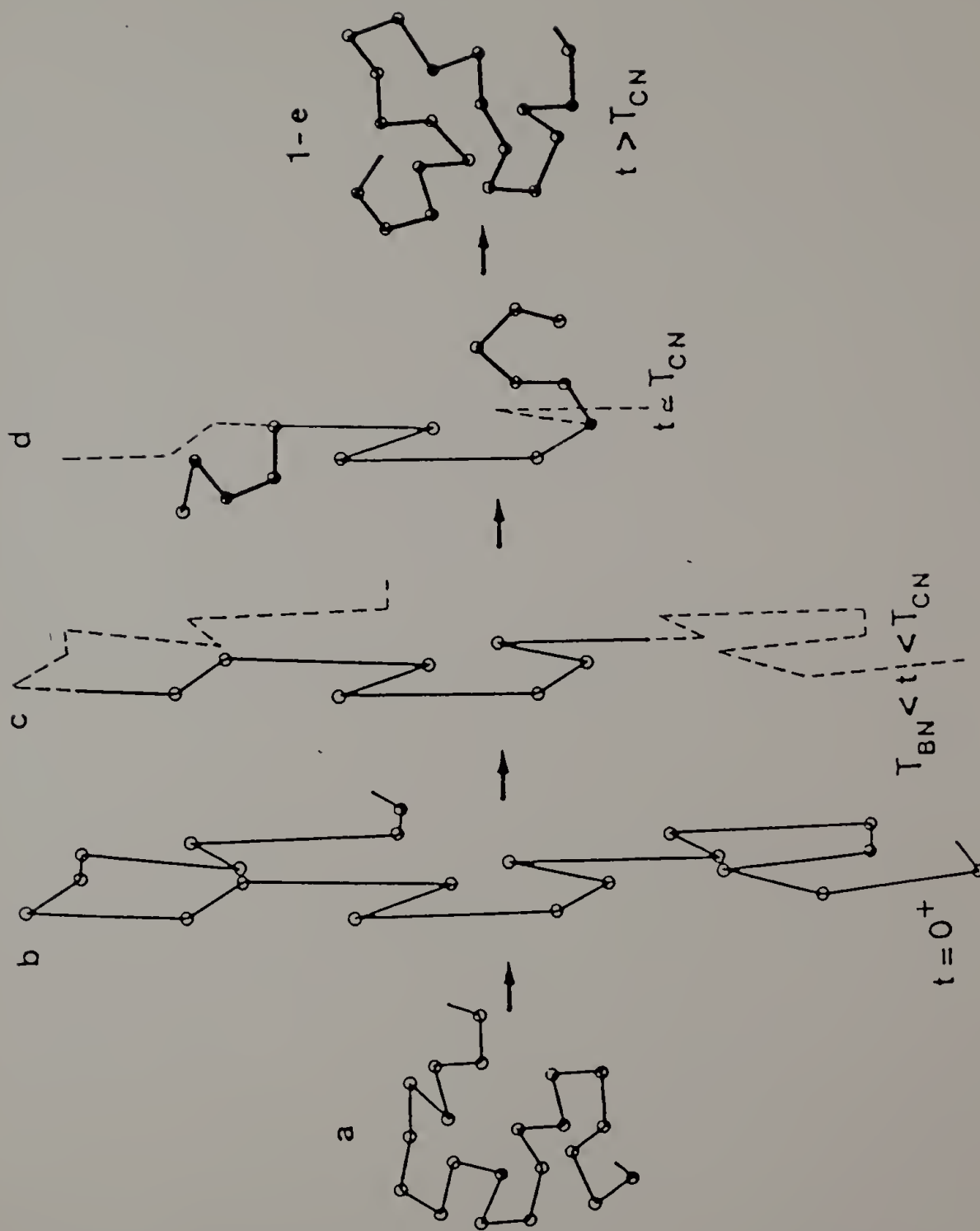


Figure 10.

$b$  = Kuhn equivalent bond length

$N_e$  = number of Kuhn equivalent bonds between entanglements

$N_0$  = number of Kuhn equivalent bonds in chain, and

$T$  = absolute temperature.

The inverse temperature proportionality and chain length dependence are particularly important. For polymer chains of high molecular weight, the three relaxation times should differ from one another by an order of magnitude or more. The first relaxation, local re-equilibration, is very rapid and should show no net orientation change. Viovy, Monnerie, and Tassin (VMT) (25) have proposed a revision of the DE theory which incorporates a fourth distinct relaxation mechanism (Figure 11). As postulated in this theory, entanglement points forming the constraining tube of a chain relax and allow the chain to make localized jumps which decrease its path length. This mechanism, tube relaxation, competes with chain retraction and has its own characteristic time of  $T_B'$ .

Molecular motions of polymeric chains in blends are even more complicated. For miscible blends of stiff PS chains of high molecular weight and flexible PVME chains of relatively low molecular weight, one would expect a greater number of available relaxation mechanisms. For example, reductions in path length for a PS chain may arise from renewal of tube constraints by both retraction and reptation of PVME chains

Figure 11. Modification of path of primitive chain due to retraction of constraining chains: (a) isotropic initial state; (b) step-strained primitive chain; (c) path of primitive chain after retraction of neighboring chains, showing tube relaxation (local loosening) due to random loss of chain entanglement points.

(from Viovy et al, ref. 25).

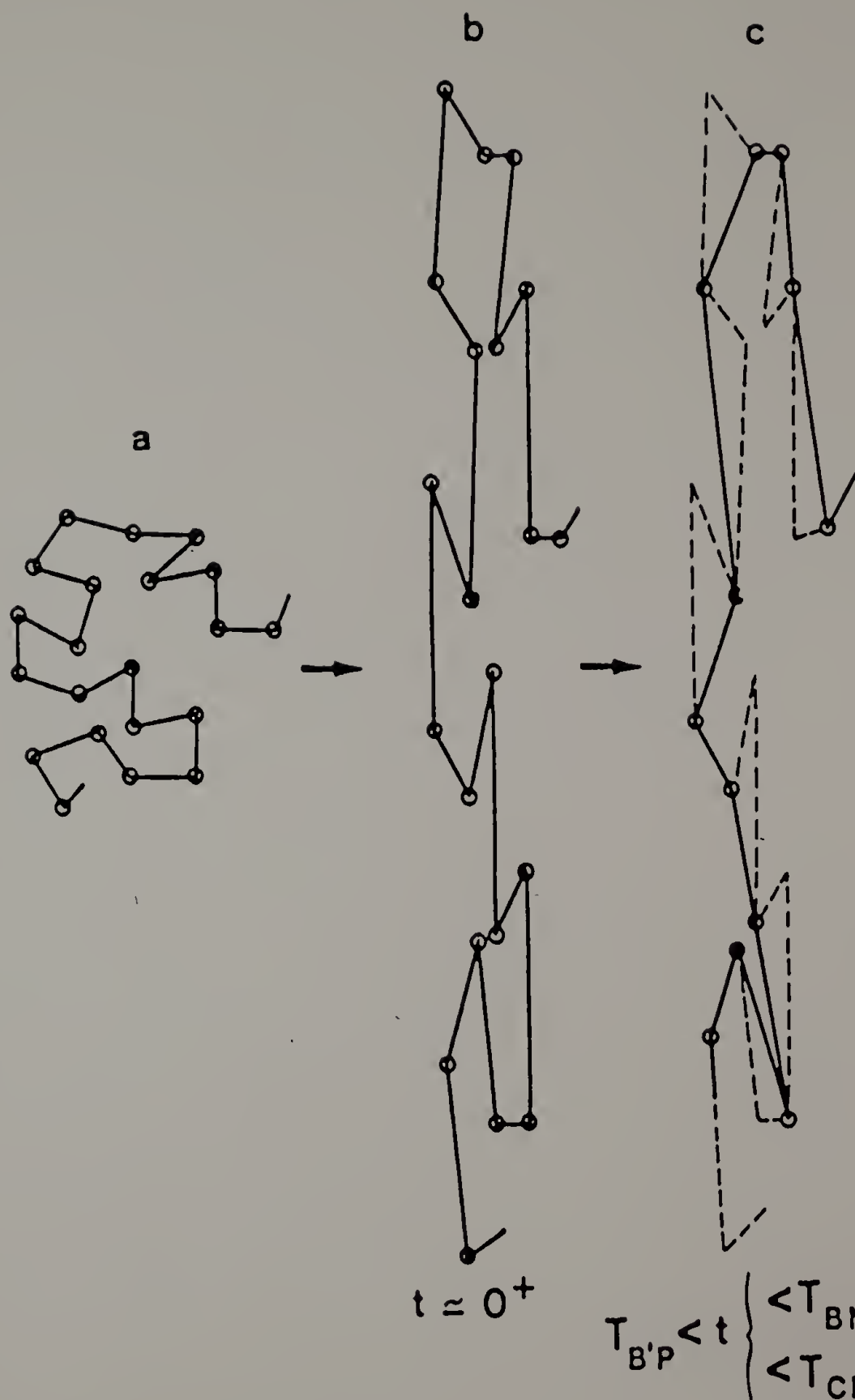


Figure 11.



and by retraction of the PS chain itself. The rapidity, or time scale, of each type of motion, as well as the frequency of occurrence of each type of motion will determine the overall stress and orientation relaxation spectra. Herein lies the inherent advantage of step strain-relaxation experiments over other rheological experiments: different types of molecular motion are more easily separated.

In miscible blends there is also the additional complication of attractive interactions between components. As was stated earlier, the presence of PVME has been shown to induce an enhancement in the orientation of the PS component during deformation of these blends. In terms of the DE and VMT models the chain relaxation time constants for PS are increased over their respective values for homopolymeric PS. This increase must largely arise from increases in the value of the monomeric friction (equations 3-5) coefficient of PS in the presence of PVME.

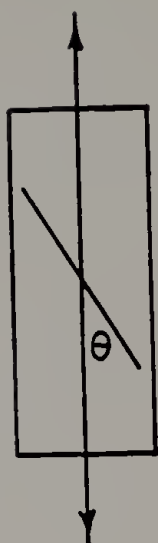
### 2.3.2 Orientation Function

The objective of these experiments was to measure the time dependence of the second moment orientation function for both components of the blend and to interpret these measurements in terms of the previously described molecular model. The second moment orientation function (Figure 12) describes

Figure 12. Definitions of dichroic ratio and second moment orientation function.

$$D = A_{\parallel} / A_{\perp}$$

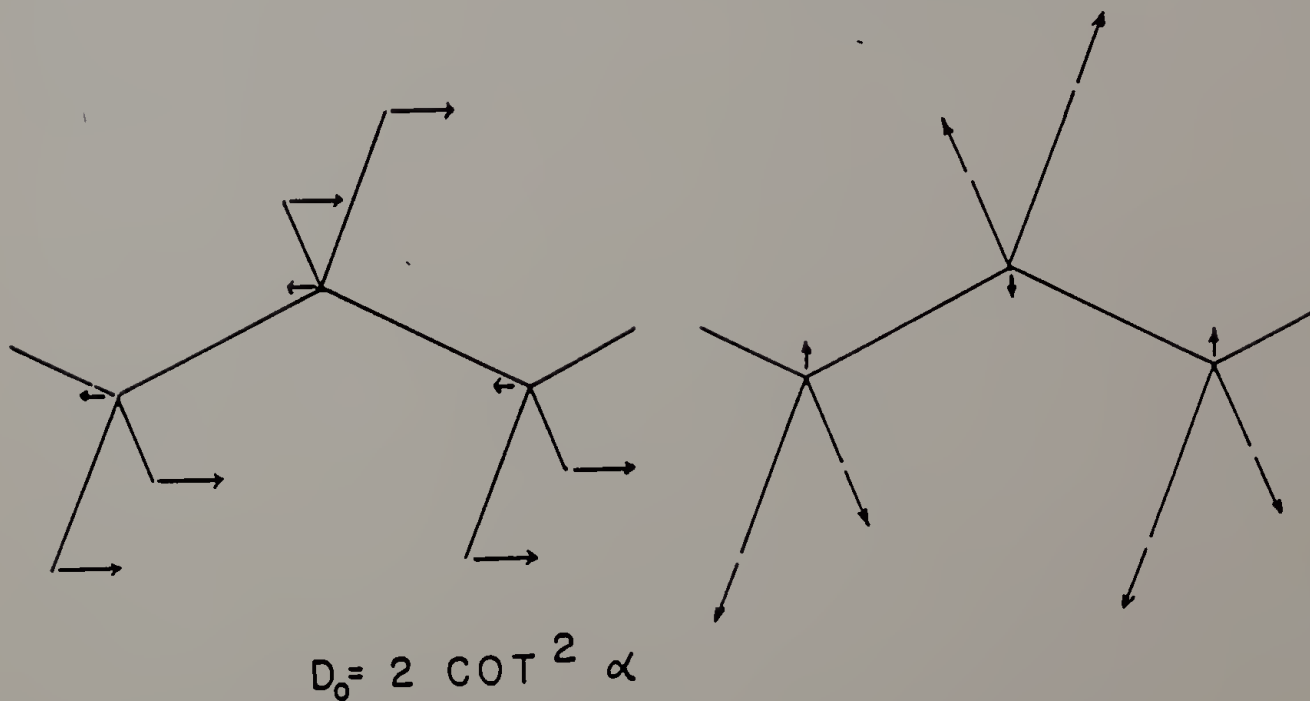
DICHROIC RATIO



ORIENTATION  
FUNCTION

$$F = \frac{3 \overline{\cos^2 \theta} - 1}{2}$$

$$F = \frac{D-1}{D+2} \frac{(D_0 + 2)}{(D_0 - 1)}$$



$$D_0 = 2 \cot^2 \alpha$$

Figure 12.

the extent of chain segment alignment at the microstructural level and serves as a parameter to follow segmental motion in dynamic experiments. It is defined for uniaxially oriented systems as:

$$F = \frac{1}{2} \left( 3 \overline{\cos^2 \theta} - 1 \right) \quad (6)$$

where  $\theta$  is the angle between the chain axis and the direction of stretching and where  $\overline{\cos^2 \theta}$  represents the spatial average quantity of  $(\cos^2 \theta)$ .

Infrared dichroism is a means for determining the orientation function for specific components in a multicomponent polymer system. For any absorption band the dichroic ratio,  $D$ , is defined as

$$D = \frac{A_{||}}{A_{\perp}} \quad (7)$$

where  $A_{||}$  and  $A_{\perp}$  represent, respectively, the absorbances of radiation polarized parallel and perpendicular to the direction of stretching.

The dichroic ratio and orientation function have the relationship given by

$$F = \frac{D-1}{D+2} \cdot \frac{D_0+2}{D_0-1} \quad (8)$$

and

$$D_0 = 2 \cot^2 \alpha \quad (9)$$

The right-hand fraction of Equation (8) corrects for the angular difference  $\alpha$  between the directions of the chain axis and the absorbing transition moment. The transition moment for the C-H stretch (in the ring) at  $3026 \text{ cm}^{-1}$ , used to follow PS orientation, was determined to be  $37^\circ$  from the chain axis. This value was found by applying previous data on constant strain rate deformation of PS/PVME blends to the method of Samuels (29) using known transition moments of other PS bands. For PVME its C-H stretching vibration at  $2819 \text{ cm}^{-1}$  was assumed to have a transition moment  $90^\circ$  to the chain axis.

### 2.3.3 Data Analysis

For the data on the relaxation of the second moment orientation function of PS chains after application of step-strains to various PS/PMVE blends, three relaxation times, in general, were found to be sufficient for fitting the data to the VMT theory. Least square fits were attempted for two equations (25).

$$F_{PS}(t) = F_{PS}(0^+) \alpha^{-2} g(t/T_B', PVME) [h(t/T_C', PVME)]^2 f(t/T_C, PS) \quad (10)$$

$$F_{PS}(t) = F_{PS}(0^+) \alpha^{-2} g(t/T_B', PVME) [k(t/T_B, PS)]^2 f(t/T_C, PS) \quad (11)$$

where  $F_{PS}$  = uniaxial orientation function for PS

$F_{PS}(0^+)$  = uniaxial orientation function for PS

immediately following deformation and local

re-equilibration

$\alpha$  = average orientation of bonds following deformation

$$g(t/T) = 1 + [\alpha - 1] \exp(-t/T)$$

$$h(t/T) = 1 + [\alpha^{1/2} - 1] f(t/T)$$

$$f(t/T) = \sum_{j \text{ odd}=1}^N (8/j\pi^2) \exp(-j^2 t/T) \simeq \exp(-t/T)$$

$$k(t/T) = 1 + [\alpha^{1/2} - 1] \exp(-t/T)$$

$T_{B,PS}$  = chain retraction time constant for PS

$T_{C,PS}$  = chain reptation time constant for PS

$T_{B',PVME}$  = PS tube relaxation time constant due to PVME retraction

$T_{C',PVME}$  = PS tube relaxation time constant due to PVME reptation

Equation 10 assumes that  $T_{C',PVME} \ll T_{B,PS}$  while equation 11 assumes  $T_{B,PS} \ll T_{C',PVME}$ . Generally the approximate expression given for  $f(t/T)$  will be equivalent within experimental error to its exact expression. This has the effect of making the functional forms of Equations 10 and 11 identical. Varying the molecular weight of the PS component should show whether the bulk of the second relaxation mechanism is due to PS retraction or PVME reptation. The long term relaxation to an isotropic state of the PS chain should, as usual, depend

upon its reptation time, although, as pointed out previously (30,31), the process of tube renewal will contribute to the long-term relaxation.

Shown in Figure 9 is the measured decay in orientation for polystyrene of molecular weight 600,000 in a 40% PS/60% PVME blend. A smooth line representing a least-squares fit for three relaxation times from the VMT model and an extrapolated initial orientation function is shown superimposed on experimental data points. Multiple zones of chain relaxation, with their associated relaxation times, are apparent in the data. Because these relaxation times differ from one another by at least an order of magnitude, each relaxation time can be fit to the data almost independently of the other two.

Least-squares fits to the VMT model from experimental data are shown in Figure 13. The molecular weight of the PS content was varied, keeping the overall PS/PVME composition constant. As expected, initial orientation of the PS component increases and relative decay rates of orientation are slowed for high molecular weights of PS. It is also readily apparent that discrete zones of relaxation exist, and that they are indeed separable to a degree.

Similar results were obtained when the relative composition of the blend was changed, as shown in Figure 14. Slower rates of orientation decay and higher initial orientation of

Figure 13. Relaxation of orientation function of PS components of varying molecular weight in 40% PS/60% PVME blends; (X)  $M_n = 233,000$ , (Y)  $M_n = 410,000$ , (+)  $M_n = 600,000$ .



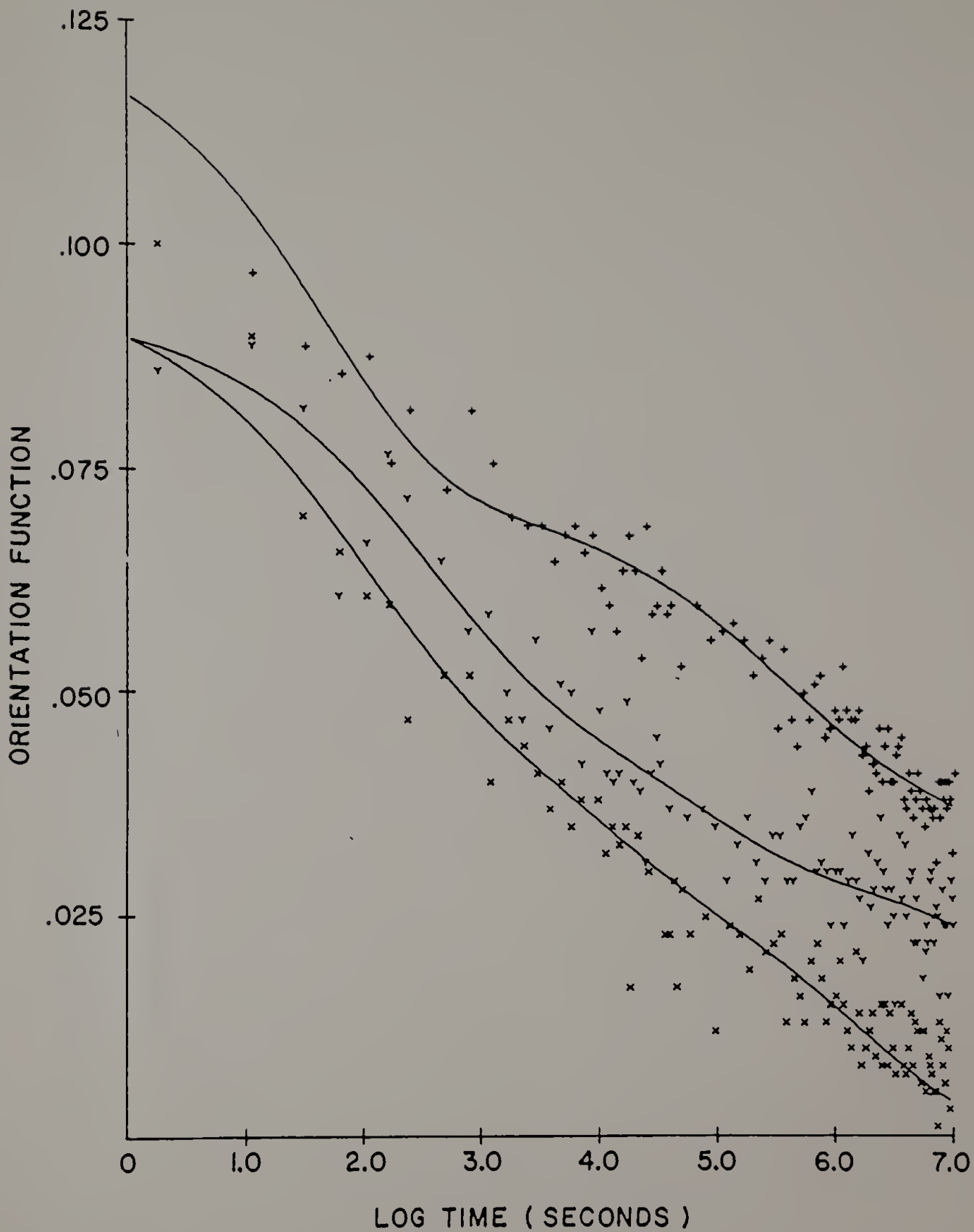


Figure 13.

Figure 14. Relaxation of orientation function of PS components ( $M_n = 600,000$ ) in PS/PVME blends of varying composition; (X) 30% PS/70% PVME blend, (+) 40% PS/60% PVME blend.

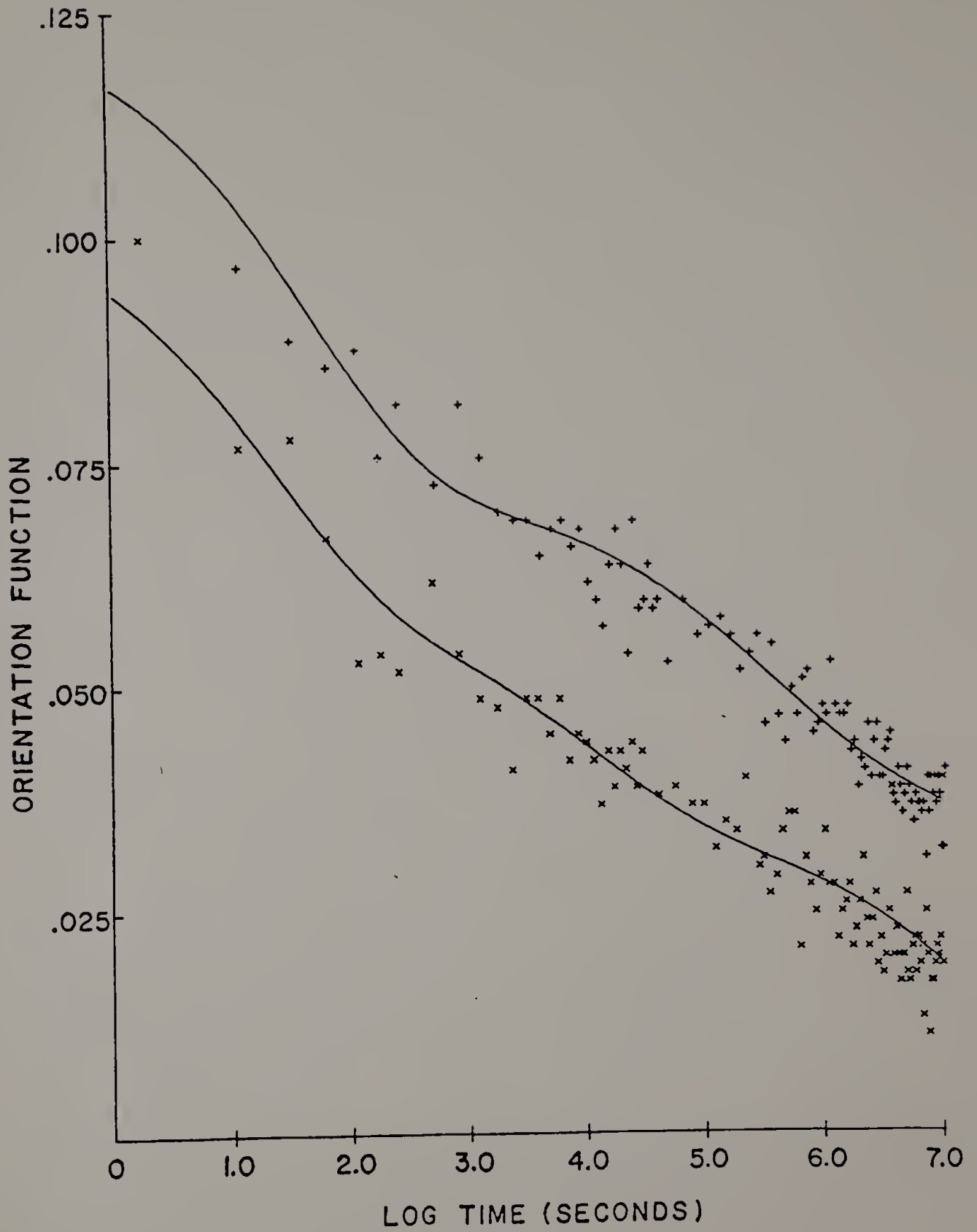


Figure 14.

PS occurs as the PS content is increased in the blend. Quantitative results are given in Table 1 for both sets of data. The calculated initial orientation function for PS  $[F(O^+)]$  as well as the three relaxation times for PS relaxation are given. As previously mentioned,  $T_{B',PVME}$ ,  $T_{B,PS}$ , and  $T_{C,PS}$  correspond to PS tube relaxation due to PVME retraction, PS retraction, and PS reptation, respectively. The second relaxation has been labeled as such due to its large variation with the molecular weight of the PS component. Reptation of PVME segments should also contribute to this relaxation domain, although the extent of its contribution is uncertain. Values of  $T_{C,PS}/T_{B,PS}$  are also shown in Table 1. If the experimental systems strictly conformed to the Doi-Edwards model, then  $T_{C,PS}/T_{B,PS}$  would in all cases be equal to  $3N/M_{eq}$  where  $N$  is the number of Kuhn equivalent bonds in the PS chain and  $M_{eq}$  is the number of Kuhn equivalent bonds between entanglement points. If  $M_{eq}$  remains constant, as predicted by scaling and mean field theories (23), then  $T_{C,PS}/T_{B,PS}$  should roughly be proportional to the PS molecular weight. This trend is not apparent in the data due mostly to the large scatter in the experimental data, especially at the earliest times of the deformation experiments. Deviation from the Doi-Edwards model might be expected anyway due to polydispersity effects (25).

Table 1

Calculated relaxation times for second moment orientation function of PS during stress relaxation experiments.

EFFECT OF MOLECULAR WEIGHT/40% PS  
(relaxation times given in seconds)

	$F(0^+)$	$T_{B',PVME}$	$T_{B,PS}$	$T_{C,PS}$
233,000	.096	136	969	9,880
410,000	.089	259	2000	61,000
600,000	.126	104	5080	147,000

EFFECT OF COMPOSITION/600,000 MW PS

	$F(0^+)$	$T_{B',PVME}$	$T_{B,PS}$	$T_{C,PS}$
30% PS	.1054	74.2	1170	34,100
40% PS	.1260	104	5080	147,000

Figures 15 and 16 show the molecular weight dependence and composition dependence for stress relaxation of PS/PVME blends. There are no perceptibly discrete relaxation domains as was the case for the orientation measurements. This demonstrates the sensitivity and selectivity of infrared dichroism in studying mechanical behavior of complex systems. Motions of chain segments of one component and their relative contributions to mechanical properties may only be discernible from orientation measurements.

It must also be pointed out that the experimental values of  $T_{C,PS}$  are probably somewhat larger than their actual values due to slight temperature rises ( $\sim 4^\circ$ ) occurring in the stretching apparatus. This is borne out by the rising tail of the stress measured at long times. The rubber-like elasticity of the blends also manifests itself when the samples are removed from the stretcher and allowed to relax in the unstressed state. Typical strain recoveries were 80% of the elongation length or more.

In accord with previous results, no substantial orientation occurred for PVME (4,18). Orientation function measurements for the PVME component did not exceed .03 and showed even greater scatter than did the measurements for PS. It has been suggested that stress response of these blends depends only on the PS component (18). However, the contribution of PVME segments to PS relaxation, in the form of the

Figure 15. Relaxation of stress in 40% PS/60% PVME blends with varying molecular weight of PS component.

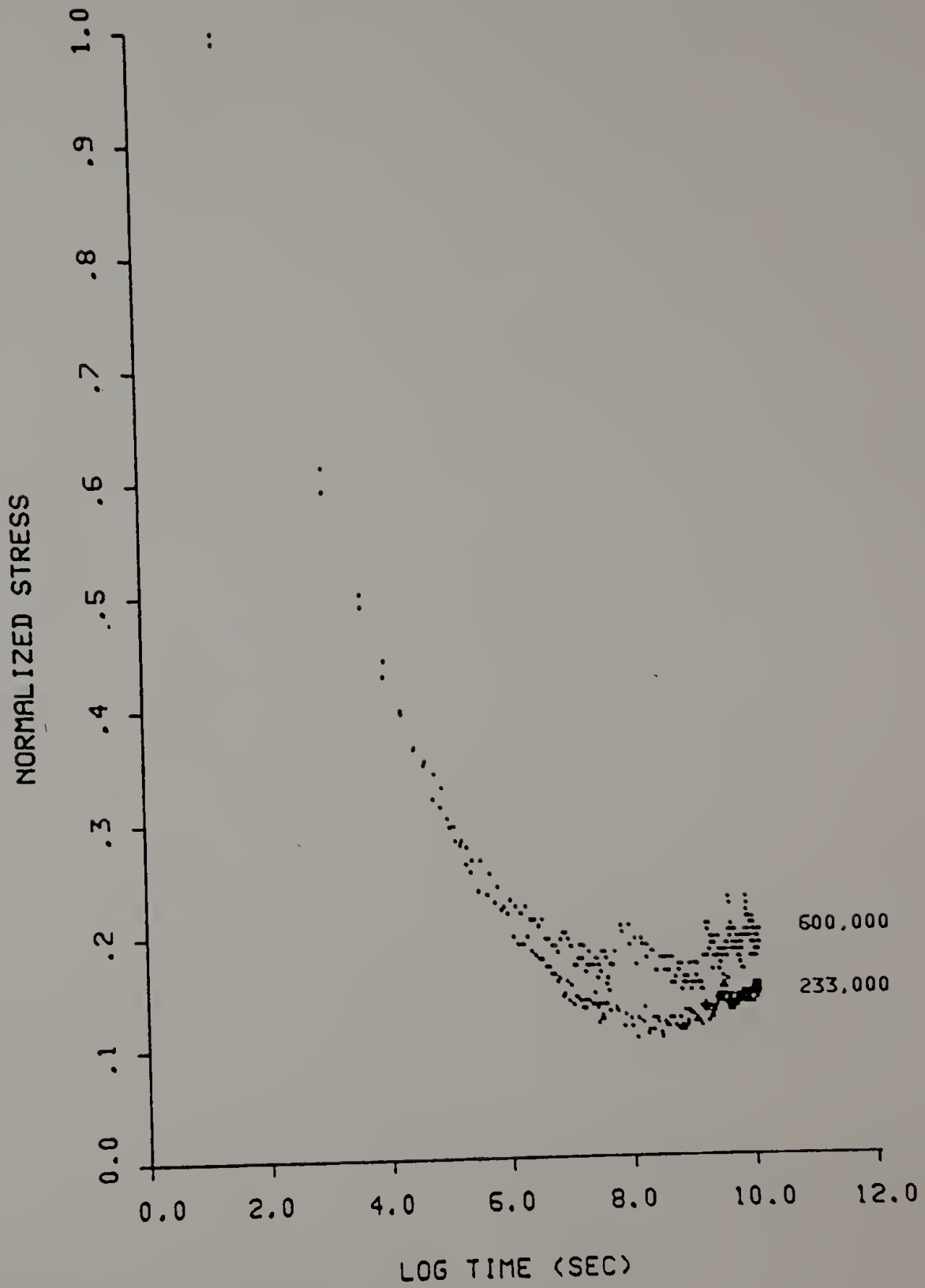


Figure 15.



Figure 16. Relaxation of stress in PS/PVME blends with varying composition (PS  $M_n = 600,000$ ).

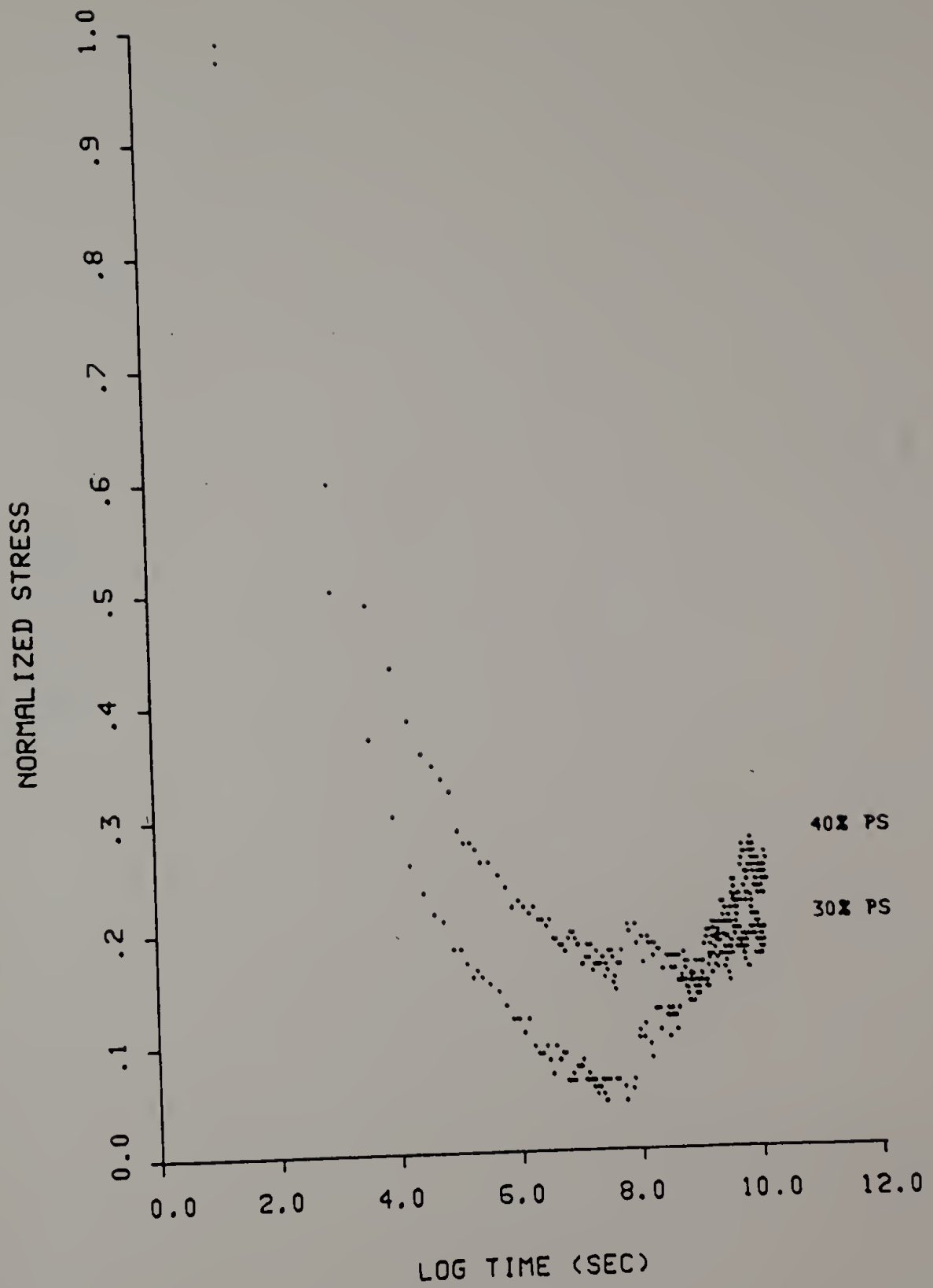


Figure 16.

short-term chain relaxation mechanism previously described, cannot be overlooked. The overall relaxation of PVME, within experimental error, occurs on the same time scale as the short term relaxations of PS.

#### 2.4 Conclusions

The mechanical behavior of miscible PS/PVME blends is more complex due to the availability of more chain relaxation mechanisms at the microscopic level and due to the intermolecular attractions between the two components. Mechanical measurements of stress alone are not sufficient in segregating the relative contributions of these chain relaxation mechanisms in the overall relaxation behavior of the PS/PVME blends. The second moment orientation function, measured by infrared dichroism, turns out to be a more intricate method of following chain relaxation phenomena in these blends.

The selectivity of infrared dichroism allows one to monitor the relaxation behavior of both the PS and PVME components simultaneously. Although the PVME component orients to only a very slight degree and relaxes at a much faster rate than the PS component, the motion of PVME segments is intrinsically important in the relaxation of the PS component. As indicated by analysis of the data using the VMT theory for polymer deformation, relaxation of PVME segments initiates

the process of tube relaxation for PS chains. Two other PS relaxations apparent from the experimental data were ascribed to chain retraction and chain reptation as postulated in the original DE model.

The time constants for these processes did not conform quantitatively to predictions of the DE model for molecular weight dependence due in large part to the excessive scatter of the data. Nonetheless, the time constants differed from one another by at least an order of magnitude showing that the use of the VMT and DE models represents a logical approach for delineating the relaxation behavior of compatible PS/PVME blends.

## CHAPTER 3

### SPECTROSCOPIC STUDIES OF THE CHROMIC TRANSITION IN POLYDIACETYLENE SOLUTIONS

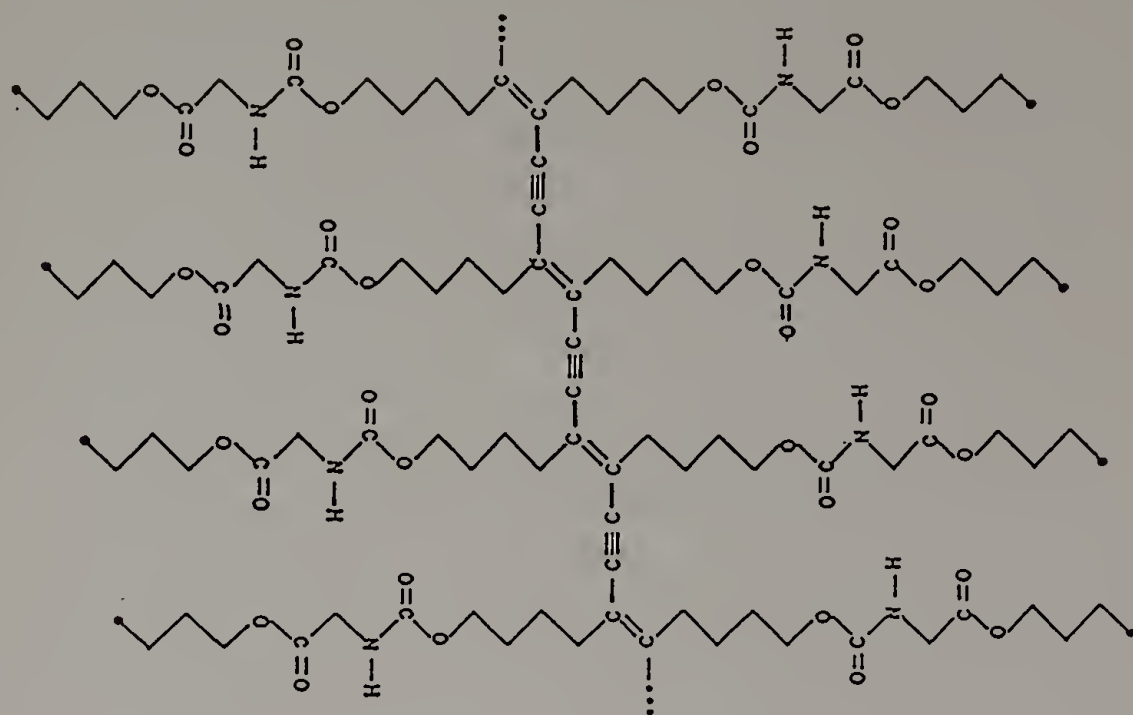
#### 3.1 Introduction

##### 3.1.1 Initial Observations of Solution Behavior

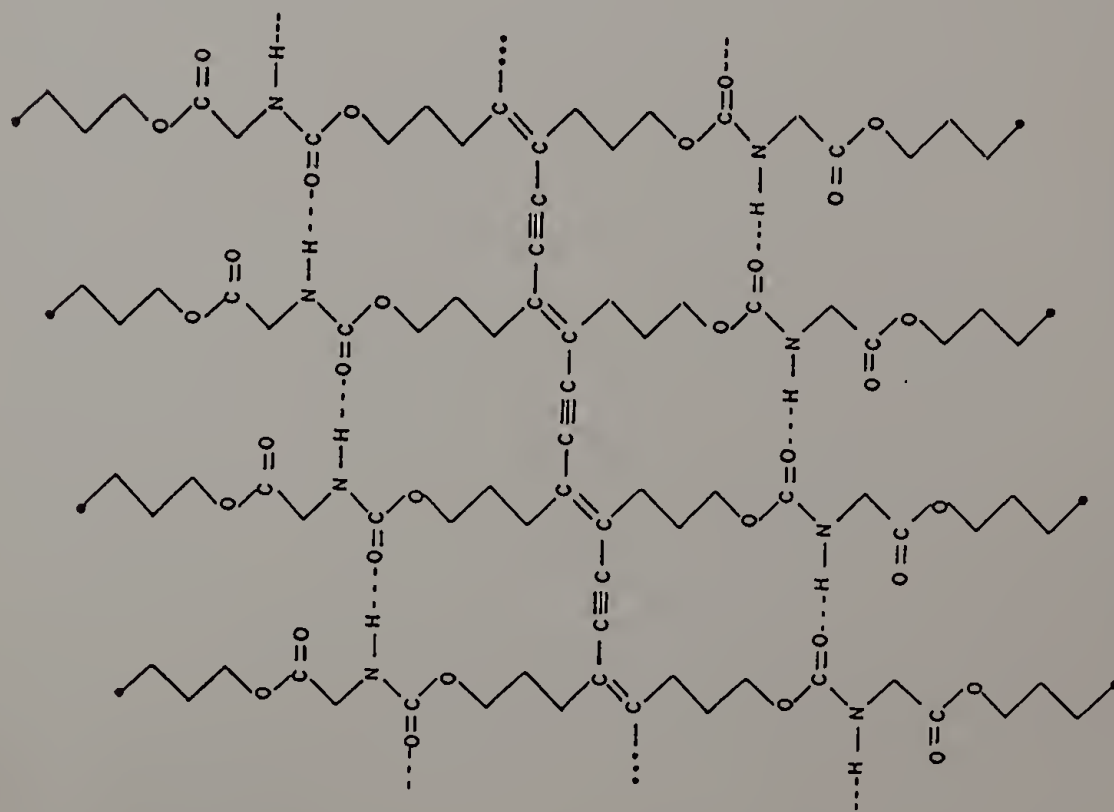
Behavior of polydiacetylenes in solution presents a major challenge in terms of understanding the relationship between electronic structure in the chain backbones of these materials and the overall conformational order of these polymers in solution. Associated with these conjugated systems are an assortment of unusual physical properties whose molecular origins are poorly understood. Reversible chromic transitions in solution and gelation at exceedingly small polymer concentrations are two such properties. The key to discerning molecular origins for these and other phenomena lies in understanding the nature of and the extent of the coupling of electronic structure and conformational structure of these polydiacetylenes in solution.

Initially, conformational properties of polydiacetylenes in solution could not be studied due to the general insolubility of most of these materials (32). However, in 1978, Patel (33) first demonstrated that the polydiacetylenes (Figure 17) poly[4,6-decadiyne-1,10-diol bis((n-butoxycar-

Figure 17. Planar hydrogen-bonded conformations of poly(3BCMUs) and poly(4BCMUs).



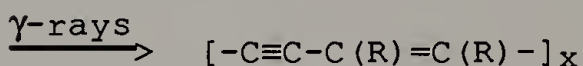
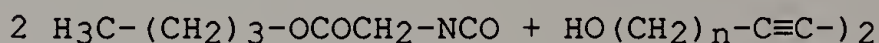
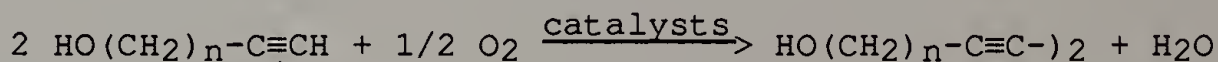
STRUCTURE OF POLY(4BCMU)



STRUCTURE OF POLY(3BCMU)

Figure 17.

bonyl)-methyl)urethane] (denoted as poly(3BCMU)) and poly[5,7-dodecadiyne-1,12-diol bis((n-butoxycarbonyl)-methyl)urethane] (denoted as poly(4BCMU)) are both soluble in common organic solvents such as chloroform and tetrahydrofuran. A wide range of soluble polydiacetylenes with varying side-groups have been synthesized since then, and a partial listing is given in Table 2. The basic scheme of synthesis for poly(3BCMU) and poly(4BCMU) is as follows (34):



where R is the pendant sidegroup

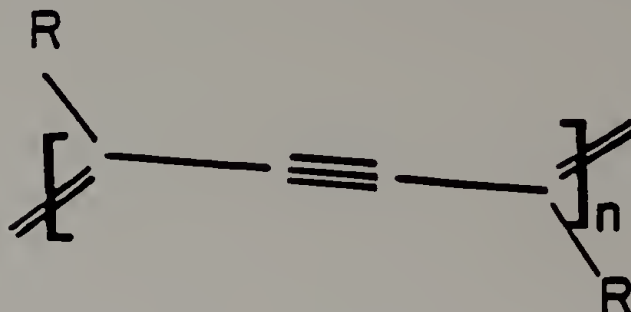


In addition to their observation of the solubility of the BCMU polydiacetylenes, Patel et al. (10) discovered that variation of the solvent/non-solvent ratio could induce the aforementioned reversible chromic transition in solutions of these polydiacetylenes. Upon addition of the poor solvent, hexane, yellow solutions of poly(3BCMU) and poly(4BCMU) were observed to turn blue and red respectively. The transitions



Table 2

Listing of structures, abbreviations, and solvent types for some soluble polydiacetylenes.



SIDEGROUP STRUCTURE (R)	ABBREVIATION	SOLVENT TYPE
(CH <sub>2</sub> ) <sub>3</sub> OCONHCH <sub>2</sub> CO <sub>2</sub> C <sub>4</sub> H <sub>9</sub>	POLY (3BCMU)	POLAR
(CH <sub>2</sub> ) <sub>4</sub> OCONHCH <sub>2</sub> CO <sub>2</sub> C <sub>4</sub> H <sub>9</sub>	POLY (4BCMU)	POLAR
(CH <sub>2</sub> ) <sub>9</sub> OCONHCH <sub>2</sub> CO <sub>2</sub> C <sub>4</sub> H <sub>9</sub>	POLY (9BCMU)	POLAR
(CH <sub>2</sub> ) <sub>3</sub> OCONHCH <sub>2</sub> CO <sub>2</sub> C <sub>2</sub> H <sub>5</sub>	POLY (3ECMU)	POLAR
(CH <sub>2</sub> ) <sub>4</sub> OCONHCH <sub>2</sub> CO <sub>2</sub> C <sub>2</sub> H <sub>5</sub>	POLY (4ECMU)	POLAR
CH <sub>2</sub> OCONHC <sub>6</sub> H <sub>5</sub>	POLY (H DU)	POLAR
(CH <sub>2</sub> ) <sub>3</sub> OCONHC <sub>6</sub> H <sub>5</sub>	POLY (D DU)	POLAR
(CH <sub>2</sub> ) <sub>4</sub> OCONHC <sub>6</sub> H <sub>5</sub>	POLY (T CDU)	POLAR
(CH <sub>2</sub> ) <sub>9</sub> OCOCH <sub>2</sub> C <sub>6</sub> H <sub>5</sub>	POLY (9 PA)	POLAR
CH <sub>2</sub> OSO <sub>2</sub> C <sub>6</sub> H <sub>4</sub> CH <sub>3</sub>	POLY (TS-6)	POLAR
(CH <sub>2</sub> ) <sub>4</sub> OSO <sub>2</sub> C <sub>6</sub> H <sub>4</sub> CH <sub>3</sub>	POLY (TS-12)	POLAR
(CH <sub>2</sub> ) <sub>9</sub> OCOCH(CH <sub>3</sub> ) <sub>2</sub>		POLAR
(CH <sub>2</sub> ) <sub>9</sub> OCOCH <sub>2</sub> (1-naphthyl)		POLAR
(CH <sub>2</sub> ) <sub>11</sub> CH <sub>3</sub>		NON-POLAR
(CH <sub>2</sub> ) <sub>3</sub> OCONHCH <sub>2</sub> COO <sup>-</sup> K <sup>+</sup>	POLY (3KAU)	WATER
(CH <sub>2</sub> ) <sub>4</sub> OCONHCH <sub>2</sub> COO <sup>-</sup> K <sup>+</sup>	POLY (4KAU)	WATER
(CH <sub>2</sub> ) <sub>2</sub> COO <sup>-</sup> K <sup>+</sup>		WATER
(CH <sub>2</sub> ) <sub>3</sub> COO <sup>-</sup> K <sup>+</sup>		WATER

could be reversed with the addition of the good solvent, chloroform, although the transitions from blue to yellow and red to yellow occurred at higher chloroform contents than did the reverse transitions. It has also been demonstrated that addition of thermal energy (heating) can induce the chromic transition (8).

Patel et al. surmised from optical data that major changes in polymer conformation and conjugation length in the polydiacetylene molecules were responsible for the chromic transitions. (Conjugation length is defined as the chain backbone length over which portions of the  $\pi$  electron network can be described as continuous.) A  $5000\text{ cm}^{-1}$  shift in the peak maxima for visible absorption was shown to occur for the transition in the poly(3BCMU)/chloroform/hexane system, and a  $2500\text{ cm}^{-1}$  shift was demonstrated for the poly(4BCMU)/chloroform/hexane system. Patel et al. used the free electron gas model of Kuhn (35) to calculate average conjugation lengths of molecules of poly(3BCMU) in yellow solutions. According to Kuhn's model, which had previously been applied to oligoenes (conjugated low molecular weight hydrocarbons with alternating single and double bonds in the backbone) (36), the optical bandgap energy  $E$ , as determined by maxima in visible absorption spectra, has a reciprocal dependence on the number of conjugated double bonds per molecule as follows:

$$E = V_o + \left( \frac{h^2}{4mL_o} - \frac{V_o}{4} \right) \frac{1}{N + 0.5} \quad (12)$$

where E = optical bandgap energy

$V_o$  = correction term for bond length alteration

h = Planck's constant

$L_o$  = length of conjugated unit

N = number of conjugated double bonds per molecule  
or per conjugated segment

Using this model, Patel et al. calculated that poly(3BCMU) molecules in yellow solution have a distribution of relatively short conjugation lengths extending over an average of seven monomeric units. Upon occurrence of the transition, the average conjugation length increases substantially to values approaching the effectively infinite conjugation lengths of poly(3BCMU) molecules in the crystalline state.

### 3.1.2 Models for Chain Structure in Yellow Solutions

The actual structure of polydiacetylenes in yellow solutions is a matter of great controversy. The shortening of polydiacetylene conjugation lengths in yellow solutions may arise either from discrete conformational defects along the planar trans structure of the polydiacetylene molecules (10) or from a continuous distortion of bond angles and bond lengths in the planar trans structure (37). The planar trans

structure of single crystals of polydiacetylenes has been evidenced by X-ray analysis (32), and the close correlation of optical data for crystalline polydiacetylenes and solvated polydiacetylenes demonstrates that the planar trans structure accounts for the conformational structures in the blue or red (poor solvent) solution state.

To account for the reduced conjugation length of polydiacetylenes in good solvents, Patel et al. (10) argued for discrete defects consisting of  $90^\circ$  rotations about carbon-carbon single bonds (Figure 18A). The estimated energetic cost of 1 kcal per mole of monomeric repeat units (10) would be compensated for by the increased entropy of the side groups. Although the main backbone  $\pi$ -orbital overlap is broken completely, the  $90^\circ$  rotation would still allow conjugation to occur by the orthogonal  $\pi$  orbitals associated with the carbon triple bond.

Heeger et al. (38) argued for another type of discrete defect in which  $180^\circ$  rotations about single bonds would introduce cis defects (Figure 18B), and supposedly a more freely coiling structure would result. This model would account for the precipitous five-fold drop in the measured hydrodynamic radii of poly(4BCMUs) molecules in toluene in proceeding from red solutions at room temperature to yellow solutions at  $72^\circ\text{C}$  (39). The hydrodynamic radius, as measured by quasi-elastic light scattering, was found to decrease from

- Figure 18. (A) Patel model for chromic transition: planar structure goes to chain with electronically decoupled adjacent segments.
- (B) Heeger model for chromic transition: trans isomer goes to cis isomer.
- (C) Wegner model for chromic transition: (aggregated) planar structure goes to (isolated) wormlike chain with continuous curvature of the chain skeleton.

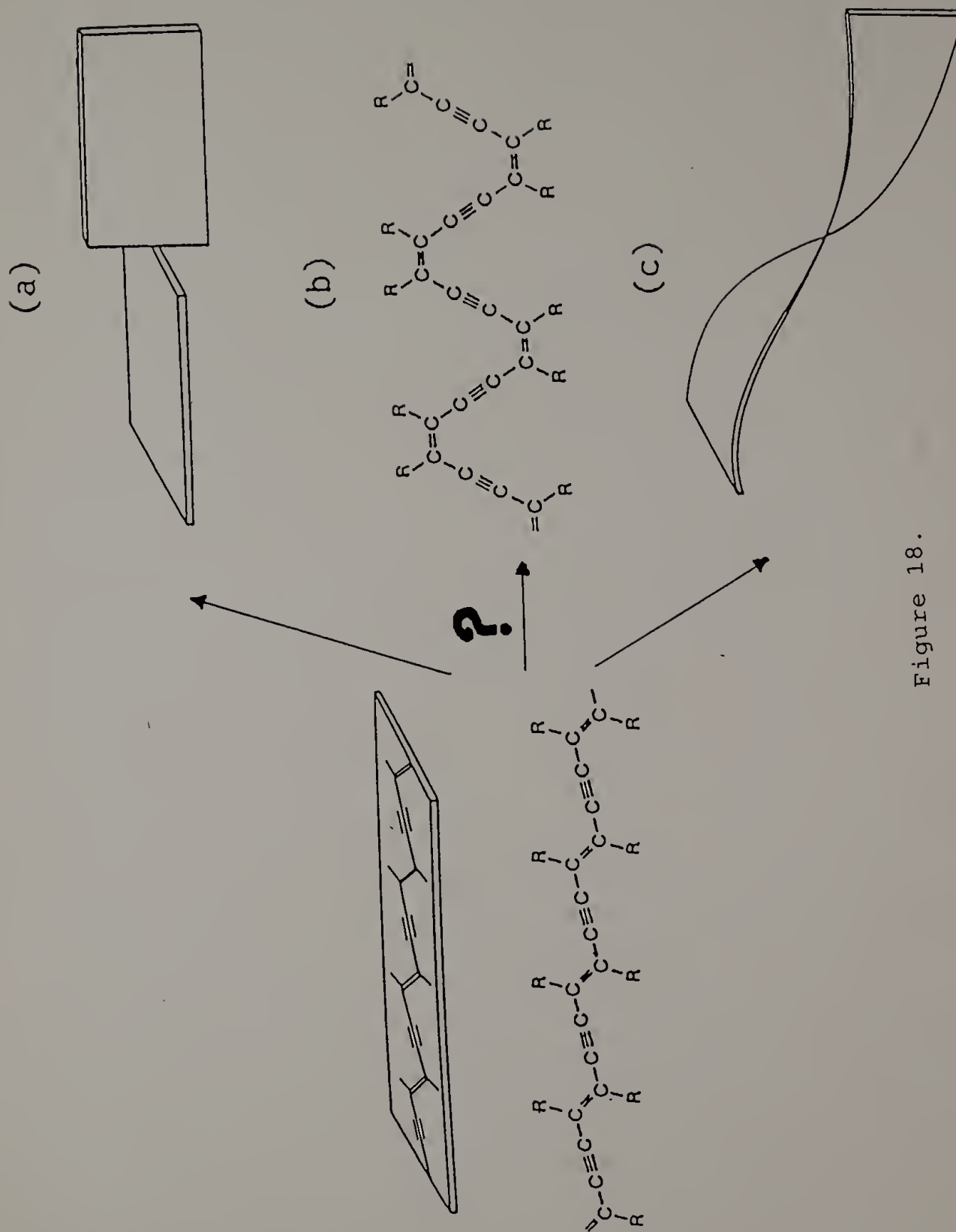


Figure 18.

0.11  $\mu\text{m}$  to 0.02  $\mu\text{m}$  under these conditions. It is unclear, however, as to whether the incorporation of cis defects into the main chain backbone would appreciably affect the extent of conjugation within the  $\pi$  electron network or would in fact induce greater flexibility or coiling ability into the chain backbone.

A third model accounting for the decreased conjugation lengths of polydiacetylene molecules in yellow solutions has been proposed by Wegner et al. (37). This model incorporates a Porod-Kratky (40-42), or wormlike, chain (Figure 18C) as a means of explaining the apparent coil-like conformations of the chain in yellow solutions. Instead of discrete conformational defects, bond angle deformations and bond stretches compose a continuous deformation of the chain backbones. These bond angle deformations would be on the order of about  $12^\circ$  per monomeric repeat unit (37). At present, however, there have been no theoretical investigations as to whether loss of conjugation can occur by continuous deformations of ideal chain geometries and therefore serve as an explanation for the observed coil-like behavior of the chains. Experimental evidence from Wegner et al. (37) employing light-scattering and viscometric data have shown that the polydiacetylene PTS-12 ( $R=(\text{CH}_2)_4\text{OSO}_2\text{C}_6\text{H}_4\text{CH}_3$ ) probably exists as coils in good solvents. Calculated dependencies of radii of gyration on molecular weight and persis-

tence lengths were consistent with values expected for coiled macromolecules in good solvents.

### 3.1.3 Models for Mechanism of Transition

The specific mechanism of the chromic transition, as well as the molecular source of decreased conjugation lengths, has been a subject of controversy in solution studies of polydiacetylenes. Patel et al. (10) and Heeger et al. (38) regarded the chromic transition to be intramolecular in nature, i.e. occurring by a single chain mechanism. Possible driving forces for the chromic transition include formation or dissociation of intramolecular hydrogen bonding, the introduction of entropy in the side-chains in the form of greater conformational flexibility and disorder, and solvent-polymer interactions which would be stronger in the presence of more highly conjugated chain backbones.

The first factor, intramolecular hydrogen bonding, which can occur between urethane substituents of neighboring side groups, was suggested by Heeger et al. (14) in analogy with the observed helix-coil transitions in polypeptides (43). Heeger et al. (14) have analyzed optical data on the temperature induced chromic transition for poly(4BCMU) in toluene according to the Zimm and Bragg (44) model for helix-coil transitions. This theory attempts to account for the ob-



served transitions of polypeptides from a helical state at low temperatures or in poor solvents to randomly coiled structures at high temperatures or in good solvents. The theory incorporates two main parameters 's' and ' $\sigma$ '. 's' denotes the equilibrium constant for conversion to a helical segment of a coiled segment bonded to another helical segment. ' $\sigma$ ' is a term accounting for the high boundary energy between coiled and helical segments. The relative sharpness of the transition depends upon this latter parameter.

Heeger et al. (14) attempted to apply this theory to the conformational transition of poly(4BCMU) in toluene. They reasoned that formation or dissociation of hydrogen bonding in the sidegroups of this polydiacetylene spur the transition between rod-like states and coiled states in the same manner as in polypeptides. Heeger et al. found reasonable fits to the theory (Figure 19). However, the presence of long range cooperativity among hydrogen bonds, which is an integral part of the Zimm and Bragg model, is uncertain in the case of polydiacetylene. As opposed to hydrogen bonds within the main chains of polypeptides, the hydrogen bonds in the flexible side groups of polydiacetylenes would not be expected to be highly correlated over a long range. More importantly, the chromic transition has been observed in a number of polydiacetylenes which cannot form intramolecular hydrogen bonds (45,46). Therefore, intramolecular hydrogen

Figure 19. Application of visible spectroscopic data on chromic transition to Zimm-Bragg model for helix-coil transition. Fraction of molecular segments of polydiacetylene in the trans state as a function of temperature; circles: experimental data from intensities of red (rod-like) absorption peak for poly(4BCMU) in toluene; solid line: three parameter fit to Zimm-Bragg theory.  
(from Berlinsky et al., ref. 14)

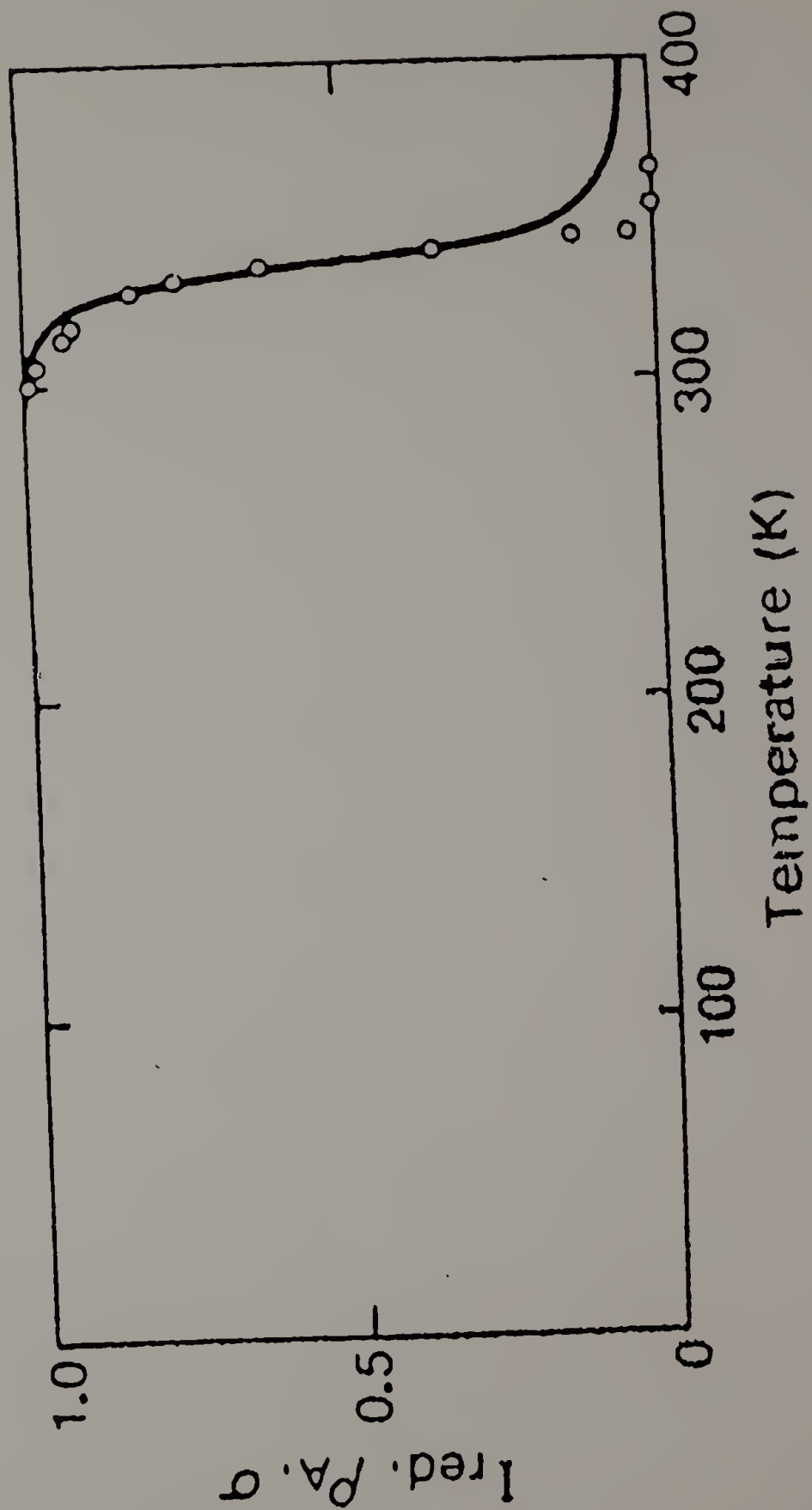


Figure 19.

bonding cannot, as a general case, be the driving force for the chromic transition.

The second possible driving force for an intramolecular transition is the ordering or disordering of side chains, as suggested by Bloor et al. (15). This would be a possible mechanism for both hydrogen-bonded and non-hydrogen-bonded polydiacetylenes. According to Bloor et al. formation of gauche conformers in the alkane sequences introduces sufficient disorder in the coupled side groups and chain backbone such that the chain backbone adopts a worm-like conformation. These conclusions were reached by Bloor et al. from visible absorption studies on poly(9BCMU), which has a total of nine methylene units between the chain backbone and the urethane substituents in mixed solvents of chloroform and n-hexane. This system was particularly interesting in that Bloor and his coworkers were able to detect a long-lived metastable intermediate as evidenced by the appearance of transient red solutions which eventually turned blue. Bloor et al. attributed these intermediates to aggregated chains with disorder frozen in initially. Introduction of partial ordering into the side chains allows the formation of crystalline aggregates, and on a longer time scale the side chains order more fully yielding the stable blue solution.

Some objections have been raised to the supposition that ordering and disordering of side chains serve as driving

forces for the chromic transition (17). Firstly, the degree of coupling between chain backbone conformation and side chain conformation would generally be expected to be weak. Secondly, order-disorder transitions, very similar to those observed for polydiacetylene solutions, have been observed for conjugated polysilanes in solution (47,48) and have been found to be nearly unaffected by the degree of conformational flexibility or entropic content in the alkyl side groups. The order-disorder transitions in solution occurred within a range of 10°C for polysilanes (-SiR<sub>2</sub>-) with alkyl sidegroups (R) ranging from C<sub>2</sub>H<sub>5</sub> to C<sub>12</sub>H<sub>25</sub>. Thirdly, x-ray scattering (49) and infrared spectroscopic (50) experiments on polydiacetylene films have shown that disordering of side chains occurs at substantially lower temperatures than does the disordering of chain backbones.

A third possible driving force for an intramolecular transition involves energetic stabilization of the rod-like conformation of polydiacetylenes in solution arising from solvent interactions with delocalized electrons in the chain backbone (16,17). At high temperatures or in good solvents the entropically favored disordering of the chain backbones would have the interactions between solvent and delocalized electrons due to the reduction of conjugation in the backbones. This model has received extensive theoretical treatment by Schweizer, and a limited number of semi-quantitative

predictions from the theory concerning transition temperature and temperature ranges were found to be consistent with experimental results on polydiacetylenes in solution (17).

The chromic transition of polydiacetylenes in solution has also been postulated to be intermolecular in nature with attractions between polymers and tendencies to form aggregates spurring the ordering transition. Wegner et al. (37) found from spectrophotometric measurements on heated and cooled solutions of poly(3BCMU) in dichloroethane that the relative concentrations of the blue (low temperature) and yellow (high temperature) forms of poly(3BCMU) were dependent not only upon time and temperature but upon the history of the sample as well. This is behavior typical of a nucleation-controlled crystallization or aggregation phenomenon. In addition, Wegner and his co-workers (51) have detected aggregates composed of roughly 30 chains occurring for polydiacetylene solutions at concentrations as low as  $1.0 \times 10^{-6}$  mole/liter. Observations such as these have led Wegner and his coworkers to conclude that the chromic transition for polydiacetylenes in solution is intermolecular.

Chance et al. (52) and Heeger et al. (13,38,39,53,54) have disputed Wegner's conclusions and have offered a limited amount of experimental evidence in support of their conclusions that the chromic transition occurs by an intramolecular mechanism. In particular, Heeger et al. (39) found that for

sufficiently dilute concentrations of poly(4BCMU) in toluene, the rod-like polydiacetylene molecules have, as measured by quasi-elastic light scattering, hydrodynamic radii which are independent of polymer concentration (Figure 20). Furthermore, they found that the hydrodynamic radii of poly(4BCMU) molecules in toluene remain constant with temperature below the chromic transition temperature (Figure 21). Heeger et al. (54,55) also found that electric field induced birefringence of poly(4BCMU) molecules in toluene increases by a factor of more than 300 in going from the coiled, yellow phase to the rod-like, red phase. The hydrodynamic radius is obtained from the Stokes equation:

$$D = k_B T / 6\pi\eta R_H \quad (13)$$

$D$  = translational diffusion constant

$\eta$  = solution viscosity

$R_H$  = hydrodynamic radius

$k_B$  = Boltzmann constant

$T$  = absolute temperature

where  $D$  is obtained from an autocorrelation time

constant determined by quasielastic light scattering.

Also, a measured free rotational relaxation time of 0.1 second, measured for poly(4BCMU) molecules in toluene by a birefringence decay technique, was consistent with theoretical values expected for single rod-like polydiacetylene molecules in solution. This particular experiment consisted of observ

Figure 20. Hydrodynamic diameter (from quasi-elastic light scattering) of poly(4BCMU) in toluene as a function of polymer concentration.

(from Lim and Heeger, ref. 39)



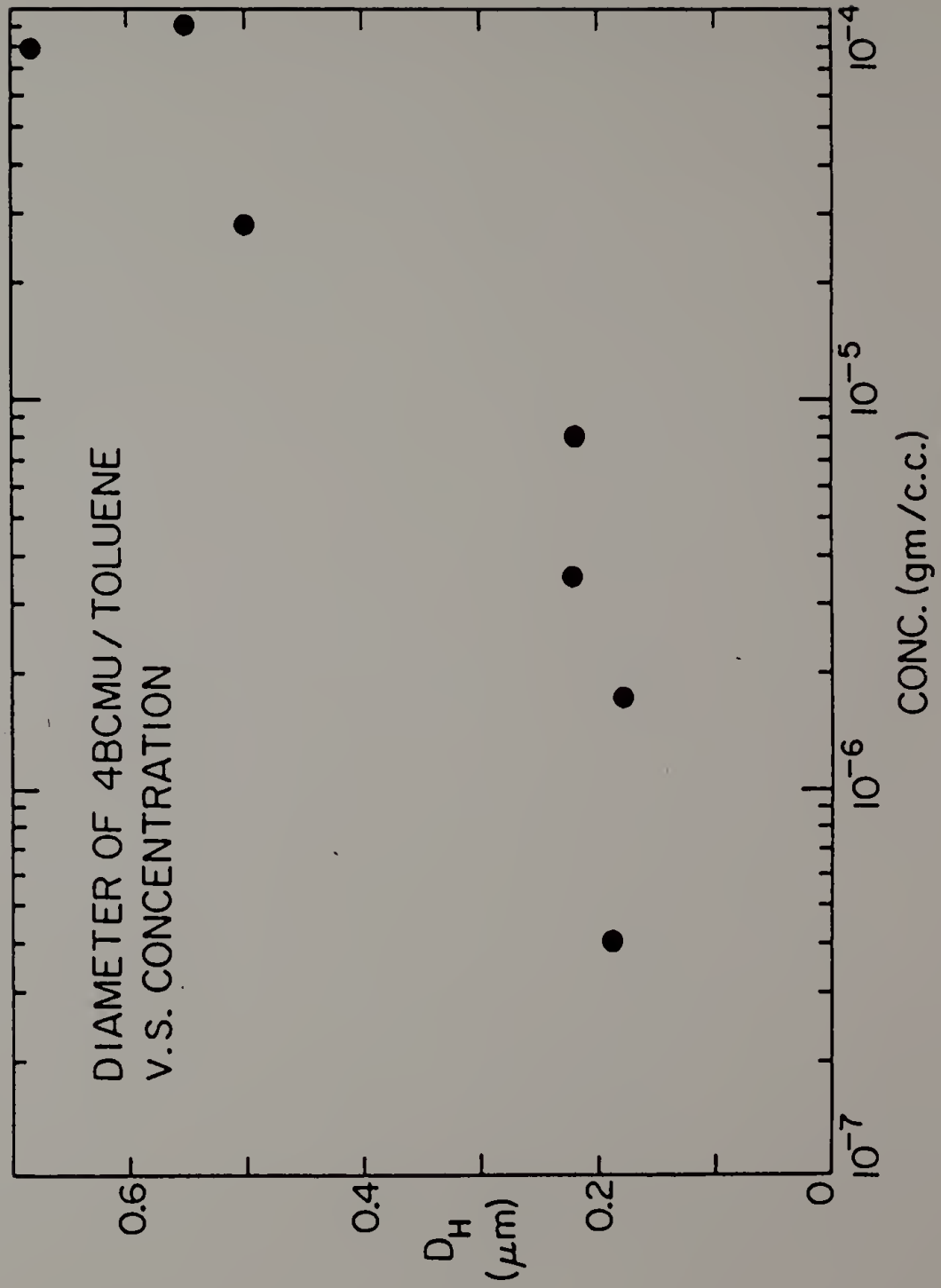


Figure 20.

Figure 21. Hydrodynamic diameter of poly(4BCMU) in toluene as a function of temperature.  
(from Lim and Heeger, ref. 39).

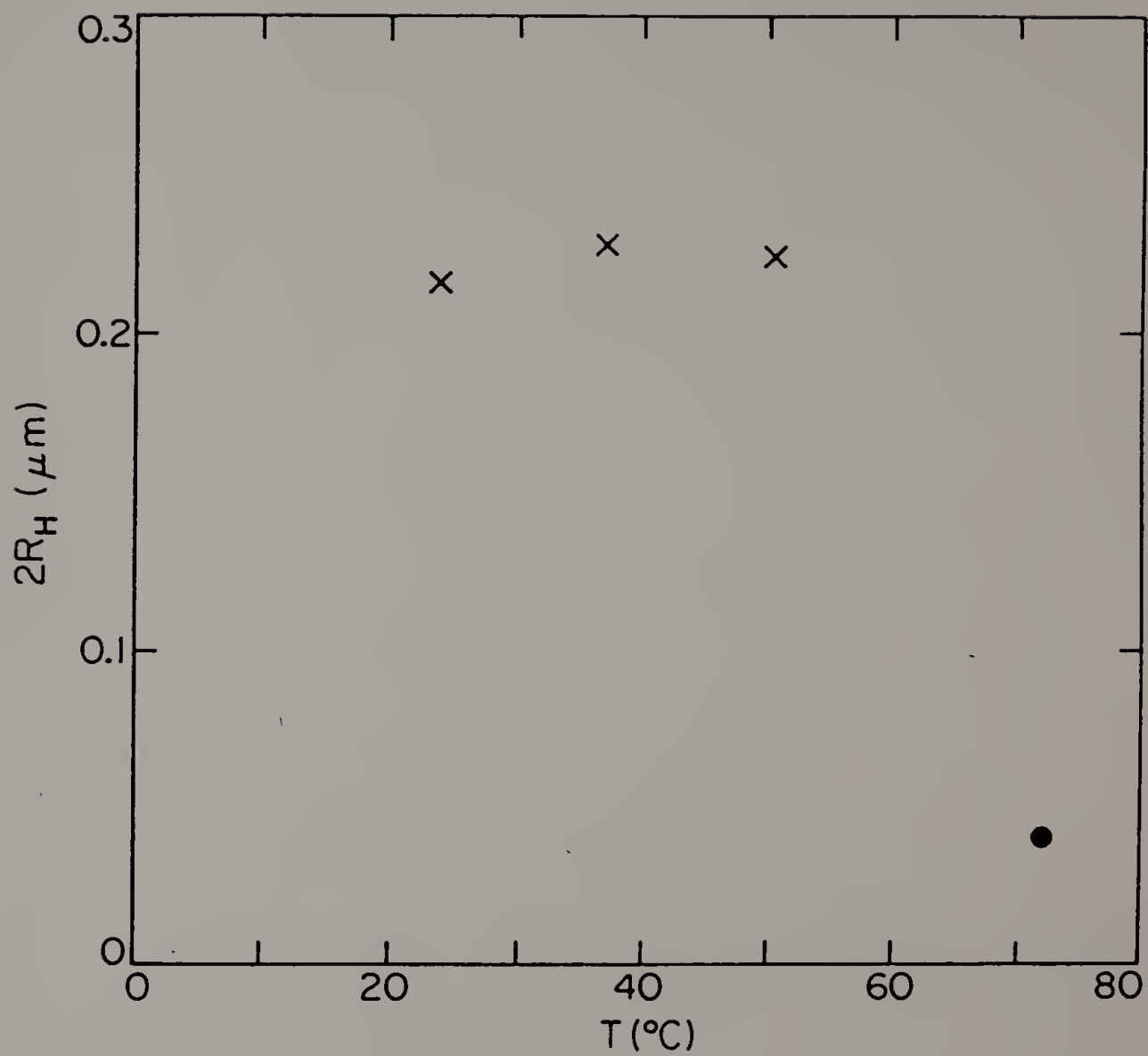


Figure 21.

ing the decay in birefringence of the poly(4BCMU) molecules in solution after suddenly switching off an applied electric field.

Chance and co-workers have presented additional evidence favoring an intramolecular interpretation for the chromic transition. Chance et al. (52) and Patel et al. (10) have constructed phase diagrams (Figure 22) of poly(3BCMU) in a mixed solvent of chloroform and n-hexane, the former being a good solvent for poly(3BCMU) and the latter being a non-solvent. Occurrences of the blue, or 'planar' conformational phase, and the yellow, or nonplanar, phase were determined as functions of solvent quality (i.e. proportion of solvent to non-solvent) and polymer concentration. As was expected, precipitation of the polymer in the form of visual aggregates showed a substantial polymer concentration dependence. However, the yellow-to-blue and blue-to-yellow transitions occurred at unique values of solvent composition and showed no detectable polymer concentration dependencies. This was taken by Chance and his co-workers to be strong evidence that the chromic transition is a single chain phenomenon and that any intermolecular aggregation phenomena occur subsequent to the transition. Chance et al. (52,56) have also shown, through spectrophotometric measurement on poly(3BCMU) in various mixed solvents, that the kinetics of the chromic transition are independent of polymer concentration over a two or

Figure 22. Partial phase diagram for poly(3BCMU) in mixed solvents of  $\text{CHCl}_3$  and n-hexane.  $X_c$  is the mole fraction of  $\text{CHCl}_3$  (good solvent) in n-hexane (nonsolvent). The phase boundaries for the formation of precipitate (clouding point) and blue solution (color transition) were determined by titration with hexane, whereas the formation of yellow solution was determined by titration with  $\text{CHCl}_3$ . A red-purple end point was arbitrarily chosen for the boundary of the yellow-to-blue transition, while a yellow end point was used for the blue-to-yellow transition.

(from Patel et al., ref. 10).

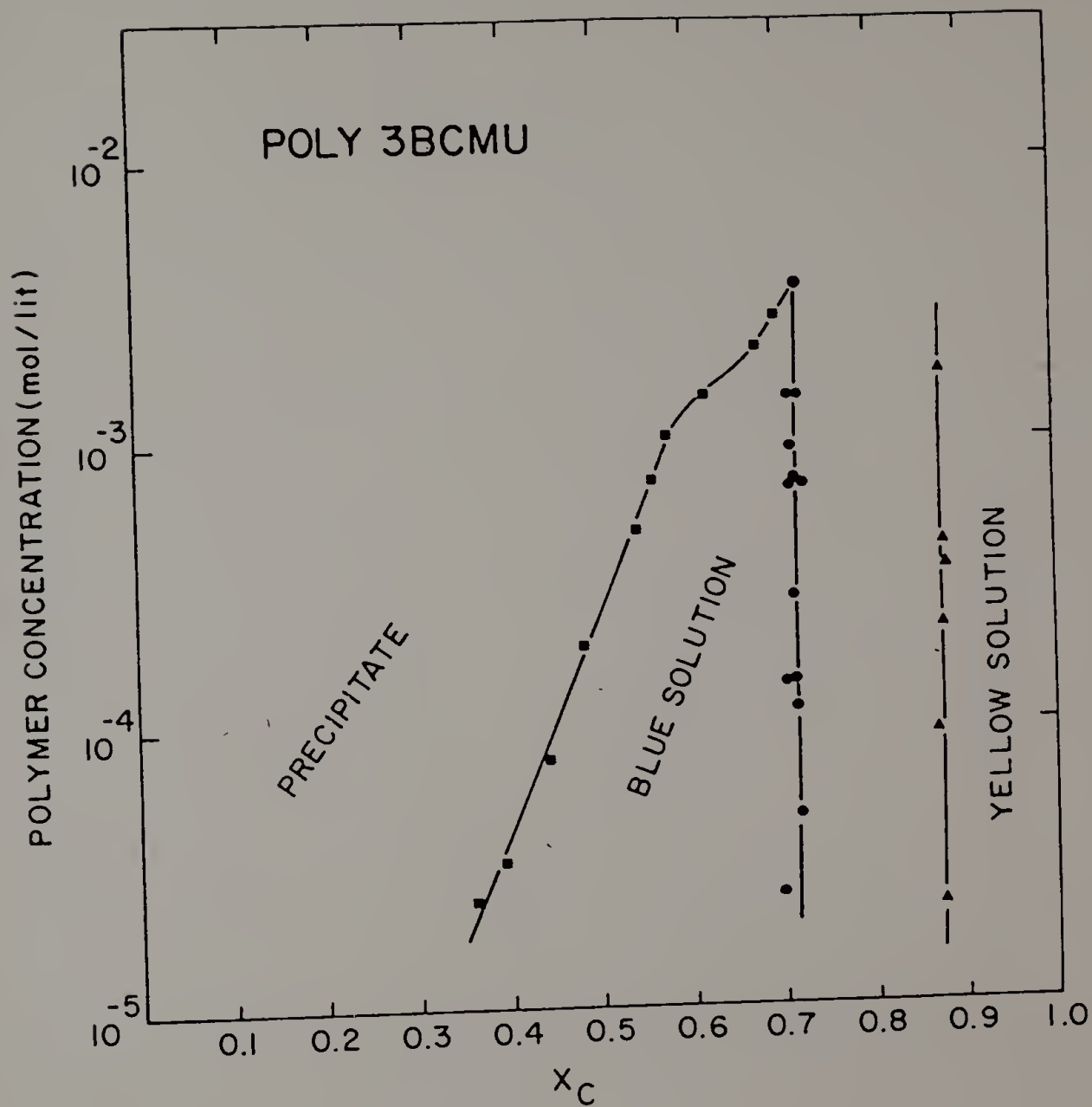


Figure 22.

der of magnitude concentration difference. This was taken to be further evidence of the single chain nature of the transition.

The aforementioned assortment of theories and seemingly contradictory experimental evidence concerning the chromic transition makes it clear that the transition is still very poorly understood. Part of the complications regarding understanding of the transition undoubtedly arise from the supposition that a unique chain mechanism must be responsible for the chromic transitions of any soluble polydiacetylene in any solvent. This presumption is erroneous as will be demonstrated by research efforts recounted here.

Specifically, it will be shown that a single chain mechanism cannot uniquely describe the transition for polydiacetylenes in all solvent systems. A simple set of spectroscopic experiments showed that poly(3BCMU) in mixed solvents of chloroform and carbon tetrachloride, a poor solvent for poly(3BCMU), undergoes a chromic transition with a weak but plainly observable polymer concentration dependence (57). This shows that any observed independence of polydiacetylene concentration for the chromic transition (10,52,58) is a reflection of the particular solvent system employed and does not in any way represent an intrinsic property of polydiacetylene molecules in solution.

Additional observations were also made concerning the kinetics of the chromic transition and the observed presence or absence of hysteresis in the chromic transition for differing solvent systems. It was observed that the poly(4BCMU)/chloroform carbon tetrachloride ( $\text{CCl}_4$ ) system, unlike the poly(4BCMU)/ $\text{CHCl}_3$ /n-hexane system (39) (Figure 23), shows significant hysteresis in the yellow-to-red and red-to-yellow transitions when such solutions are cooled or heated. This again demonstrated the fact that any observed solution properties of polydiacetylenes cannot be taken to be universal, but rather must be regarded as dependent upon the particular solvent system used.

### 3.2 Experimental

Well characterized samples of poly(3BCMU) and poly(4BCMU) were furnished by Professor G. Wegner. The samples were synthesized according to the scheme outlined in the introduction to this chapter. Infrared absorption spectra of samples extracted with acetone were identical to those of unextracted samples, thus showing the absence of significant amounts of unreacted monomer.

For studying the solvatochromic transition, various weights of poly(3BCMU) were initially dissolved in measured amounts of  $\text{CHCl}_3$  (ca. 20 ml) and titrated in a stepwise fashion with  $\text{CCl}_4$ . Dilution in larger amounts of  $\text{CHCl}_3$  was re



Figure 23. Fraction of total intensity of visible absorption spectra associated with the red (rod-like state) phase of poly(4BCMU) in mixed solvents of  $\text{CHCl}_3$  and n-hexane as a function of temperature.  $X_C$  is the mole fraction of  $\text{CHCl}_3$  (good solvent) in n-hexane (nonsolvent). The curves are the same on heating and on cooling to within experimental accuracy.

(from Lim and Heeger, ref. 39)

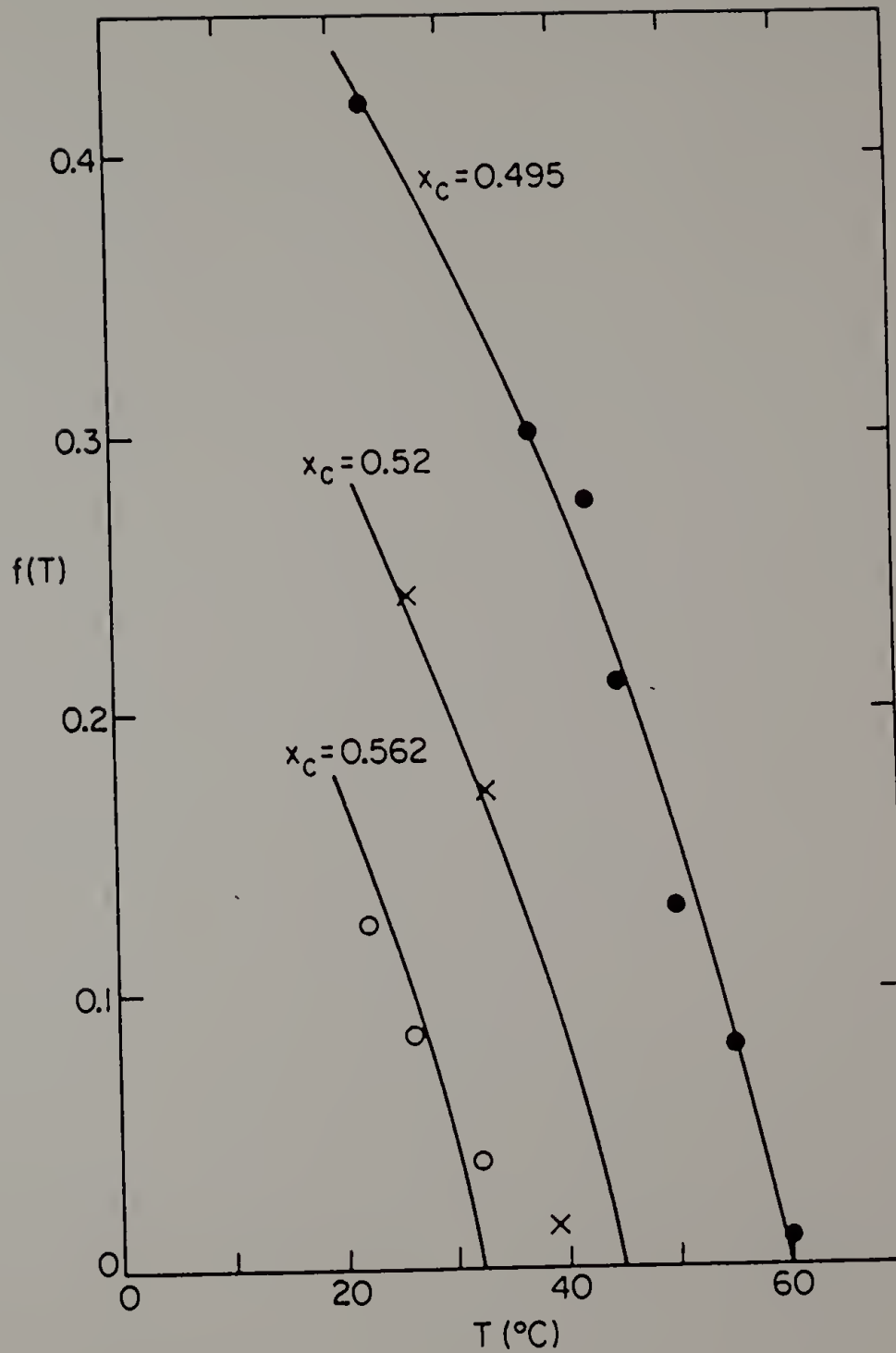


Figure 23.

quired to obtain the samples of lowest concentrations. Solutions were titrated with  $\text{CCl}_4$  once through the yellow-to-blue transition and back titrated with  $\text{CHCl}_3$  once through the blue-to-yellow transition. Titrated samples were sealed, shaken vigorously, and allowed to stand for 13 minutes. Small, carefully measured samples were then withdrawn from the titrated solutions to be measured for optical absorption. Measurements were obtained on a Beckman DU-40 spectrophotometer with a scanning speed of 750 nm per min. Absorbance values were kept below 2.0 for all samples through the use of a Harrick cell with glass windows for high concentrations or a quartz cuvette for low concentrations. For studying the thermochromic transition in the poly(4BCMU)/ $\text{CHCl}_3$ / $\text{CCl}_4$  system, 1.14 mg of poly(4BCMU) was dissolved in 40 ml of solution composed of 14 vol.%  $\text{CHCl}_3$ /86 vol.%  $\text{CCl}_4$  solution and placed in a quartz cuvette equipped with a heating jacket. The sample was heated and cooled at an approximate rate of 1 K/3 min.

### 3.3 Results and Discussion

#### 3.3.1 Solvatochromic Transition

Shown in Figure 24 are absorption spectra for poly(3BCMU) in solutions of 43%  $\text{CHCl}_3$ /57%  $\text{CCl}_4$  and 60%  $\text{CHCl}_3$ /

Figure 24. Visible absorption spectra obtained for solutions of poly(3BCMU) in 43% CHCl<sub>3</sub>/57% CCl<sub>4</sub> and poly(3BCMU) in 60% CHCl<sub>3</sub>/40% CCl<sub>4</sub>. The left curve represents the yellow solution and the right curve represents the blue solution.

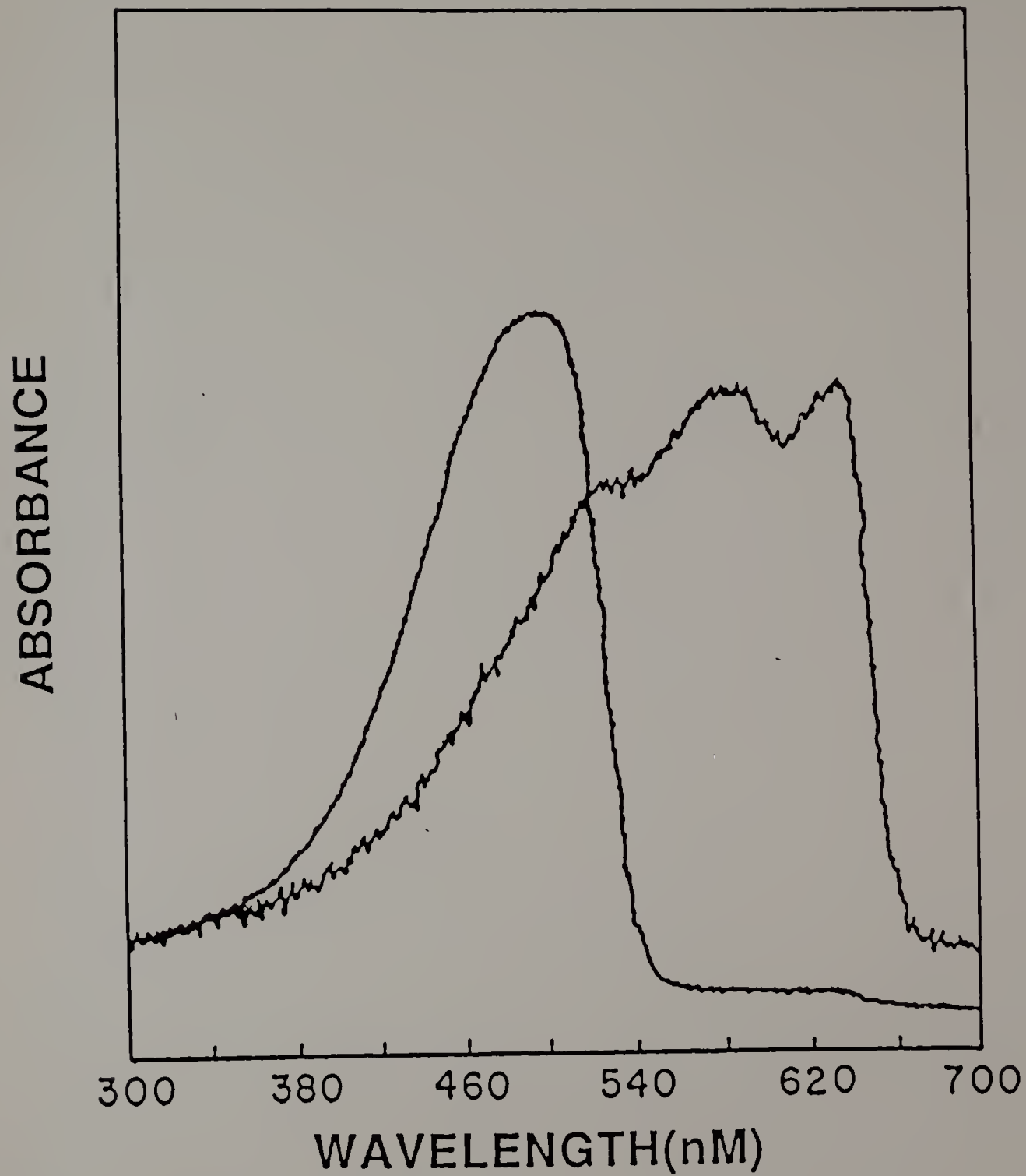


Figure 24.

40%  $\text{CCl}_4$ . Intensities of the peaks at approximately 630 nm and 580 nm increase with  $\text{CCl}_4$  content corresponding to an increase of the blue phase, whereas the peak at approximately 480 nm increases with  $\text{CHCl}_3$  content, corresponding to an increase of the yellow phase. Simple ratios of the height of the "blue peak" at 630 nm to the height of the "yellow peak" at 480 nm will therefore give a good indication of to what extent a chromic transition has taken place. This ratio method was used so that spectra at differing polymer concentrations could be correlated directly. This analysis assumes that absorption coefficients do not change as a function of solvent composition.

In Figure 25 representative data points obtained from absorption spectra are plotted for titrated samples as functions of polymer concentration and chloroform fraction in the mixed solvent. Each plotted data point is labeled with a ratio of its "blue peak" height to its "yellow peak" height. The yellow-to-blue transition range is designated as occurring between ratio values of 0.2 and 1.0 for the sake of convenience. The actual transition extends somewhat beyond these limits. Values below 0.2 occur over greatly expanded solvent composition ranges. Values well over 1.0 are avoided so as not to induce precipitation of polymer. The blue-to-yellow transition range, which does not coincide with the yellow-to-blue range, was designated as occurring between ra

Figure 25. Partial phase diagram for poly(3BCMU) in mixed solvents of  $\text{CHCl}_3$  and  $\text{CCl}_4$ . Relative intensities of the 630 nm peak (blue solution) to the 510 nm peak (yellow solution) representing for each sample point of specific polymer concentration and solvent composition the relative extent of the chromic transition (ranging from 0.2 to 1.0: blue  $\longleftrightarrow$  yellow); ( ● ) represents yellow-to-blue titration; ( ○ ) represents blue-to-yellow titration. The regions between each set of vertical boundaries correspond to the solvent composition ranges over which the transitions occur.

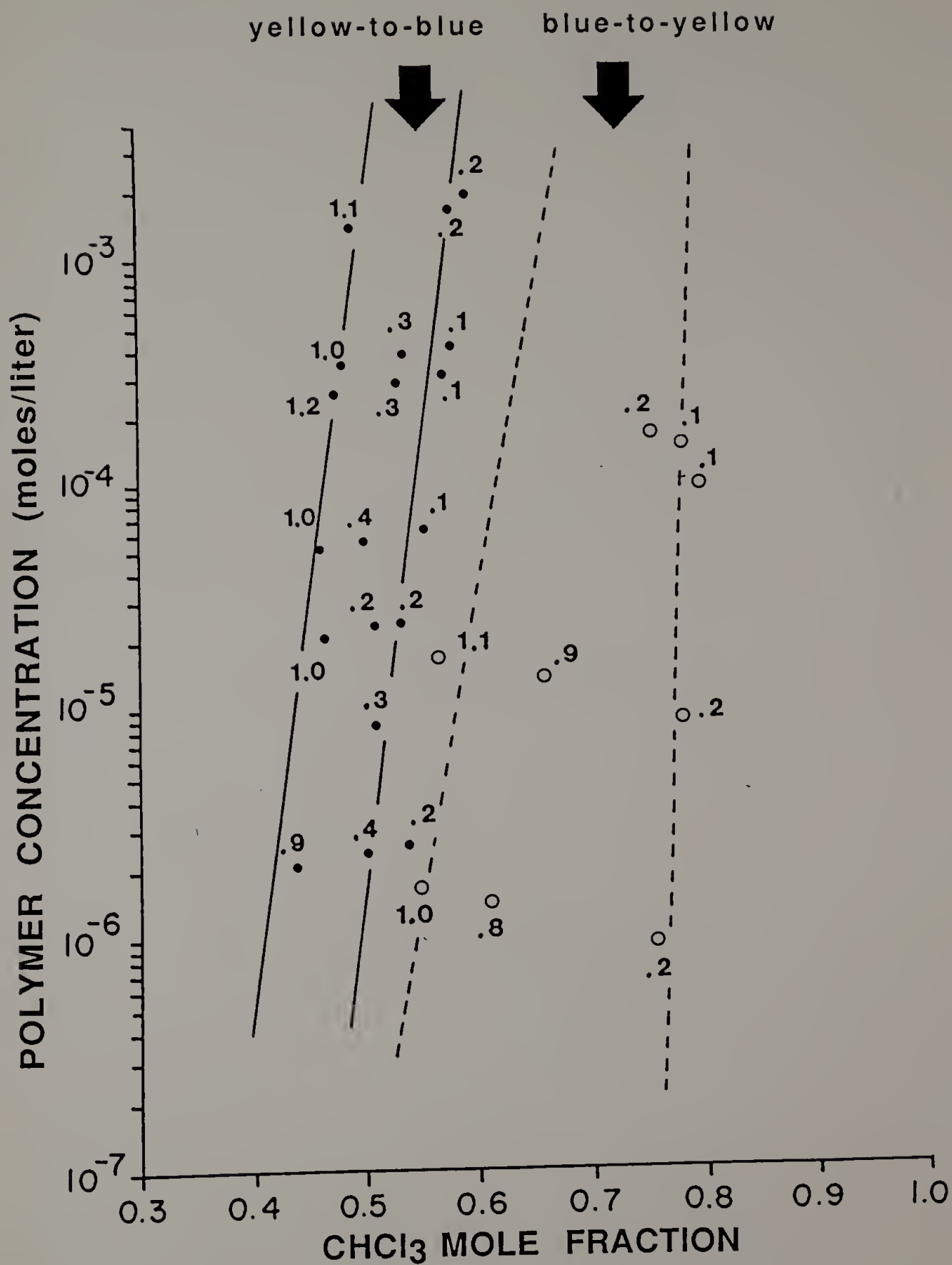


Figure 25.



tio values of 1.0 and 0.2 as well. The lines drawn in Figure 25 were fitted by a standard linear regression routine. Explanation for the greater amount of scatter for the blue-to-yellow transition will be given later.

It can be readily seen that there is indeed a pronounced polymer concentration dependence for both transition ranges, suggesting that the chromic transitions in this solvent system cannot be explained easily by a single chain mechanism. The extreme insolubility of poly(3BCMU) in hexane means that one must be cautious about deriving any conclusions concerning general behavior of polydiacetylenes in solution when such a specific solvent is used. Also, large molar volume differences between solvent components may lead to differences between the global solvent composition and the local solvent composition in the vicinity of the urethane side-groups in polydiacetylene molecules due to restricted accessibility of the more voluminous solvent. Conditions such as these may lead to relative insensitivity of polymer-solvent interactions to moderate changes in solvent composition. Carbon tetrachloride, used in these experiments has a molar volume excess of less than 20% over that of chloroform whereas hexane is over 60% greater in molar volume than chloroform, as calculated from their respective molecular weights and densities.

From Figure 25 one can see that the blue-to-yellow transition occurs over a much larger composition range than does the yellow-to-blue transition showing clearly the difference in kinetics between the two transitions. For the yellow-to-blue transition the period of time between initial mixing and optical absorption measurement (ca. 13 min.) is long in comparison with the time required for the transition to occur. The blue-to-yellow transition, however, is slow in comparison to the time allowed for the transition to occur before measurement (52,56). The data in Figure 25, therefore, do not define true equilibrium curves since the transition ranges are dependent upon allotted time before measurement. Also, there is expected to be greater scatter in the points measured for the blue-to-yellow transition since spectral changes are still proceeding at the time of the measurement, whereas the spectra for the yellow-to-blue transition are changing very slowly at the time of the measurement. These observations agree with the results of Chance et al. (52,56) for the poly(3BCMU)/CHCl<sub>3</sub>/hexane system. In their experiments, the yellow-to-blue transition proceeded rapidly at short times, but continued to progress slowly at longer times, whereas the reverse transition rate was slow at short times and accelerated at longer times. Chance et al. theorized these kinetics to be indicative of a single chain mechanism due to an observed independence of polymer concentra-

tion for the transition kinetics. However, in the experiments, similar transition behaviors were observed in the presence of a distinct polymer concentration dependence for the chromic transition, which rules out the postulation that this particular form of kinetics may uniquely describe a single chain mechanism for the conformational transition. The multi-chain transitions may be ascribed to formation of aggregates (yellow-to-blue) and dissociation of these structures (blue-to-yellow). At least initially, the aggregation process occurs at a faster rate.

### 3.3.2 Thermochromic Transition

Differences in solution behavior of polydiacetylenes are also observed for the thermochromic transition of polydiacetylenes when solvent components are varied. In Figure 26 are shown visible absorption spectra of solutions of poly(4BCMU)/15% CHCl<sub>3</sub>/85% CCl<sub>4</sub> between 39°C and 59°C. The peak at 460 nm predominates when the solution is yellow, or when the polydiacetylene molecules assume coiled conformations. As the solution is cooled to 39°C, the molecules assume rod-like conformations, and the solution turns red. A peak at 540 nm appears and grows in intensity with decreasing temperature.

Figure 26. Visible absorption spectra of poly(4BCMU)/15% CHCl<sub>3</sub>/85% CCl<sub>4</sub> obtained as a function of temperature. CHCl<sub>3</sub> and CCl<sub>4</sub> are respectively good and very poor solvents for poly(4BCMU).

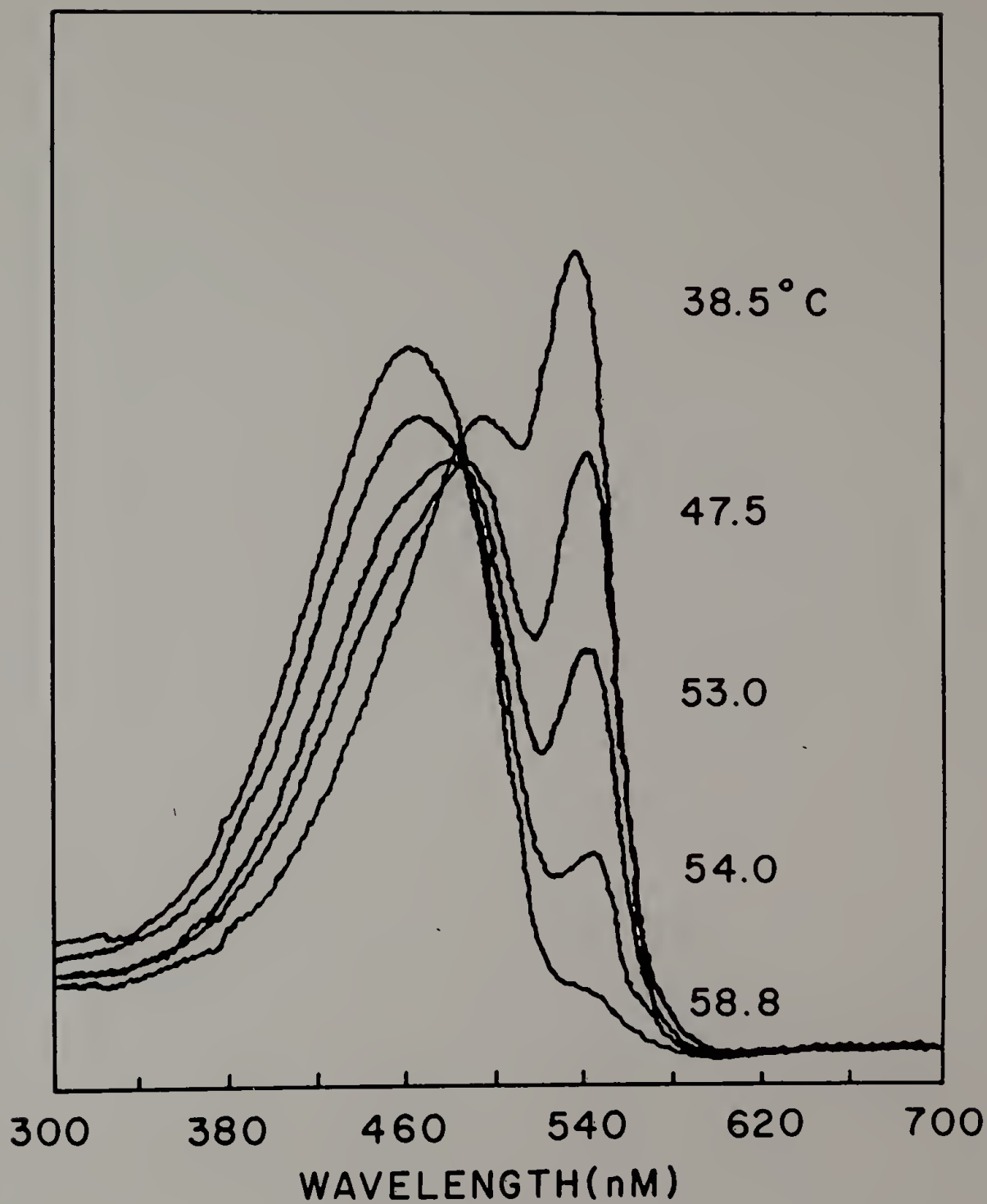


Figure 26.

Lim et al. (39) found that the thermochromic transition for the poly(4BCMU)/CHCl<sub>3</sub>/hexane system shows no hysteresis (see Figure 23). The changes in the optical spectra coincide for the heating and cooling cycles. As seen in Figure 27, this is not the case for the poly(4BCMU)/CHCl<sub>3</sub>/CCl<sub>4</sub> system. The red-to-yellow transition upon heating occurs at higher temperatures than does the yellow-to-red transition upon cooling. The transitions also occur over narrower temperature ranges than those found in the CHCl<sub>3</sub>/hexane system. Carbon tetrachloride partially dissolves poly(4BCMU) at higher temperatures due to van der Waals interactions of solvent with polymer, whereas no solubility at elevated temperatures can be detected for poly(4BCMU) in hexane. This indicates that short-range van der Waals interactions, between solvent and polymer as well as solvent-polymer hydrogen bonding, contribute to stabilizing polydiacetylene molecules in their coiled conformation.

### 3.4 Conclusions

Previous experiments on solutions of poly(3BCMU) in CHCl<sub>3</sub> and n-hexane have detected no polymer concentration dependencies for the solvatochromic transition in this system

Figure 27. The absorbance of the 540 nm (red phase) peak observed for poly(4BCMU)/15% CHCl<sub>3</sub>/85% CCl<sub>4</sub> solution as a function of temperature; ( □ ) represents the heating cycle; ( ● ) represents the cooling cycle.

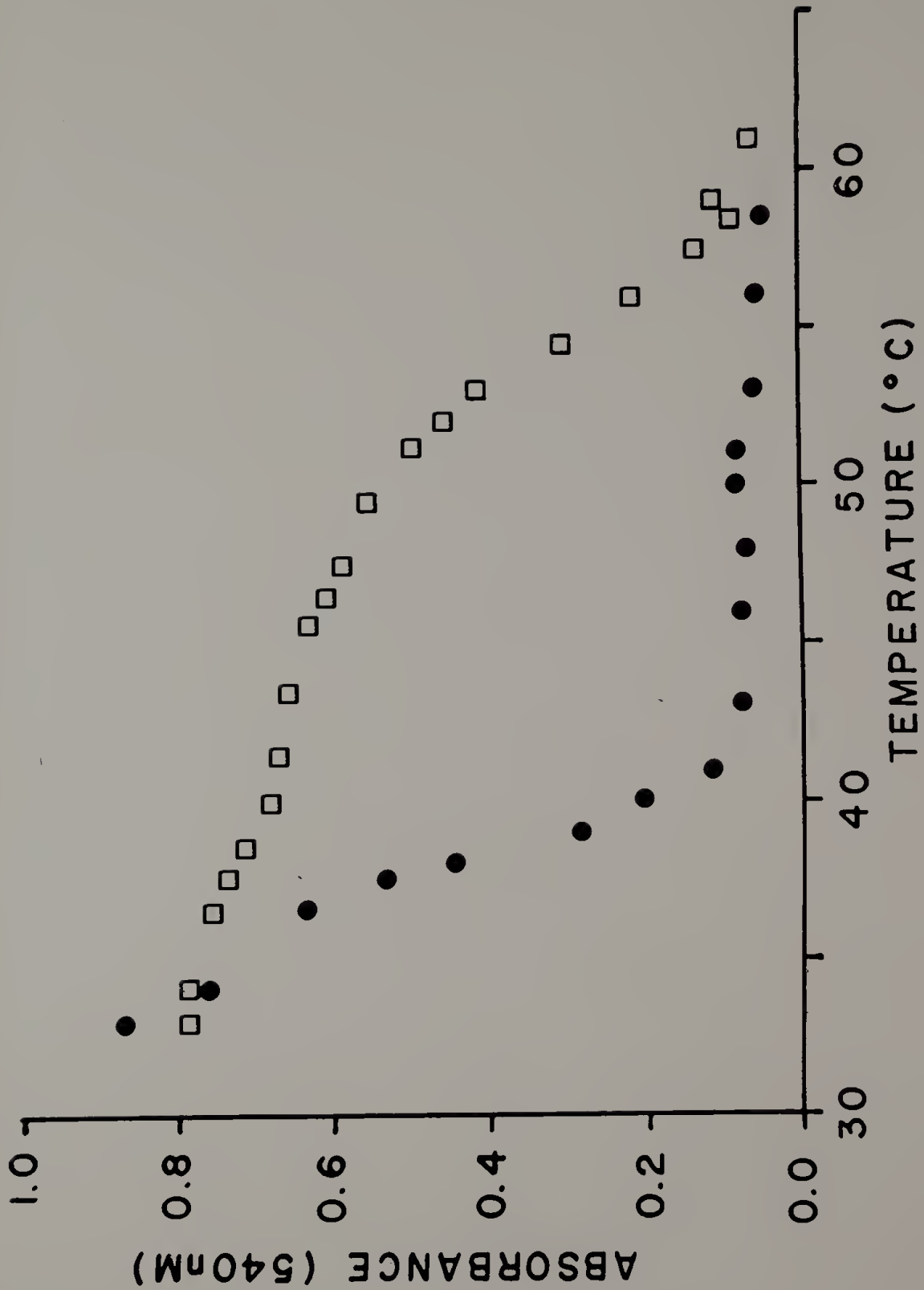


Figure 27.



(10,52,58). This observation was taken to be conclusive evidence that the chromic transition of polydiacetylenes in solution occurs by a single chain mechanism.

However, as the experimental results in this chapter demonstrate, the transition does not occur by a single chain mechanism in all solvent systems. Substitution of a more highly polarizable poor solvent,  $\text{CCl}_4$ , for n-hexane induces a pronounced polymer concentration dependence for the solvatochromic transition.

These experiments also showed that the kinetics of the transition from the coiled state (good solvent dominant) to the rod-like state (poor solvent dominant) significantly differs from the kinetics of the reverse transition. In these multi-chain transitions the formation of aggregated species occurs, at least initially, at faster rates than do the breakup of these aggregates.

Studies of the thermochromic transition for the poly(4BCMU)/ $\text{CHCl}_3$ / $\text{CCl}_4$  system demonstrated once again the critical role of the solvent in determining the mechanism of the transition. It was found that the blue-to-yellow (heating) and yellow-to-blue (cooling) transitions show a considerable hysteresis, as measured by visible absorption. This observation is in sharp contrast to the lack of hysteresis found in the poly(4BCMU)/ $\text{CHCl}_3$ /n-hexane system (39).

## CHAPTER 4

### SPECTROSCOPIC STUDIES OF HYDROGEN BONDING IN SOLUTIONS, GELS, AND FILMS OF POLYDIACETYLENES

#### 4.1 Introduction

Polydiacetylenes are unique in that an intricate coupling exists between molecular conformational structure and the extent of delocalization of  $\pi$  electrons in the main chain backbone. As was shown in the work of the previous chapter, visible absorption spectroscopy may be used to monitor the degree of conjugation within the  $\pi$  bond network of polydiacetylene chains. A number of other physical characterization techniques can be employed to probe changes in conformational structure of polydiacetylenes. Infrared spectroscopy, in particular, finds extensive use in the study of those polydiacetylenes containing substituents capable of undergoing intramolecular hydrogen bonding. In these cases, utilization of infrared spectroscopy permits one to follow the formation and dissociation of intramolecular hydrogen bonding in polydiacetylene solutions, gels, and films. Dissociation of hydrogen bonding species in the sidegroups would be expected to be indicative of loss of side chain order. If it can also be shown that a strong correlation exists between the extent of intramolecular hydrogen bonding and the degree of conjugation in the main chain backbone, then it is possi-

ble to use a variety of developed techniques of infrared spectroscopy to investigate conformational and electronic structure in polydiacetylenes. As the work that is described in this section will show, establishment of this correlation was possible for solutions and gels of polydiacetylenes but was not obtainable for films of polydiacetylenes. In summary, the work presented in this chapter examines the role of intramolecular hydrogen bonding in the chromic transitional behavior and the structure of polydiacetylenes in the solution, gel, and film states.

The correlation between intramolecular hydrogen bonding and electronic structure in polydiacetylenes was first considered by Patel et al. (33) after their discovery that the polydiacetylenes (see Figure 17) poly[4,6-decadiyne-1,10-diol bis((n-butoxycarbonyl)-methyl) urethane] (denoted as poly(3BCM)) and poly[5,7-dodecadiyne-1,12-diol bis((n-butoxycarbonyl)-methyl) urethane] (denoted as poly(4BCM)) are both soluble in common organic solvents such as chloroform and tetrahydrofuran. Patel et al. also discovered that changes in solvent quality (10) and temperature changes (8) could induce reversible color changes, or chromic transitions, in these solutions. Solutions of poly(3BCM) and poly(4BCM) were observed to turn from blue to yellow and from red to yellow respectively with the addition of good solvent or thermal energy. These chromic transitions were

manifested in visible absorption measurements in which solutions of poly(3BCMUs) and poly(4BCMUs) underwent shifts of 5000 and 2000  $\text{cm}^{-1}$  respectively in visible absorption maxima. These shifts can be attributed to extensive changes in the extent of  $\pi$  electron delocalization in the conjugated chain backbone.

Patel et al. (9,10) also studied solutions and films of poly(3BCMUs) and poly(4BCMUs) using vibrational spectroscopy. They showed that there are large scale disruptions of intramolecular hydrogen bonding in proceeding from red solutions for gels of poly(4BCMUs) and blue solutions or gels of poly(3BCMUs) to yellow solutions of each. The Amide I and N-H stretching regions were observed as a function of solvent quality for poly(3BCMUs) in various mixtures of chloroform, a good solvent for poly(3BCMUs), and n-hexane, a poor solvent for poly(3BCMUs).

Shown in Figure 28 are visible absorption and infrared absorption spectra for solutions of poly(3BCMUs) for increasingly larger mole fractions ( $X_C$ ) of chloroform in the mixed solvent. The progression of the solvatochromic transition is evident from the visible absorption data. The absorption band of lowest energy at about 15,900  $\text{cm}^{-1}$  (630 nm) measured in the blue solutions is very close to the corresponding value measured for poly(3BCMUs) single crystals (9) in which conjugation lengths exceed chain lengths. A dramatic drop in

Figure 28. Visible absorption and Fourier transform infrared spectra of poly(3BCMU) in various mixtures of  $\text{CHCl}_3$  and n-hexane. The fraction of  $\text{CHCl}_3$  in n-hexane is indicated. Polymer concentrations are  $1.9 \times 10^{-5}$  mol/lit for the visible spectra and  $1.3 \times 10^{-3}$  mol/lit for the FTIR spectra.  
(from Patel, et al., ref. 10)

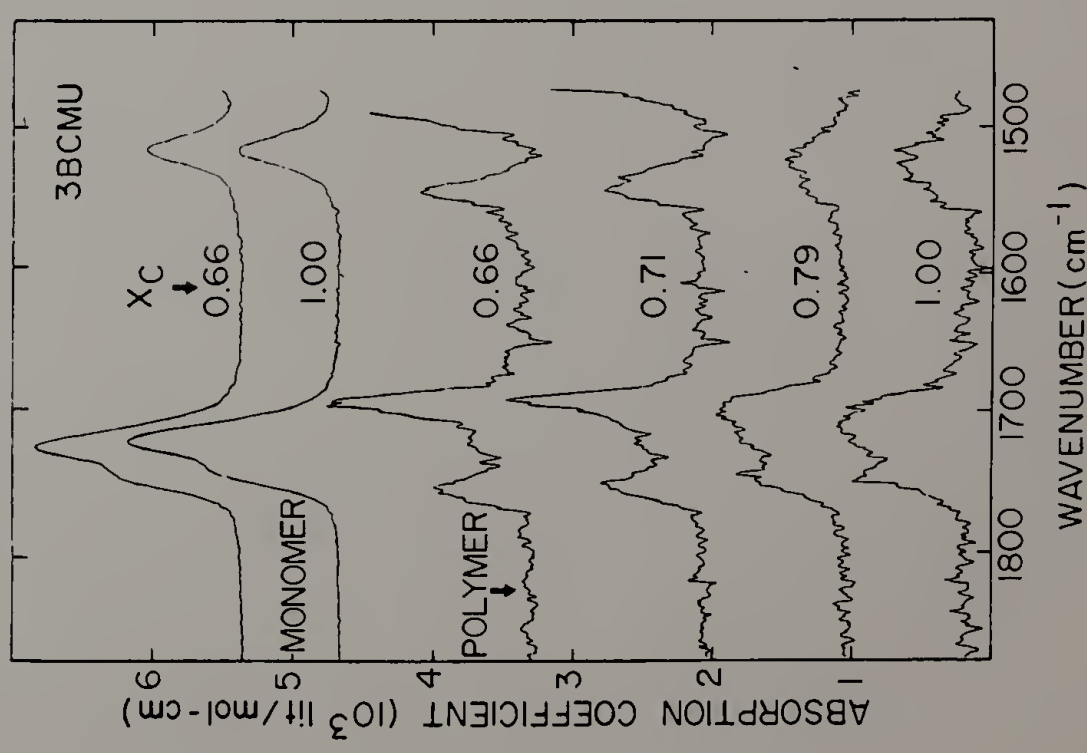
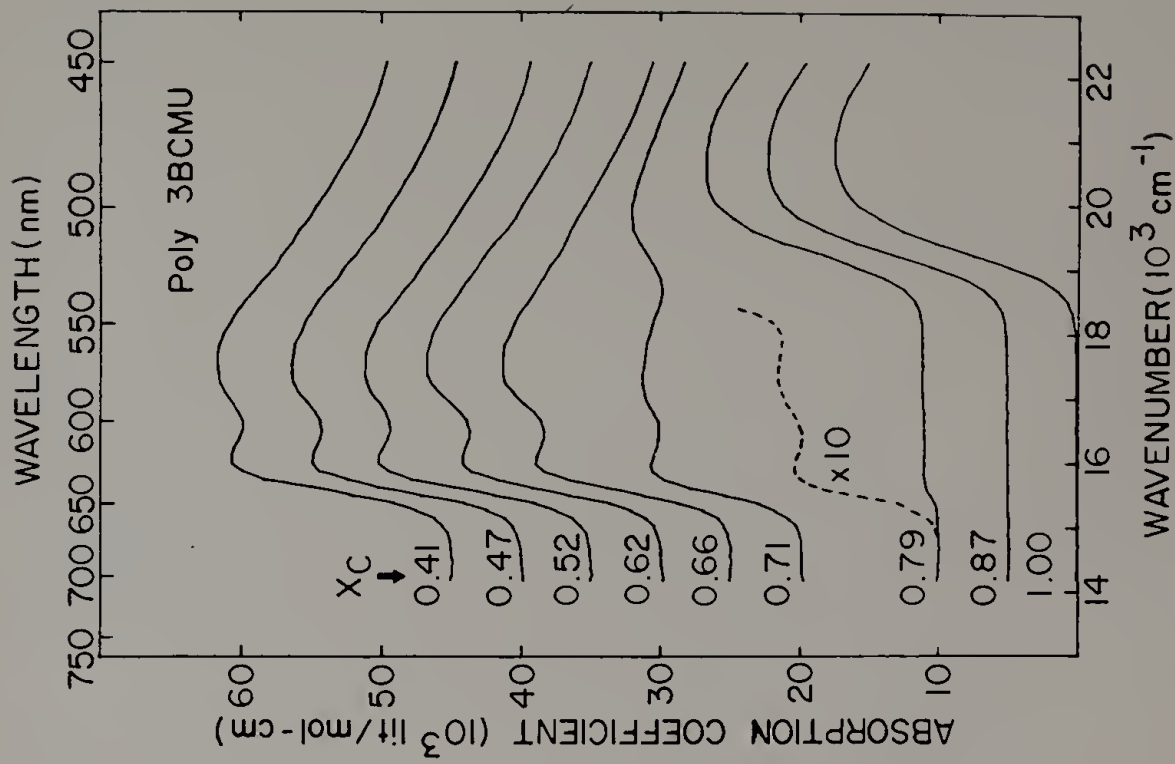


Figure 28.

conjugation length occurs when the mole fraction of chloroform in the solvent exceeds 0.71. This is evidenced by the  $5000\text{ cm}^{-1}$  shift of absorption maxima to a broad peak of higher energy centered around  $21,000\text{ cm}^{-1}$  (480 nm). From this data Patel et al. surmised that the conjugation lengths of poly(3BCMU) molecules in solution range over about 6 or 7 monomeric repeat units.

Also displayed in Figure 28 are corresponding infrared spectra for the solvatochromic transition of poly(3BCMU) in chloroform and n-hexane. The Amide I and Amide II regions are shown. The monomer spectrum, which is virtually unaffected by solvent composition variations, displays two sharp peaks at  $1725$  and  $1520\text{ cm}^{-1}$  respectively corresponding to Amide I and Amide II group vibrations free of intramolecular hydrogen bonding. The shoulder band at  $1745\text{ cm}^{-1}$  corresponds to a carbonyl stretching within the ester group. This band becomes distinct in the solution spectra and is relatively unaffected by solvent quality changes. However, the intensities of the non-bonded components of the Amide I and Amide II are dramatically reduced in the blue solutions ( $X_C \leq 0.71$ ) at the expense of hydrogen bonded components at about  $1695\text{ cm}^{-1}$  for the Amide I region and about  $1545\text{ cm}^{-1}$  for the Amide II region. These latter peaks abruptly decrease in intensity as the blue to yellow transition occurs, and the non-bonded components intensify.

The abrupt dissociation and reformation of intramolecular hydrogen bonding between urethane substituents are seen to accompany the extensive changes in chain backbone conjugation apparent from the visible absorption data. Chance et al. (52) thus speculated that formation of intramolecular hydrogen bonding induces and stabilizes planarity of the chain backbone in these molecules. Chance et al. (52) have also postulated conformational transitions from fully extended molecules with planar backbones to molecules with numerous discrete non-planar defects or rotations in the chain backbones (Figure 18A). Therefore, according to Chance et al., the conformational transition, which is responsible for the large scale changes in electronic conjugation associated with the chromic transition, has a driving force consisting of the formation and dissociation of hydrogen bonds between side group substituents.

Heeger et al. (38) have reached similar conclusions and have gone so far as to model the conformational transition of polydiacetylenes in solution according to the Zimm and Bragg (44) model for helix-coil transitions. According to Heeger et al. (14) a cooperative type transition from a rod-like state to a coiled state occurs due to the relative energetic and entropic stabilities of intramolecularly hydrogen bonded sequences would then give rise to cooperative type restructuring within single chains of polydiacetylene molecules.



The Heeger model, as well as the general idea of formation and disruption of intramolecular hydrogen bonding serving as a driving force for the chromic transition, has been criticized on a number of grounds. Schweizer (17) has argued that correlations between hydrogen bonding groups on polydiacetylene side chains are nonexistent beyond neighboring monomeric units. He further argued these bonds can form or dissociate locally unlike the case of polypeptides in which formation of isolated hydrogen bonds within the chain backbone is highly unfavorable from an energetic standpoint. Schweizer also invoked the examples of polysilanes (47,48) and non-hydrogen bonded polydiacetylenes (45,46) as conjugated systems which undergo distinct conformational order-disorder transitions in the absence of any intramolecular hydrogen bonding.

Furthermore, Painter et al. (50) have shown through infrared spectroscopic and differential scanning calorimetric measurements on films of poly(4BCMU) that dissociation of intramolecular hydrogen bonding reflective of side chain disordering occurs at lower temperatures than does the disordering transition in the chain backbone. Thus, in the case of polydiacetylene films, at least, formation or disruption of intramolecular hydrogen bonding does not serve as the driving force for the chromic transition.

Regardless of the fact that the chromic transitions of polydiacetylene in solutions are not driven by changes in intramolecular hydrogen bonding in all cases, or perhaps in any case, it is still of general interest to establish, when possible, definitive correlations between intramolecular hydrogen bonding in sidegroups and the extent of conjugation or electronic delocalization in the main chain backbones. Intramolecular hydrogen bonding certainly contributes to the stability of the rod-like, highly conjugated conformations of polydiacetylenes in solution as evidenced from the higher transition temperatures for hydrogen-bonded polydiacetylenes over non-hydrogen-bonded polydiacetylenes in similar solvents.

Although a one-to-one correspondence between the dissociation of hydrogen bonds in sidegroups and the disruption of the rod-like conformation of the main chain is suggested by the infrared and visible spectroscopic data of Patel et al. (Figure 28), a truly definitive correlation cannot be made from this data for a number of reasons. Firstly, any observed correlation between the two sets of data can only be qualitative at best due in part to the relatively low signal-to-noise of the infrared data arising from solvent absorption band interference. Secondly, intermediate stages of the solvatochromic transition are not apparent from these sets of data, and it is possible that the one-to-one correspondence

does not hold during the stages where the changes in side-groups and backbone structure are occurring most rapidly. Thirdly, the varying kinetics of the solvatochromic transition as discussed in the previous chapter, makes precise determination of the one-to-one correspondence difficult. The rates of cooling and heating in studies of the thermochromic transition are more easily controlled than the solvent compositions, polymer concentrations, solvent mixing times, etc. in studies of the solvatochromic transition. Lastly, the polymer concentration used in the studies of Patel et al. differed greatly between that used in the visible absorption studies ( $1.9 \times 10^{-5}$  mole/liter) and those used in the infrared absorption studies ( $\geq 1.3 \times 10^{-3}$  mole/liter). Given the data outlined in the previous chapter showing that the chromic transition is concentration dependent (57), it is important to study solution of the same polymer concentration for both the visible and infrared absorption studies. A major goal of this work was to definitively establish a one-to-one correspondence, under the correct conditions cited above, between changes in intramolecular hydrogen bonding and changes in electronic delocalization within polydiacetylene backbones.

Establishing such a correlation between changes in side chain structure and changes in backbone structure is important in that it becomes possible to use a number of special-

ized techniques developed for infrared spectroscopy as indirect probes of changes in chain conformation of polydiacetylenes in solution. For example, polarized infrared spectroscopy can be used to investigate orientation effects in gels and solutions of polydiacetylene under the effects of applied electric fields or set physical boundaries surrounding the sample.

Heeger and his co-workers (55,59-61) have conducted a number of experiments of these types using characterization techniques other than infrared spectroscopy. Heeger et al. (55) found that the electric field induced birefringence of solution of poly(4BCMU) in toluene increases by a factor greater than 300 in going from a yellow solution at 80°C to a red solution at room temperature. This data was taken by Heeger et al. to be definitive proof of a coil to rod-like conformational transition of polydiacetylene molecules. Also, from transient electric field and birefringence experiments, Heeger et al. determined a free rotational relaxation time of 0.1 second for molecules in red solutions consistent with a value expected for single isolated rod-like molecules free of any aggregation effects. Wegner et al. (51), who have postulated that rod-like polydiacetylene molecules in solution can exist only in the form of chain aggregates, have criticized Heeger's data in terms of both quantitative evaluation and interpretation.

Orientation effects in gels have also been studied by Heeger and Casalnuovo (60). They found that gels of poly(4BCMU) in toluene exhibit spontaneous, long-range, nematic alignment solely under the effects of physical boundaries enclosing the samples. This alignment within the gels, as detected by optical birefringence, occurs without the external shearing or stretching necessary to align other polymeric gels. Birefringence in these systems is reflective of ordering of chain backbones with highly anisotropic polarizability (i.e. the polarizability is large parallel to the chain direction).

The question can then be raised of whether alignment of sidegroups of polydiacetylenes in gels occurs in conjunction with backbone ordering. Polarization infrared spectroscopy could be used to detect ordering of hydrogen bonds in sidegroups of gelled polydiacetylene molecules. However, the relatively small degree of ordering obtainable for this system (second moment orientation function on the order of 0.02 (ref. 60)) would not easily be measured by ordinary polarization spectroscopy. On the other hand, polarization modulation spectroscopy (62-64), with its substantially smaller measuremental dynamic range requirements, is ideal for measuring low degrees of orientation. In our work, polarization modulation spectroscopy, which directly measures differences in absorption for two orthogonal polarizations,

was used to detect alignment of hydrogen-bonded sidegroups within these polydiacetylene gels.

The process of gelation of polydiacetylenes in solution is fascinating in itself. Poly(4BCMUs) is known to gelate at remarkably low polymer concentrations ( $\geq 6 \times 10^{-4}$  g/ml) in toluene (65) a poor solvent for poly(4BCMUs). The process is reversible and is thought to occur simultaneously with the chromic transition to the red-like form of polydiacetylene molecules (8). Although the mechanism for gelation is not clear at this time, specific interactions between polydiacetylene molecules and between polydiacetylene and solvent molecules must by some manner stabilize the gel structure in the absence of chemically bonded cross-links. It is conceivable that these interactions and the formation of a gel could perturb the chromic transition associated with poly(4BCMUs) in solution. As will be shown, the questions stated above were tested for and resolved in most cases using infrared spectroscopic techniques (66).

The correlation between extent of intramolecular hydrogen bonding and extent of conjugation within chain backbones, as measured respectively by infrared and visible spectroscopy, was used to further advantage in this work. Specifically, it was investigated as to whether significant intramolecular hydrogen bonding could occur for polydi-

acetylenes solvated at low temperatures within the presence of moderately strong hydrogen bonding solvents.

Indications that this premise would hold true come from the work of Chance et al. (67). Chance and his co-workers were able to demonstrate using visible spectroscopy that the chromic transition (yellow phase to red phase) can occur at low temperatures to varying extents for poly(4BCMU) molecules in the presence of hydrogen bonding solvents. Chance et al. found that a 55%  $\text{CHCl}_3$ /45% hexane (mole fraction) solution of poly(4BCMU) showed the most substantial increase in average conjugation lengths within the chain backbones. In experiments detailed in this chapter, solutions of poly(4BCMU) in hydrogen bonding solvents were quenched so as to promote intramolecular hydrogen bonding between polymer side groups. Infrared spectroscopy showed that such bonding did occur to a significant extent at the expense of diminished polymer-solvent interactions.

#### 4.2 Experimental

Poly(4BCMU) was prepared in Professor G. Wegner's laboratory and was synthesized according to the scheme outlined in the Introduction section of Chapter 3. Solutions used in the infrared studies were prepared by dissolving poly(4BCMU) either in reagent grade toluene or in ortho-dichlorobenzene at 85°C and 110°C respectively and then were

allowed to cool to room temperature. The concentration of the toluene solution is 0.24% by weight, four times the critical concentration required for gelation (62). However, the polymer concentration for the o-dichlorobenzene is 0.09% by weight, slightly lower than the concentration needed for gelation (8). More dilute solutions are not suitable for infrared spectroscopic studies because of solvent peak interference and poor signal-to-noise ratio.

All infrared data, except in the polarization modulation experiment, were obtained with an IBM model 98 spectrometer with a nitrogen purged box constructed in this laboratory. The spectral resolution was kept at  $2\text{ cm}^{-1}$ , and 200 scans were signal-averaged. In some cases, it was found that the most convenient way to eliminate solvent interference was to ratio solution spectra against solvent spectra obtained under identical optical conditions. Gels were sandwiched between two KBr plates. The heating and cooling rates were kept at 3 degrees every 15 minutes. A representative spectrum is shown in Figure 29. Previous studies have shown that the N-H stretching vibration is extremely sensitive to the hydrogen bonding characteristics. Representative spectra of polydiacetylene solutions and films in the red or yellow phases are shown in Figures 30 and 31, respectively.

Optical spectra were obtained with a Beckman DU-40 spectrometer with a scan speed of 750 nm/min. Gels or solutions



Figure 29. Infrared spectrum of a poly(4BCMU)/toluene gel. Strong toluene peaks occur in the regions indicated by dotted lines.

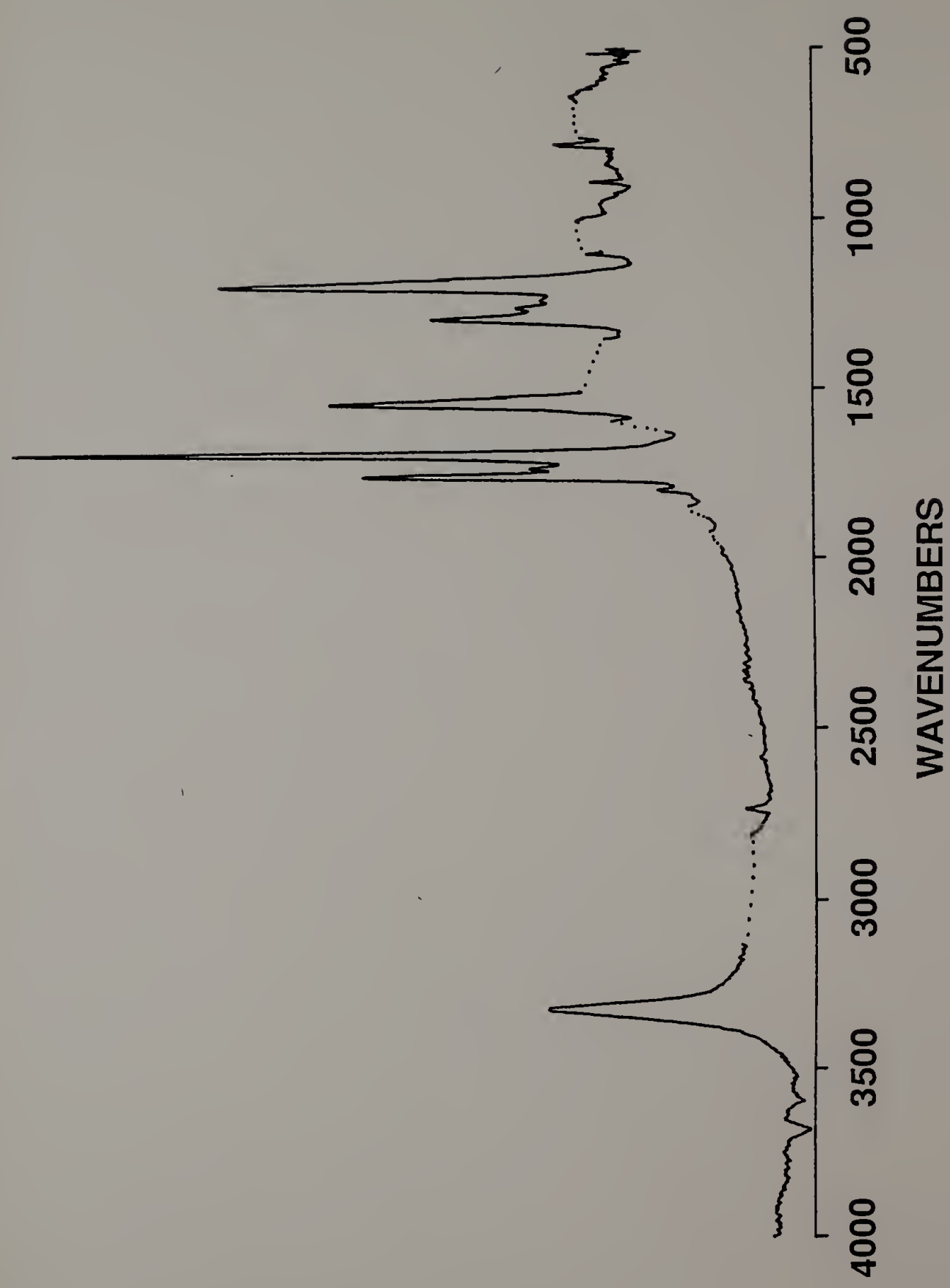


Figure 29.

Figure 30. Comparison of infrared spectra in the NH stretching region for A) film, B) toluene gel and C) o-DCB solution in the red phase.

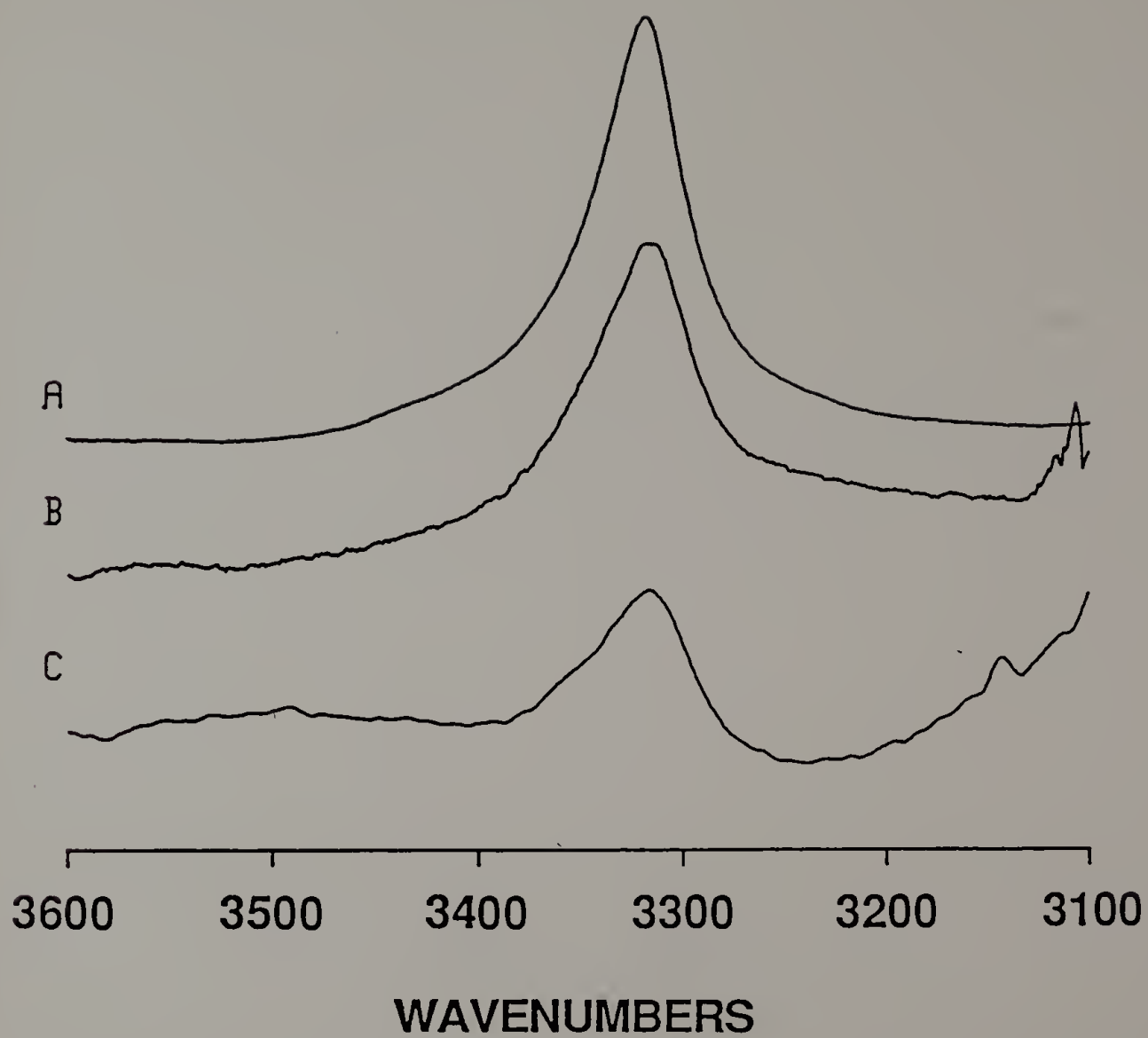


Figure 30.

Figure 31. Comparison of infrared spectra in the NH stretching region for A) yellow film, B) yellow toluene solution, and C) yellow o-DCB solution.

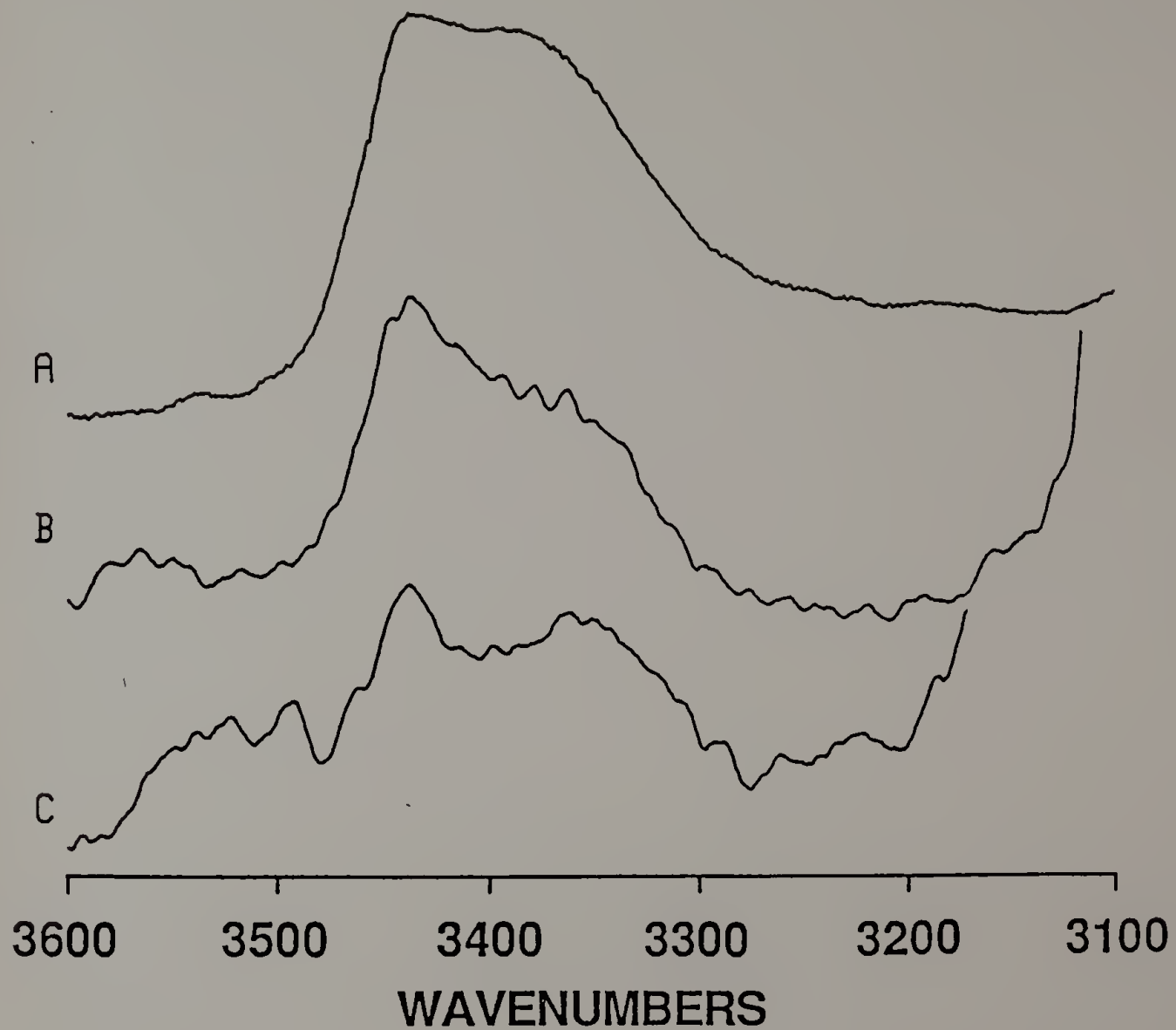


Figure 31.

were placed in a calibrated quartz cuvette with a heating jacket built in this laboratory or in a Harrick heating cell with glass windows. The optical path in this experiment was adjusted so as to keep the highest absorbance measurement below 2.0.

In the polarization modulation experiment, measurements of linear dichroism in the form of difference spectra were obtained for a gel of poly(4BCMJ) in toluene (0.2% by weight). The spectra were obtained on a Nicolet 60SXB spectrometer.

A general scheme for a modulation experiment is shown in Figure 32. Linear polarized light from the interferometer is alternately polarized between two orthogonal directions due to the action of a sinusoidally driven, stressed birefringent crystal. After the signal is detected and preamplified, it is sent to a lock-in amplifier where it is subjected to narrow band filtering (about the modulation frequency) and demodulation. The net result is a single beam difference spectrum, which when properly calibrated has intensities given by (62):

$$I_{ac}(\nu) = 0.50 [I_{\parallel}(\nu) - I_{\perp}(\nu)] \quad (14)$$

This spectrum then represents a direct measurement of the difference in intensities measured for transmission of polarized radiation parallel and perpendicular to the sample orientation direction. If however, the detected signal is subjected to low pass filtering, a spectrum is obtained

Figure 32. Block diagram of polarization modulation experiment.



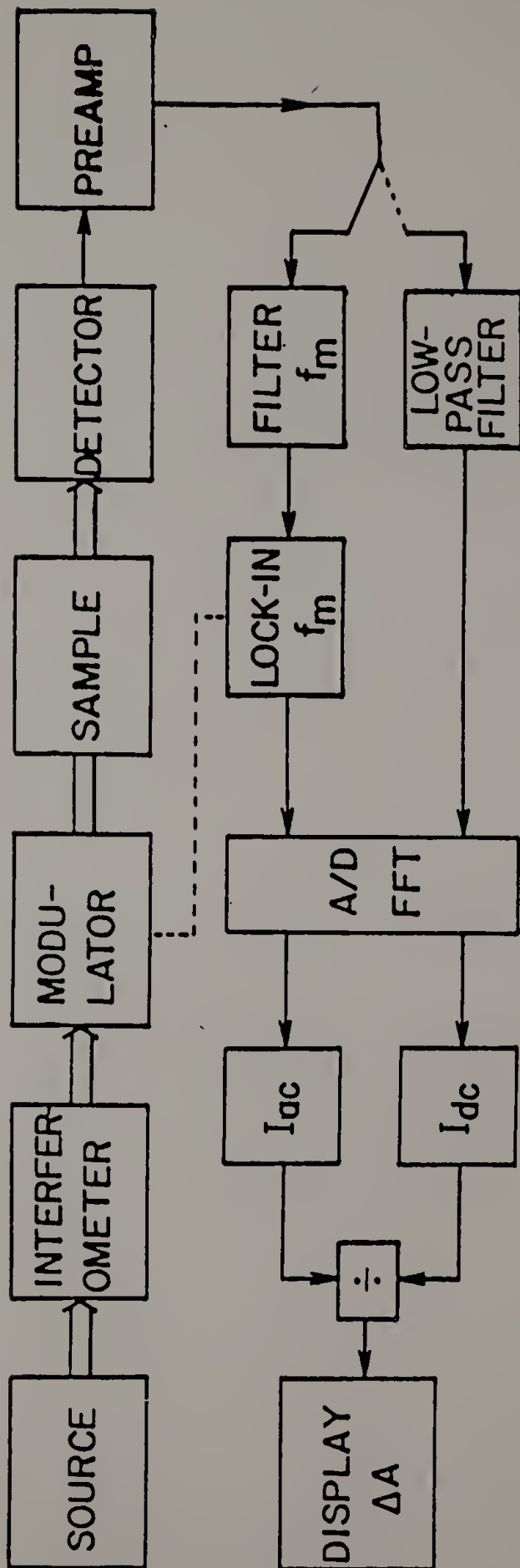


Figure 32.

representing the simple average of the intensities measured for parallel and perpendicular polarizations (62):

$$I_{dc}(\nu) = 0.50 [I_{\parallel}(\nu) + I_{\perp}(\nu)] \quad (15)$$

To provide modulation of the infrared signal, a Hinds International series II photoelastic modulator with a ZnSe crystal was used. The crystal was driven at 74 KHz, effectively alternating the polarization at 148 KHz. A Harrick quad diamond polarizer was mounted in the infrared beam path before the modulator and sample.

The detected signal was taken directly from the amplifying stage of the 60SXB detector and sent to a PAR model 124A lock-in amplifier, which serves as a phase sensitive amplifier (mixer). A model 116 preamplifier was used for the input signal to the lock-in amplifier. The input signal is mixed with the modulation signal of 148 KHz and filtered within the lock-in amplifier electronics. The demodulated signal is reinserted into the amplifier of the 60SXB detector and processed in the normal manner to yield a difference spectrum.

### 4.3 Results and Discussion

#### 4.3.1 Correlation Between Backbone Structure and Hydrogen Bonding in Sidegroups

Visually observable color changes in polydiacetylene solutions serve as a means of monitoring conformational changes in the main chains of polydiacetylene molecules. The relative intensity of the peaks associated with the red solution (540 nm) or the yellow solution (460 nm) in optical absorption spectra serve as a more quantitative measure of the chromic transition. The intensity of the red peak at 540 nm as a function of temperature is shown in Figure 33A. There is a significant hysteresis cycle associated with the main chain structural change as has been reported (39). One of the easiest ways to characterize the amount and strength of hydrogen bonding in polydiacetylene is to follow the intensity of the N-H stretching vibration (Figure 34) associated with the urethane units. This is also plotted in Figure 33B. A direct correlation between the changes in the optical spectra and the amount of hydrogen bonded components in polydiacetylenes can be observed from these two figures. This correlation between changes in the main chains and sidegroups of polydiacetylene molecules has been assumed for some time, but has never been explicitly proven until now. Obviously,

Figure 33. Temperature dependence of A) integrated intensity of NH stretching vibrations and B) absorbance of the 540 nm peak for a poly(4BCMU)/toluene system.  $\square$  denotes the heating curve;  $\triangle$  denotes the cooling curve.

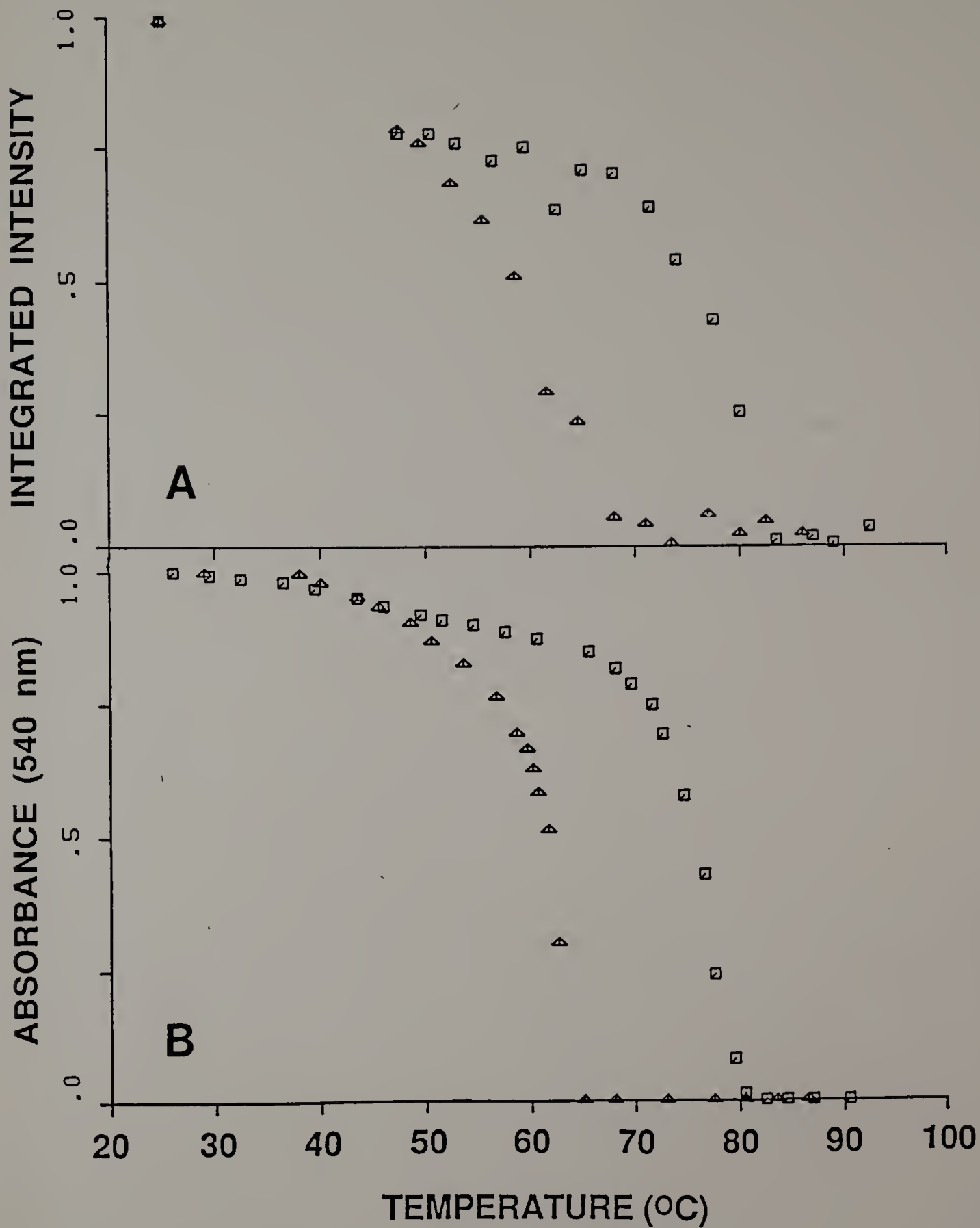


Figure 33.

Figure 34. FTIR spectra (N-H stretching region) of poly(4BCMU) in toluene (0.24 % weight polymer to volume solvent); 2  $\text{cm}^{-1}$  resolution; top spectrum corresponds to red gel at 24°C; bottom spectrum corresponds to yellow solution at 85°C.

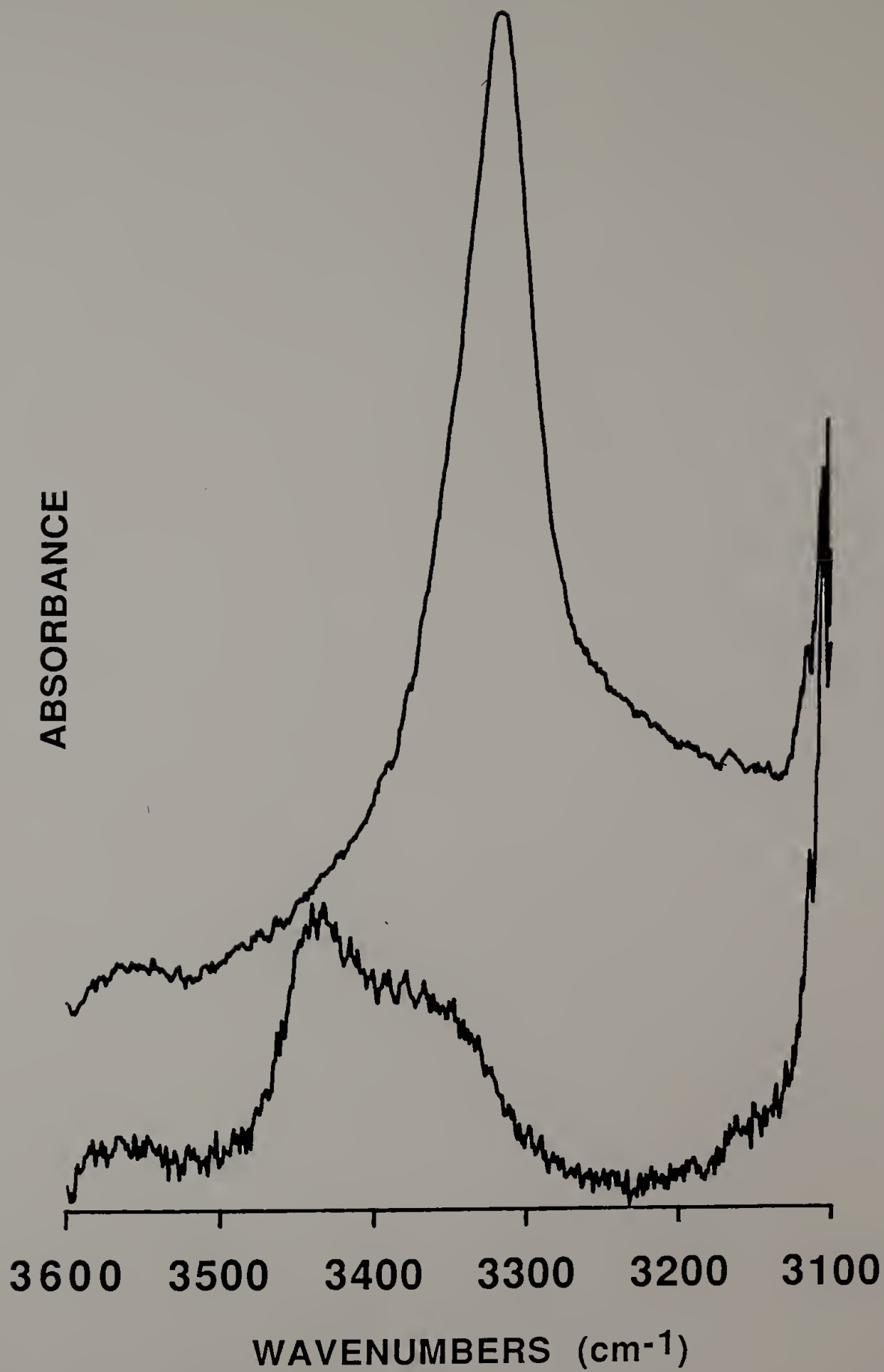


Figure 34.

this conclusion cannot be extended to polydiacetylenes which have no possibility of hydrogen bonding, yet exhibit chromic transitions as well (45,46). In that case other structural parameters must be considered to account for the disordering of the polymer chain.

Although used often in literature (1), the validity of using the N-H stretching vibration intensity as a quantitative measure of the amount of hydrogen bonding still needs to be clarified. Usually the vibrational frequency of N-H groups free from hydrogen bonding occurs at approximately 3400  $\text{cm}^{-1}$ . The groups participating in hydrogen bonds have frequencies varying from approximately 3250 to 3350  $\text{cm}^{-1}$ . The exact position depends on the strength of the hydrogen bonds formed (68). The usual practice is to compare the relative intensity of the two components, thus establishing the relative amount of hydrogen bonded components. Changing absorptivity as a function of hydrogen bond strength may severely perturb the quantitative aspect of this measurement (69). Secondly, in the polydiacetylene solutions specific polymer-solvent interactions may also change the intensity of the N-H stretching vibration measured. The spectroscopic changes that are observed may have little to do with the amount of intramolecular interactions between the urethane groups of the side chain. Lastly, although the perturbing effect is small, the possibility always exists that some of



the features or the intensity changes that are observed in the 3300 to 3400  $\text{cm}^{-1}$  region may arise from the Fermi resonance interaction of a higher order component and the fundamental N-H stretching vibration. Based on previous studies on polypeptides the last factor can be excluded since its effect is insignificant (70).

In the experiment, perturbation due to specific interactions between the polymer and the solvent is a real possibility and needs to be considered. The shape and peak position of the N-H stretching vibration for polydiacetylene in o-dichlorobenzene (o-DCB) in the red phase is basically the same as that observed for the film as shown in Figure 30. This indicates that there are no observable effects arising from specific interactions between the polymer and the solvent. The infrared spectra in the N-H stretching region, represented by the absorptions at 3350  $\text{cm}^{-1}$  and 3440  $\text{cm}^{-1}$ , of the yellow solution and films are identical as well, demonstrating that solvent does not seem to interact with the N-H groups. In the yellow solution, the intramolecular hydrogen bonds are dissociated, making it extremely favorable for hydrogen bonding to occur between the solvent and polymer when possible. The spectroscopic evidence suggests that this is not the case and the amount of hydrogen bonded species determined is not affected by specific polymer-solvent interactions.

When the poly(4BCMU) concentration is high, solution may gelate at room temperature. Previous studies (8) have not carefully considered effects of gelation and have, in fact, treated the gel and solution states as similar experiments. In order to clarify any possible effects of gelation on the chromic transition, one must examine systems in both the gel and solution states. In this work the o-DCB system is in an ungelated state while the toluene system is a gel. Integrated intensities of N-H stretching vibrations for both systems were plotted as functions of temperature in Figures 33B and 35B. The result is also compared with the extinction of the red peak (540 nm) in the optical spectrum (Figures 33A and 35A). Both the infrared and optical curves show identical hysteresis cycles and transition temperatures for either the gel or the solution. It can then be concluded that the process of gelation has no effect on the spectroscopic data.

The analysis in the C=O stretching region is more difficult, especially for the o-DCB system, due to low polymer concentration. Therefore, it is better to focus on the toluene system in which a multiplet feature was observed in this region. Among these peaks, only the one peak at  $1691\text{ cm}^{-1}$  will be used in the following discussion. In previous work, this band was unambiguously assigned to the Amide I vibration directly hydrogen bonded to the N-H group (71). Therefore the intensity of this vibration reflects the number

Figure 35. Temperature dependence of A) integrated intensity of NH stretching vibrations and B) absorbance of the 540 nm peak for a poly(4BCMU)/o-DCB solution.  $\square$  denotes the heating curve;  $\triangle$  denotes the cooling curve.

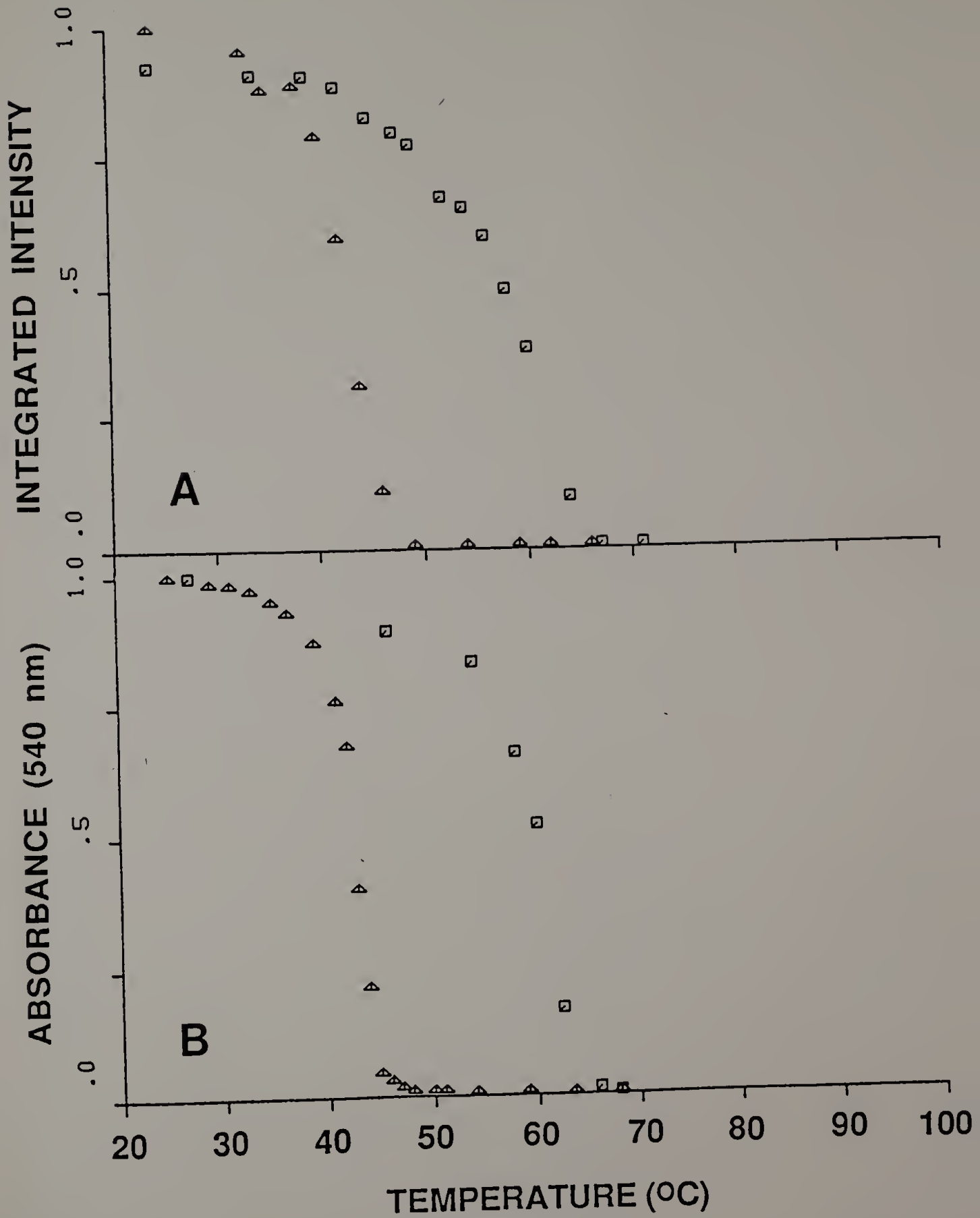


Figure 35.

of carbonyls intramolecularly bonded to the N-H groups. Least squares fitting was used to resolve this peak from others. The resulting integrated intensity of the  $1691\text{ cm}^{-1}$  band (Figure 36) is plotted as a function of temperature in Figure 37. A similar hysteresis curve to that of the N-H vibrations is observed and the transition temperature deduced from this curve is the same as that of the chromic transition. This is consistent with the claim that the change in backbone conformation and the changes in intramolecular hydrogen bonding in the side groups occur concurrently. The similar behavior between carbonyl stretching and N-H stretching in the toluene system also reveals that toluene molecules do not participate in any way in the formation of hydrogen bonding to the urethane groups of polymers.

In contrast to the above results, those obtained for the film are very different (Figure 38A,B). Firstly, both the curve for the extinction of the  $540\text{ nm}$  peak in the optical absorption spectrum and the curve for the intensity change in the N-H stretching band of a film do not recover their original values after a heating-cooling cycle. The reduction can be as high as 50% depending on thermal history and cooling rate. Secondly, the shape of each curve does not look the same as one another, even though both shapes of the curves show roughly the same transition region (between  $90$  and  $110^{\circ}\text{C}$ ). A relative sharp turn around transition is detected

Figure 36. FTIR spectra (Amide I region) of poly(4BCMU) in toluene (0.24% weight polymer to volume solvent); 2  $\text{cm}^{-1}$  resolution; red gel at 24°C has an intense peak at 1691  $\text{cm}^{-1}$ ; yellow solution at 85°C has an intense peak at 1728  $\text{cm}^{-1}$ .

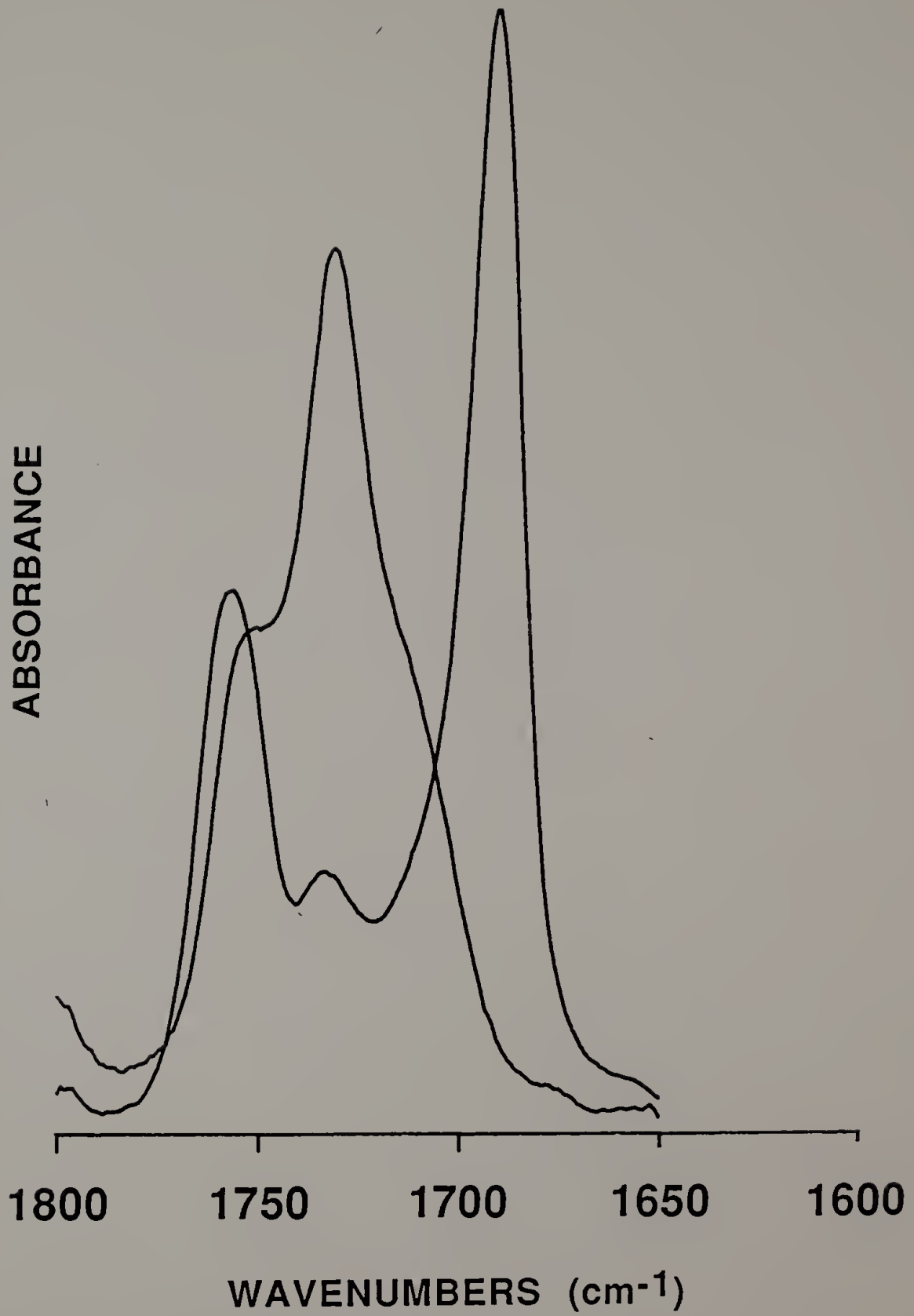


Figure 36.

Figure 37. Integrated intensity of the  $1691\text{ cm}^{-1}$  band as a function of temperature for a toluene system.  $\square$  denotes the heating curve;  $\triangle$  denotes the cooling curve.



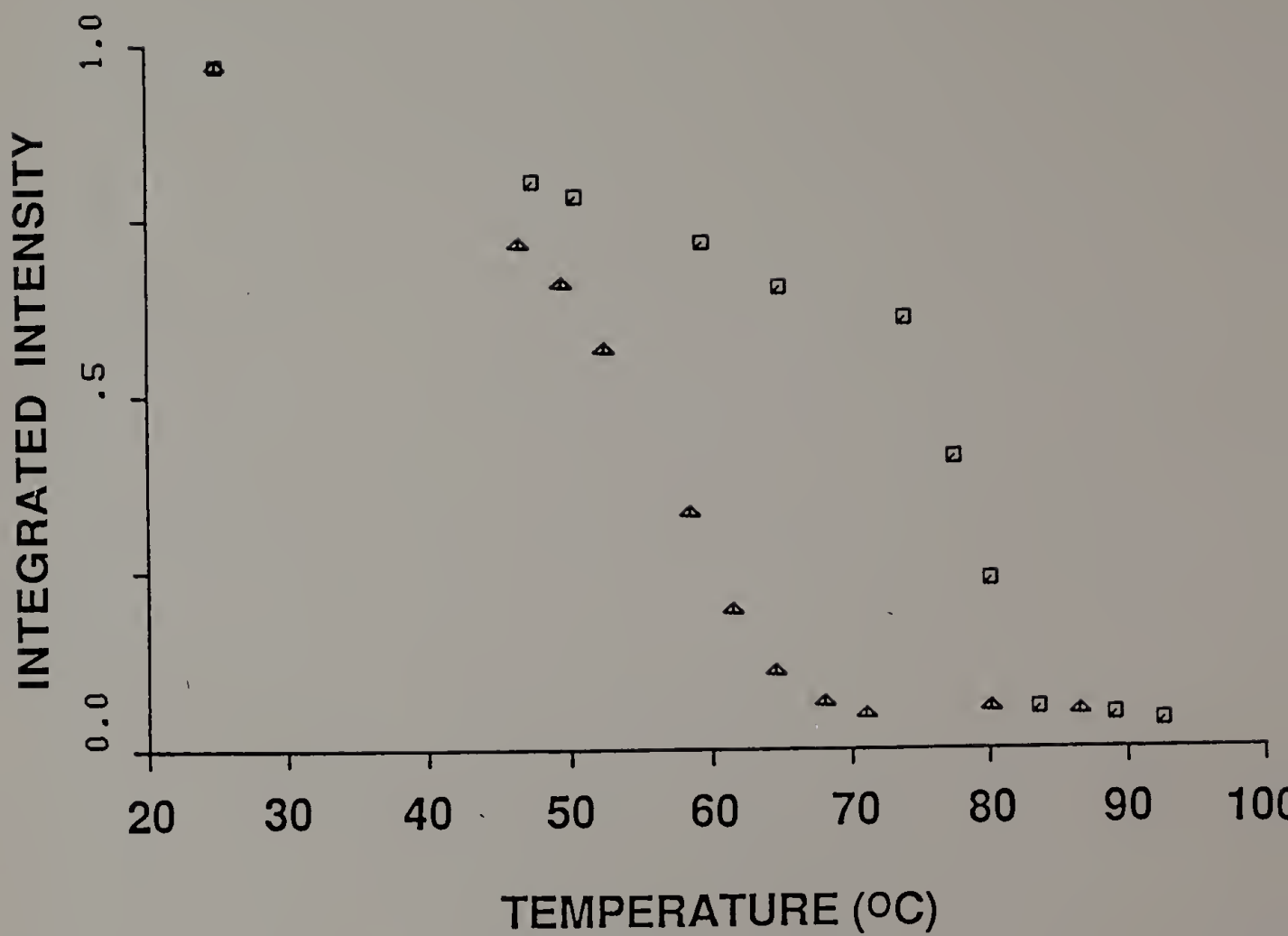


Figure 37.

Figure 38. Temperature dependence of A) integrated intensity of NH stretching vibrations and B) absorbance of the 540 nm peak for a film.  $\square$  denotes the heating curve;  $\Delta$  denotes the cooling curve.

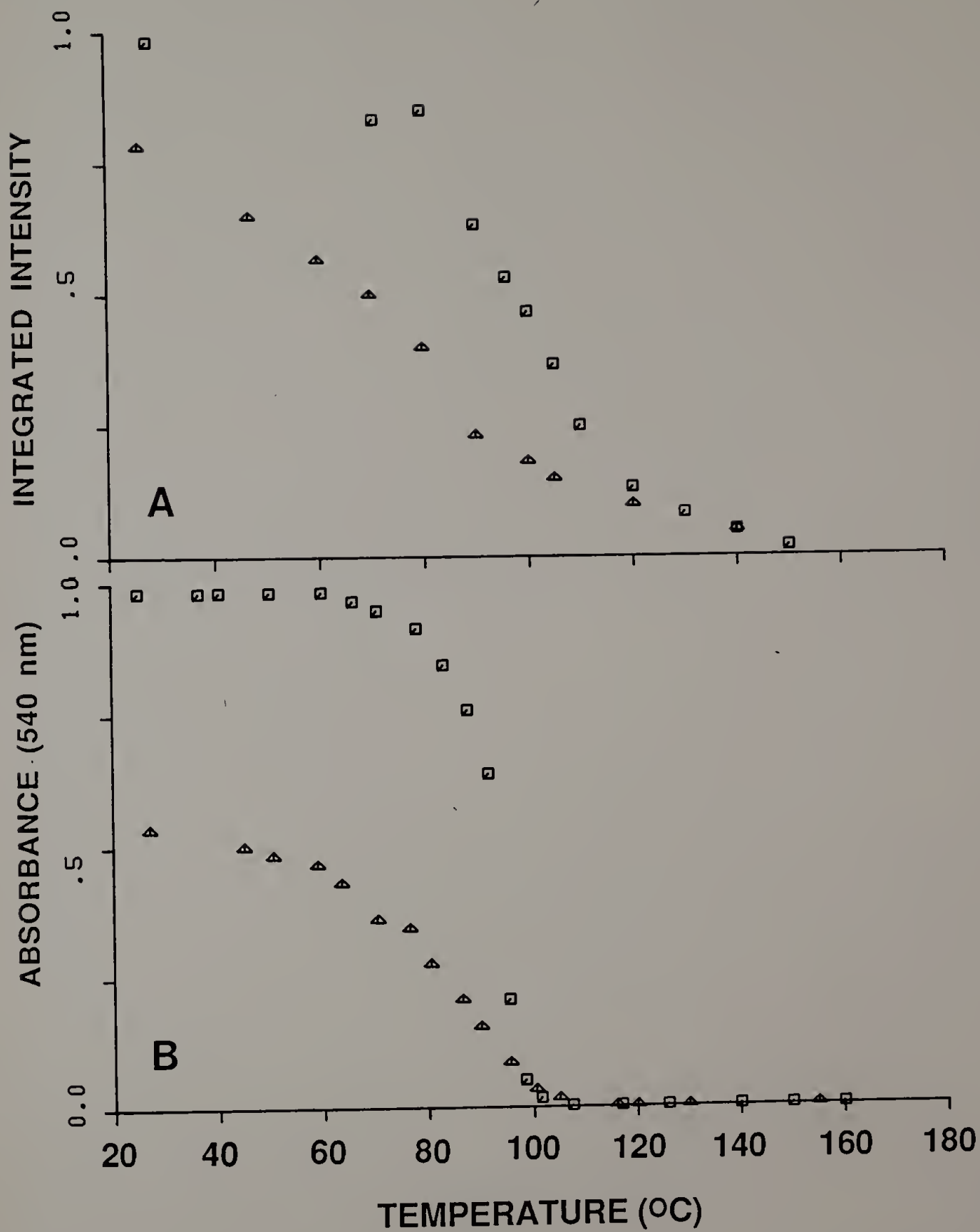


Figure 38.

in the optical curve, but a rather smooth inclination through the transition is seen in the N-H intensity curve.

A much clearer picture of the transition may be concluded from these spectral features. Through the transition only a limited amount of intramolecular hydrogen bonds are weakened. The extent of weakening is not as great as in solutions. This explains the gradual drop in the N-H intensity through the transition in films. At the same time the conformation of backbones also changes to give rise to the color change. Although the change is rather sharp, judging from the retention of the overall molecular orientation and packing order, one can conclude that the change in the backbone conformation is not as great as in solutions over similar measurement times. This means that a sharp color change may not necessarily imply a large scale disruption in the backbone conformation. A similar conclusion is reached by Peiffer and his coworkers on their study of the hydrodynamic radius change through the chromic transition (72).

The irreversibility in the intensities for films must arise for the following reason: upon cooling, large motion of polymers is necessary in order to recover the original state, but polymer-polymer interactions prevent it from happening in a short period of time. It was noticed that the time required for a film to reach an equilibrium state at a given temperature is at least one order of magnitude longer

than the time required for a solution. Therefore, changes in backbone and sidegroup structure must occur at vastly differing kinetic rates in polydiacetylene films. This may be indicative of different chain mechanisms responsible for the chromic transitions of polydiacetylenes in the film and solution states.

Overall, it was demonstrated that the chromic transition and weakening of intramolecular hydrogen bonding occur concurrently in solutions and that the transition is not perturbed by the gelation process. Although this correlation is a necessary condition for application of the cooperative rod-coil transition model, additional parameters would need to be considered; at this moment, no spectroscopic evidence is available to evaluate them. For films a similar correlation is not observed. The weakening in hydrogen bonding occurs by a slower path route and all spectral changes are irreversible. These fundamental differences between the film and solution states may be due to the effect of strong polymer-polymer interactions occurring in films.

#### 4.3.2 Hydrogen Bonding and Order in Gels

The demonstrated correlation between extents of intramolecular hydrogen bonding and extents of backbone conjugation and order in polydiacetylenes was used to further

advantage in an experiment on a polydiacetylene gel. Polarization modulation spectroscopy (62-64) was used to detect ordering and orientation of rod-like polydiacetylene molecules in a gel.

The modulation technique measures directly in a single differential spectrum the linear dichroism of a sample. Polarized infrared radiation incoming to the sample is rapidly modulated between two orthogonal directions. This results in the appearance of two interferograms in the detected signal (Figure 39). One is the normal interferogram associated with the average transmission of the sample and composed solely of Fourier frequencies ( $\omega_f$ ) (see equation 15). The other interferogram is composed of Fourier frequencies appearing as sideband modulations on a carrier frequency ( $\omega_m$ ). This latter interferogram can be demodulated in a lock-in amplifier to yield a differential spectrum (62) (see equation 14).

Shown in Figure 40 are a polarized modulation (differential) spectrum and an unpolarized single beam spectrum for a 0.2% gel of poly(4BCMU) in toluene. The single beam spectrum (smooth) shows the intense hydrogen bonded N-H stretching vibration ( $\sim 3325 \text{ cm}^{-1}$ ) associated with hydrogen bonded urethane substituents in the side groups of poly(4BCMU). Also present is solvent interference in the form of toluene bands at approximately  $3385 \text{ cm}^{-1}$  and

Figure 39. A typical distribution of Fourier frequencies in a detection signal of a polarization modulation experiment.

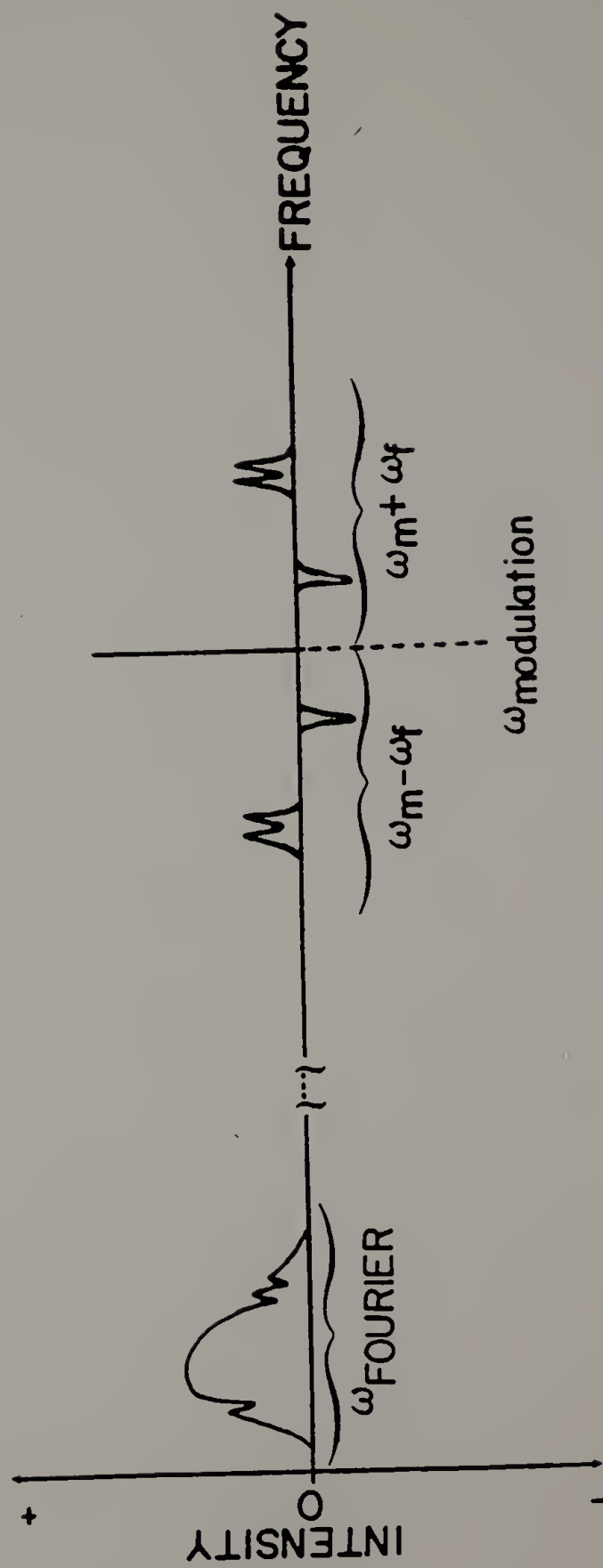


Figure 39.



Figure 40. Single beam spectrum (smooth) and modulation spectrum for a 0.2% (w/v) gel of poly(4BCMU) in toluene at  $4\text{ cm}^{-1}$  resolution. 250 scans for single beam spectrum and 1500 scans for modulation spectrum.

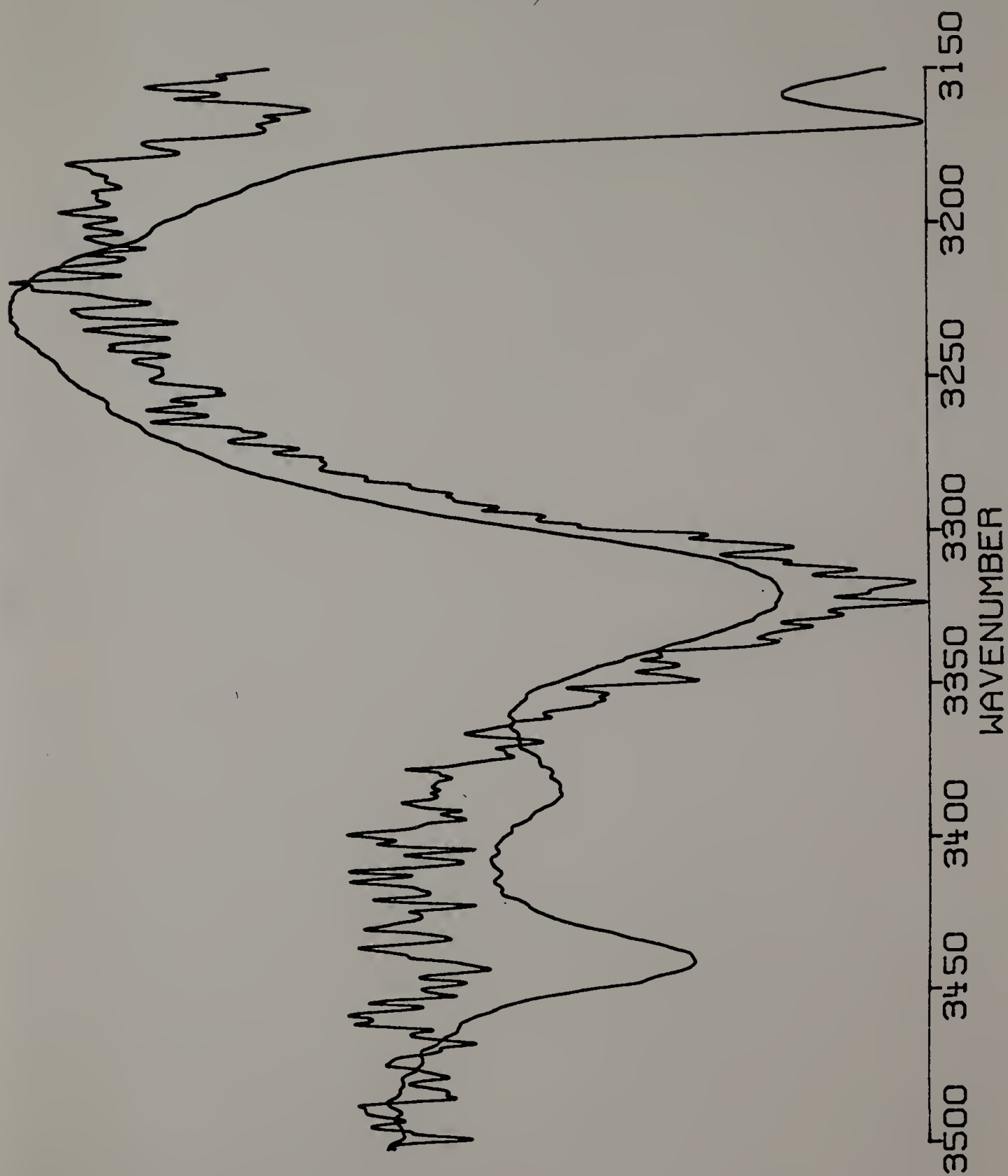


Figure 40.

3440 $\text{cm}^{-1}$ . On the other hand, the modulation spectrum shows the same poly(4BCMUs) N-H stretching vibration with no detectable solvent bands. Since the N-H stretching vibration has been determined to be polarized parallel to the main chain axis in oriented poly(4BCMUs) films (71), the alignment of intramolecular hydrogen bonds and chain backbones is indicated for poly(4BCMUs) molecules in the gel as well. This ordering is induced by the presence of parallel boundaries (0.25 cm apart) enclosing the sample. (These boundaries consist of the parallel edges of two spacer elements inserted between the KBr plates in the solution cell.) No appreciable ordering of solvent molecules occurs within the confinement of the gel as demonstrated by the absence of solvent bands in the modulation spectrum. The structure of the gel is rigid as a whole. Attempts to alter the alignment of polydiacetylene molecules in the molecules by applications of electric fields (up to 1500 V/cm) proved to be unsuccessful. The fields were applied perpendicular to the direction of alignment of the poly(4BCMUs) molecules, which have a high anisotropic polarizability along their main chain axes.

#### 4.3.3 Hydrogen Bonding in Quenched Solutions

The correlation between main chain ordering (formation of highly conjugated, rod-like structures) and side chain ordering (formation of hydrogen bonding) was again employed

in a series of quenching experiments on solutions of poly(4BCMU) in moderately strong hydrogen bonding solvents. The aim of the experiments was to determine if appreciable intramolecular hydrogen bonding, and, by correlation, chain backbone ordering, could occur if solvent interactions with the polymer molecules were minimized.

Shown in Figures 41 and 42 are spectra for yellow solutions of poly(4BCMU) at room temperature and corresponding for the quenched and gradually reheated samples. The sample in Figure 41 consists of a 2% solution of poly(4BCMU) in  $\text{CHCl}_3$ , and the sample in Figure 42 consists of a 4% solution of poly(4BCMU) in a mixed solvent of 65%  $\text{CCl}_4$ /35%  $\text{CHCl}_3$ . In both quenched samples a pronounced ordering in side chain and main chain structure is indicated by the appearance of the hydrogen bonded Amide I vibration at about  $1690 \text{ cm}^{-1}$ . This band loses intensity at the expense of a component associated with urethane groups free from hydrogen bonding at about  $1715 \text{ cm}^{-1}$ . The hydrogen bonded component is initially more intense in the mixed solvent system due to the presence of the poor solvent, carbon tetrachloride.

The initial ordering is substantially enhanced by crystallization of the solvents, and the spectra for the quenched samples remain essentially unchanged until the solvent melts. This may indicate that polymer-solvent interactions are the major factor in determining transitional behavior of solvated

Figure 41. FTIR spectra (carbonyl stretching region) for a 2% (w/v) solution of poly(4BCMU) in  $\text{CHCl}_3$  during a cooling experiment; resolution is  $4 \text{ cm}^{-1}$  and number of scans is 100.

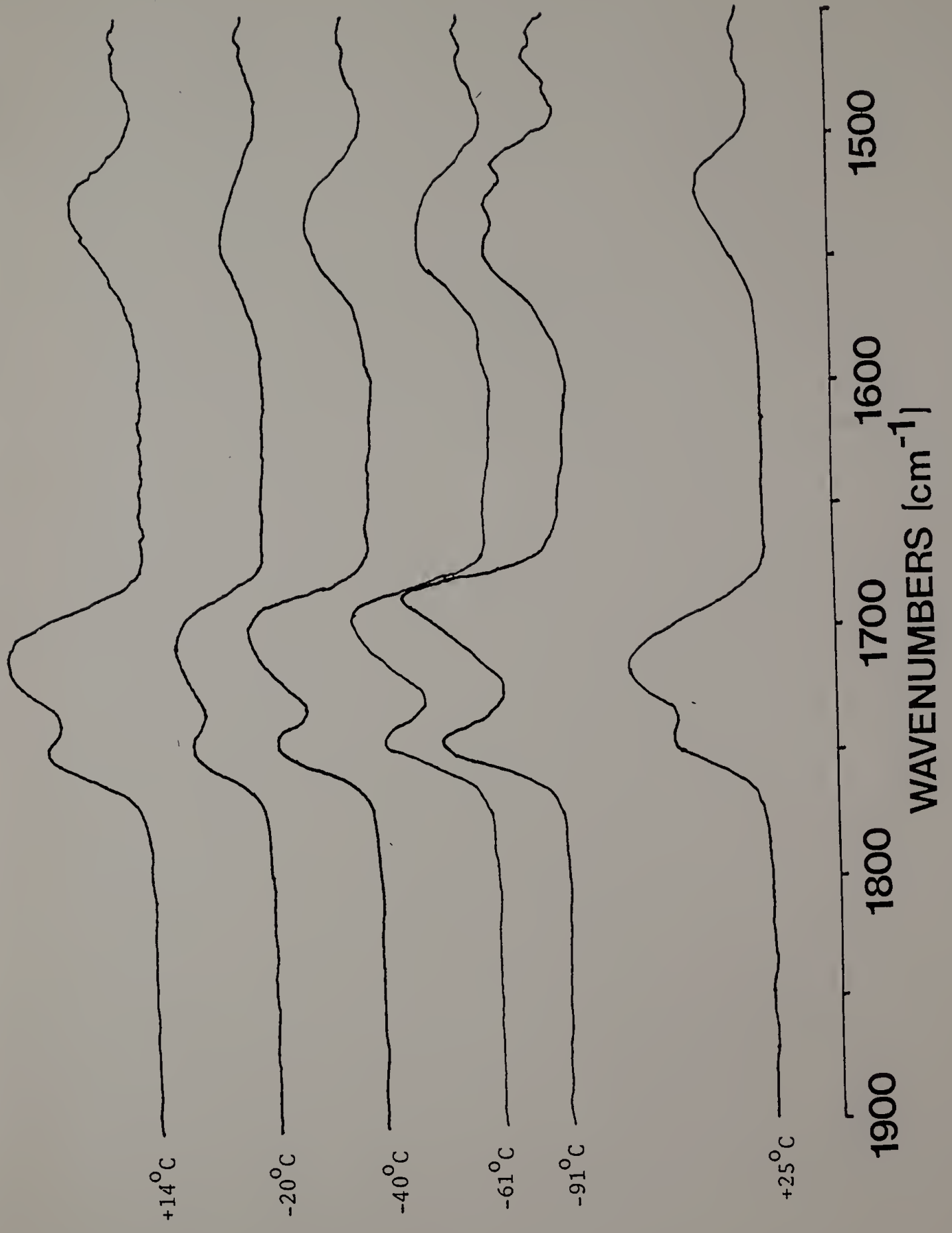
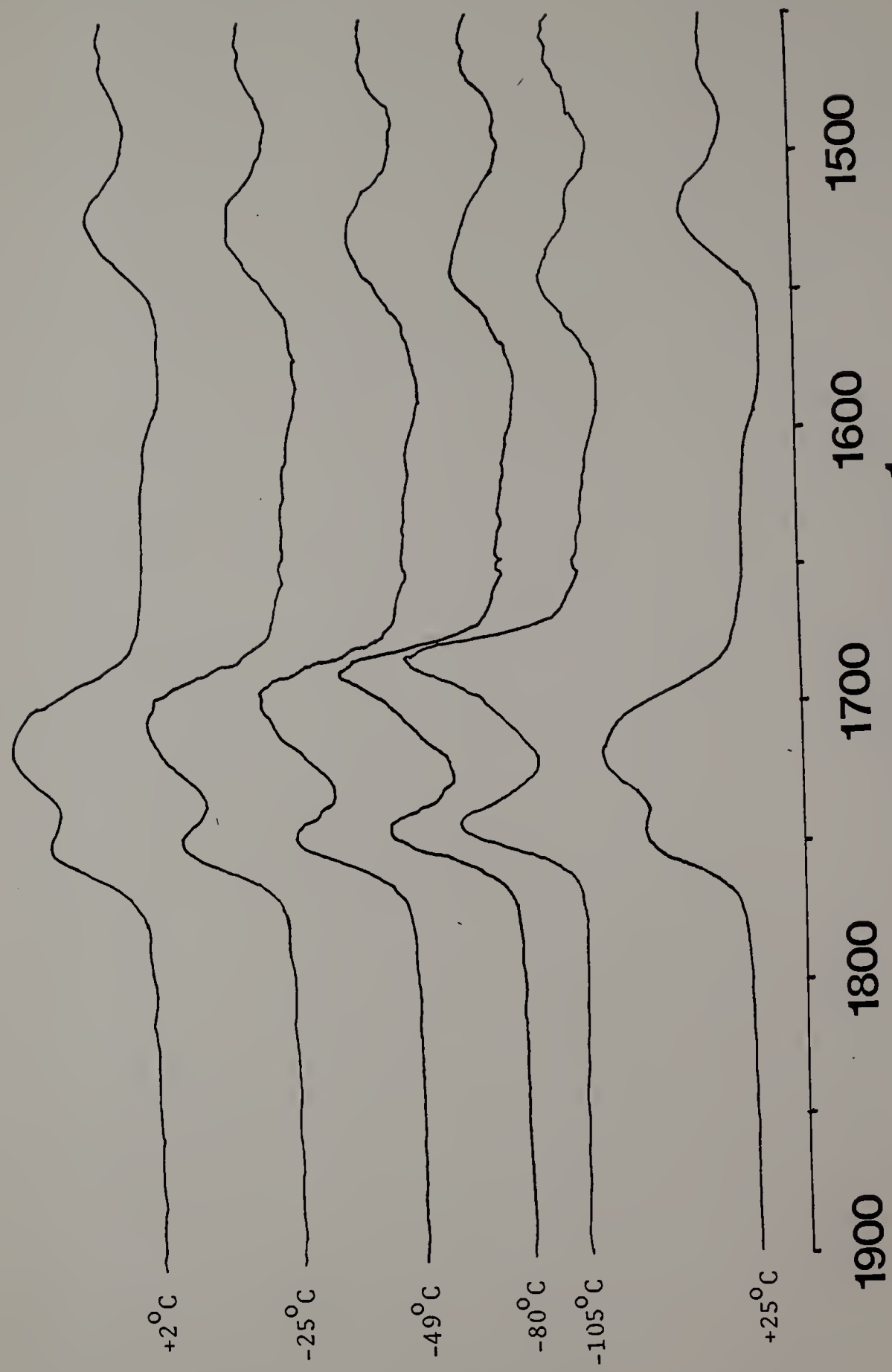


Figure 41.

Figure 42. FTIR spectra (carbonyl stretching region) for a 4% (w/v) solution of poly(4BCMU) in a mixed solvent of 65% CCl<sub>4</sub>/35% CHCl<sub>3</sub> during a cooling experiment; resolution is 4 cm<sup>-1</sup> and number of scans is 100.



WAVENUMBERS [cm<sup>-1</sup>]

Figure 42.



polydiacetylenes. Aggregated polydiacetylene molecules are observed to undergo very little additional ordering once the solvent freezes.

#### 4.4 Conclusions

A pronounced correlation between changes in the extent of intramolecular hydrogen bonding in solvated polydiacetylenes and changes in the extent of conjugation within the main chains of these materials was demonstrated unambiguously. This correlation was not detected for polydiacetylene films, and therefore the chromic transitions in films and solutions must occur at vastly differing kinetic rates, if not by different chain mechanisms. Gels, on the other hand, were shown to display similar transitional behavior to that of solutions.

The aforementioned correlation was used in a number of other infrared spectroscopic experiments. It was assumed that ordering or alignment of intramolecular hydrogen bonds, as detected by infrared spectroscopy, were indicative of ordering or alignment of the main chain backbones of the polydiacetylenes. Substantial alignment of polydiacetylene molecules in the presence of perturbing physical boundaries were detected using polarized modulation spectroscopy. In another experiment a pronounced conformational ordering of

polydiacetylene main chains was observed in quenched solutions despite the presence of moderately strong hydrogen-bonding solvents, which ordinarily disrupt the rod-like conformations of polydiacetylenes.

## CHAPTER 5

### GENERAL RESULTS AND FUTURE WORK

The utility of vibrational spectroscopy in probing conformational changes and their origins in polymeric systems has been demonstrated in the work presented in this thesis. These studies are briefly summarized in this chapter. Suggestions and considerations for related studies in the future are also given here.

A vibrational spectroscopic approach to probing the complex molecular motions responsible for the deformation behavior in miscible polymeric blends was described in Chapter 2. It was demonstrated that the selectivity of vibrational spectroscopy can be used to advantage in discriminating between the relaxational motions of chains of polystyrene and poly(vinyl methyl ether) in miscible blends of the two. Although significant scatter of data limited the extent of interpretation of results, some conclusions about the relaxational behavior in these blends could still be drawn.

It was found that long term relaxations in stress and chain orientation can be ascribed solely to the polystyrene component. Also, indications were found that the destruction of chain entanglement points between the polystyrene and poly(vinyl methyl ether) components are largely responsible for short term relaxations of the polystyrene component after

deformation of these blends. Thirdly, it was found that the poly(vinyl methyl ether) component oriented to a much smaller degree and relaxed at a much faster rate than did the polystyrene component.

In future studies of chain relaxation mechanisms in blends, the technique of polarization modulation spectroscopy could be used as a means of obtaining satisfactorily quantitative results. In the experiments of Chapter 2 time resolution is lowered due to the necessity of successively obtaining two polarized spectra, whose difference is subsequently calculated, for each orientation measurement. Time resolution can be recovered somewhat by lowering the number of signal scans per spectrum, but only at the cost of decreased signal resolution. Polarization modulation spectroscopy (62-64), on the other hand, overcomes these difficulties by directly measuring in a single spectrum the difference between two mutually orthogonal polarizations.

In polarization modulation spectroscopy the incoming beam is rapidly modulated between the two orthogonal polarizations to produce a differential ac signal. This differential signal can be measured more accurately than its counterpart, the difference of the two time-independent dc signals corresponding to the two polarization states (62). This improved signal resolution would be critical for measuring the relatively low degrees of orientation obtainable in these

blend deformation experiments. Also, as previously stated, time resolution would be enhanced due to the fact that fewer spectra would be required for the polarization modulation experiment.

In the studies presented in Chapters 3 and 4 the technique of vibrational spectroscopy was again used to investigate conformational changes in polymer chains. In this case, the system of interest consisted mainly of polydiacetylenes in solution. Solutions of polydiacetylenes have been shown to undergo dramatic color changes, or chromic transitions, in solution. These changes are reflective of alterations in the extent of electronic delocalization in the chain backbones and of extensive conformational restructuring of the polydiacetylene molecules.

The experimental studies outlined in Chapter 3 concerned investigations of a number of conclusions concerning the chain mechanism of the chromic transition of polydiacetylenes in solution. A series of titration experiments were performed on solutions of polydiacetylenes as a means of investigating possible polymer concentration dependencies for the chromic transition. A concentration dependence was indeed determined for the poly(3BCMU)/carbon tetrachloride/chloroform system. This amply demonstrated that a single chain mechanism cannot generically describe the transition for polydiacetylenes in all solvent systems

In Chapter 4 vibrational and visible spectroscopic techniques were used to confirm an intricate correlation between the extent of intramolecular hydrogen bonding in solvated polydiacetylenes and the extent of conjugation within the chain backbones of these molecules. This correlation was used to further advantage in a series of vibrational spectroscopic experiments. It was demonstrated that the process of gelation in these polydiacetylene solutions has no apparent effect on intramolecular hydrogen bonding extent and, by correlation, conjugation in chain backbones. It was also shown that while the formation of gel does not affect the chromic transition, gelation can induce large scale alignment and ordering of polydiacetylene molecules under the effects of physical boundaries. Lastly, it was shown that intramolecular hydrogen bonding and coil-to-rod transitions can occur in low temperature solutions composed of moderately strong intermolecular (polymer-solvent) hydrogen bonding solvents. These experiments demonstrated the vast utility of vibrational spectroscopy in the study of polydiacetylene solutions.

For future vibrational spectroscopic studies of hydrogen bonding and conformational transitions of polydiacetylenes in solution, studies of polydiacetylene systems other than poly(3BCMUs) and poly(4BCMUs) would prove of great interest. For example, Bloor, et al.(15) have shown that poly(9BCMUs), a

member of the butoxycarbonyl methyl urethane substituted polydiacetylenes, undergoes in solution a multistage transition between ordered and disordered forms with the formation of long-lived metastable intermediates. Hydrogen bonding characteristics have not been investigated as of yet in this system. In poly(9BCMUs) nine methylene units in the side chains separate the hydrogen bonding urethane groups from the main chain, as opposed to only three and four methylene units in poly(3BCMUs) and poly(4BCMUs) respectively. Investigation of the extent of correlation between intramolecular hydrogen bonding and backbone structure of poly(9BCMUs) in solution would have vast ramifications on the question of whether hydrogen bonding serves as a driving force for the transition in hydrogen bonded polydiacetylenes.

## REFERENCES

1. Schroeder, L.R. and Cooper, S.L., J. Appl. Phys. 47, 4310 (1976).
2. Garcia, D. and Starkweather, H.W., J. Polym. Sci., Polym. Phys. Ed. 23, 537 (1985).
3. Skrovanek, D.J., Painter, P.C., and Coleman, M.C., Macromolecules 19, 699 (1986).
4. Faivre, J.P., Jasse, B., and Monnerie, L., Polymer 26, 879 (1985).
5. Lu, F.J., Benedetti, E., and Hsu, S.L., Macromolecules 16, 1525 (1983).
6. Zhao, Y., Jasse, B., and Monnerie, L., Polym. Bull. 13, 259 (1982).
7. Ferry, J.D., "Viscoelastic Properties of Polymers", 3rd edition, John Wiley and Sons, New York, 1980.
8. Patel, G.N., Witt, J.D., and Khanna, Y.P., J. Polym. Sci., Polym. Phys. Ed. 18, 1383 (1980).
9. Chance, R.R., Patel, G.N., and Witt, J.D., J. Chem. Phys. 71, 206 (1979).
10. Patel, G.N., Chance, R.R., and Witt, J.D., J. Chem Phys. 70, 4387 (1979).
11. Chance, R.R., Macromolecules 13, 396 (1980).
12. Patel, G.N. and Khanna, Y.P., J. Polym. Sci., Polym. Phys. Ed. 20, 1029 (1982).
13. Lim, K.C., Fincher, C.R., and Heeger, A.J., Phys. Rev. Lett. 50, 1934 (1983).
14. Berlinsky, A.J., Wudl, F., Lim, K.C., Fincher, C.R., and Heeger, A.J., J. Polym. Sci., Polym. Phys. Ed. 22, 847 (1986).
15. Bloor, D., Ando, D.J., and Obhi, J.S., Makromol. Chem., Rapid Commun. 7, 665 (1986).



16. Schweizer, K.S., Chem. Phys. Lett. 125, 118 (1986).
17. Schweizer, K.S., J. Chem. Phys. 85, 1156 (1986); 85, 1176 (1986).
18. Lu, F.J., Burchell, D.J., Li, X., and Hsu, S.L., Polym. Eng. Sci. 23, 861 (1981).
19. Lefebvre, D., Jasse, B., and Monnerie, L., Polymer 22, 1616 (1981); 23, 706 (1982); 25, 318 (1984).
20. Flory, P.J., "Principles of Polymer Chemistry", Cornell University Press, Ithaca, NY, 1953.
21. Stein, R.S., J. Polym. Sci. 31, 327 (1958).
22. Roe, R.J. and Krigbaum, W.R., J. Appl. Phys. 35, 2215 (1964).
23. Doi, M. and Edwards, S.F., J. Chem. Soc. Faraday Trans. 2, 74, 1789, 1802, 1818 (1978).
24. Doi, M., J. Polym. Sci., Polym. Phys. Ed. 18, 1005 (1980).
25. Viovy, J.L., Monnerie, L., and Tassin, J.F., J. Polym. Sci., Polym. Phys. Ed. 21, 2427 (1983).
26. Coyne, L.D. and Hsu, S.L., unpublished work.
27. Burchell, D.J., Lasch, J.E., Farris, R.J., and Hsu, S.L., Polymer 23, 965 (1982).
28. Burchell, D.J., Lasch, J.E., Dobrovolny, E., Page, N., Domian, J., Farris, R.J., and Hsu, S.L., Appl. Spectrosc. 38, 343 (1984).
29. Samuels, R.J., Makromol. Chem., Suppl. 4, 241 (1981).
30. Klein, J., Macromolecules 11, 852 (1978).
31. Marrucci, G., J. Polym. Sci., Polym. Phys. Ed. 23, 159 (1985).
32. Wegner, G., in "Molecular Metals", Hatfield, W.E., ed., Plenum Press, New York (1979).

33. Patel, G.N., Chance, R.R., and Witt, J.D., Polym. Preprint Am. Chem. Soc. Div, Polym. Chem. 19, 160 (1978).
34. Patel, G.N., Polym. Preprint Am. Chem. Soc. Div. Polym. Chem. 19, 154 (1978).
35. Kuhn, H., Fortschr. Chem. Org. Naturst. 16, 169 (1958); 17, 404 (1959).
36. Baughman, R.H. and Chance, R.R., J. Polym. Sci., Polym. Phys. Ed. 14, 2037 (1976).
37. Wenz, G., Muller, M.A., Schmidt, M., and Wegner, G., Macromolecules 17, 837 (1984).
38. Lim, K.C., Kapitulnik, A., Zacher, R., Casalnuovo, S., Wudl, F., and Heeger, A.J., in "Polydiacetylenes", Chance, R.R. and Bloor, D., eds., Martinus Nijhoff, Netherlands (1985).
39. Lim, K.C. and Heeger, A.J., J. Chem. Phys. 82, 522 (1985).
40. Porod, G., Monatsh. Chem., 80, 251 (1949).
41. Kratky, O. and Porod, G., Recl. Trav. Chim. Pays-Bas 68, 1106 (1949).
42. Flory, P.J., "Statistical Mechanics of Chain Molecules", Interscience, New York (1969).
43. Doty, P., Holtzer, A.M., Bradbury, J.H., and Blatt, E.R., J. Amer. Chem. Soc. 76, 4493 (1954); Doty, P., Bradbury, J.H., and Holtzer, A.M., J. Am. Chem. Soc. 78, 498 (1956); Doty, P., Bradbury, J.H., and Holtzer, A.M., J. Am. Chem. Soc. 78, 947, (1956).
44. Zimm, B.H. and Bragg, J.K., J. Chem. Phys. 31, 526 (1959).
45. Rughooputh, S.D.D.V., Phillips, D., Bloor, D., and Ando, D.J., Polym. Commun. 25, 242 (1984).
46. Tieke, B., Makromol. Chem. 185, 1455 (1984).
47. Harrah, L.A. and Ziegler, J.M., J. Polym. Sci., Polym. Lett. Ed. 23, 209 (1985).

48. Harrah, L.A. and Ziegler, J.M., Bull. Am. Phys. Soc. 30, 540 (1985).
49. Plachetta, C., Rau, N.O., and Schulz, R.C., Mol. Cryst. Liq. Cryst. 96, 141 (1983).
50. Walters, G., Painter, P., Ika, P., and Frisch, H., Macromolecules 19, 888 (1986).
51. M. Schmidt, M. and Wegner, G., J. Chem. Phys. 84, 1057 (1986).
52. Chance, R.R., Washabaugh, M.W., and Hupe, D.J., in "Polydiacetylenes", Chance, R.R. and Bloor, D., eds., Martinus Nijhoff, Netherlands, 1985.
53. Lim, K.C., Sinclair, M., Casalnuovo, S.A., Fincher, C.R., Wudl, W., and Heeger, A.J., Mol. Cryst. Liq. Cryst. 105, 329 (1984).
54. Lim, K.C., Kapitulnik, A., Zacher, R., and Heeger, A.J., J. Chem. Phys. 84, 1058 (1986).
55. Lim, K.C., Kapitulnik, A., Zacher, R., and Heeger, A.J., J. Chem. Phys. 82, 516 (1985).
56. Chance, R.R., Washabaugh, M.W., and Hupe, D.J., Chemtronics 1, 36 (1986).
57. Coyne, L.D., Chang, C., and Hsu, S.L., accepted, Makromol. Chem.
58. Se, K., Ohnuma, H., and Kotaka, T., Polym. J. 14, 895 (1982).
59. Kapitulnik, A., Casalnuovo, S., Lim, K.C., and Heeger, A.J., Phys. Rev. Lett. 53, 2254 (1984).
60. Casalnuovo, S.A., and Heeger, A.J., Phys. Rev. Lett. 53, 2254 (1984).
61. Kapitulnik, A., Lim, K.C., Casalnuovo, S.A., and Heeger, A.J., Macromolecules 19, 676 (1986).
62. Nafie, L.A. and Vidrine, D.W., in "Fourier Transform Infrared Spectroscopy", Vol. 3, Ferraro, J.R. and Basile, L.J., eds., Academic Press, New York, 1982.

63. Noda, I., Dowrey, A.E., and Marcott, C., J. Polym. Sci., Polym. Lett. Ed. 21, 99 (1983).
64. Marcott, C., Appl. Spectrosc. 38, 442 (1984).
65. Sinclair, M., Lim, K.C., and Heeger, A.J., Phys. Rev. Lett. 51, 2254 (1984).
66. Chang, C., Coyne, L.D., and Hsu, S.L., accepted, Makromol. Chem.
67. Chance, R.R., Sowa, J.M., Eckhardt, H., and Schott, M., J. Phys. Chem. 90, 3031 (1986).
68. Cheam, T.C. and Krimm, S., J. Mol. Struct. 146, 175 (1986).
69. Skrovanek, D.J., Howe, S.E., Painter, P.C., and Coleman, M.M., Macromolecules 18, 1676 (1985).
70. Suzuki, S., Iwashita, Y., Shimanouchi, T., and Suboi, M.T., Biopolymers 4, 337 (1966).
71. Chang, C. and Hsu, S.L., Makromol. Chem. 186, 2257 (1985).
72. Peiffer, D.G., Chung, T.C., Schulz, D.N., Agarwal, P.K., Garner, R.T., and Kim, M.W., J. Chem. Phys. 85, 4712 (1986).

